SYNTHESIS, CHARACTERIZATION, AND EVALUATION OF SILICA AND POLYMER SUPPORTED CATALYSTS FOR THE PRODUCTION OF FINE CHEMICALS

A Dissertation
Presented to
The Academic Faculty

by

Rebecca Anne Shiels

In Partial Fulfillment
of the Requirements for the Degree
Doctor of Philosophy in the
School of Chemical & Biomolecular Engineering

Georgia Institute of Technology
August 2008

SYNTHESIS, CHARACTERIZATION, AND EVALUATION OF SILICA AND POLYMER SUPPORTED CATALYSTS FOR THE PRODUCTION OF FINE CHEMICALS

Approved by:

Dr. Christopher W. Jones, Advisor
School of Chemical & Biomolecular Engineering
Georgia Institute of Technology

Dr. Hang Lu
School of Chemical & Biomolecular Engineering
Georgia Institute of Technology

Dr. Pradeep Agrawal
School of Chemical & Biomolecular Engineering
Georgia Institute of Technology

Dr. Marcus Weck
School of Chemistry & Biochemistry
Georgia Institute of Technology

Dr. Dennis Hess
School of Chemical & Biomolecular Engineering
Georgia Institute of Technology

Date Approved: April 16, 2008

“Whatever you do in word or deed, do all in the name of the Lord Jesus, giving thanks through Him to God the Father.” Colossians 3:17

ACKNOWLEDGEMENTS

The completion of this degree would not have been possible without the encouragement and assistance of others. First, I would like to thank my advisor, Chris Jones, who helped me find my place here at Georgia Tech and taught me to push myself, aim high, and never settle for less than my very best. I appreciate his support throughout the past four and a half years, particularly when nothing in the lab seemed to work.

I would also like to thank my committee members, Drs. Pradeep Agrawal, Dennis Hess, Hang Lu, and Marcus Weck for their willingness to provide ideas and insights into both research and “the real world”. I especially would like to thank Marcus for all of his help with my endless chemistry questions and for always making me laugh and cheering up the room.

I owe a particular debt of gratitude to Dr. Tomlinson Fort, my undergraduate advisor at Vanderbilt. Without his encouragement, I would never have ventured down this chemical engineering path. He embodies both scientific excellence and enormous human kindness, and I value his example.

To the members of the Jones group, past and present, I would like to express my thanks for always making every day a new adventure. Particular thanks go to Mike McKittrick, Joe Nguyen, and Jason Hicks for teaching me pretty much everything I know in the lab.

To my siblings, Brian, Suzanne, and Renee, I would like to say thank you for always being there for me. We may be crazy, but we love each other and have fun

together. I especially appreciate all the help from my sister Renee over the past year with planning a wedding, moving, and generally keeping my “life” afloat.

I honestly couldn’t even begin to fit the thanks I owe my parents, Mary and Charlie Shiels, in the few lines allotted here. I cannot remember a single time when they did not do every thing in their power to support and encourage me and help me pursue my dreams. Their dedication is not taken for granted, and I thank them from the bottom of my heart.

Most importantly, I would like to thank my husband and my best friend, Jason Hicks. He literally has been there through every moment, both good and bad, of my graduate school experience. From day one, I have valued his opinion, friendship, and ability to always say what I needed to hear. His constant love, encouragement, and belief in me are the reasons I am at the finish line. I look forward to my life’s journey with you.

TABLE OF CONTENTS

LIST OF TABLES

LIST OF FIGURES

LIST OF SYMBOLS AND ABBREVIATIONS

°	degree
Å	angstrom
AIBN	2,2’-azo-bis(isobutyronitrile)
atm	atmosphere
a.u.	arbitrary units
b	broad (NMR)
BET	Brunauer-Emmet-Teller
BJH	Bopp-Jancso-Heinzinger
C	Celsius
$CDCl_3$	deuterated chloroform
cm^{-1}	inverse centimeters
CO_2	carbon dioxide
CP-MAS	cross-polarization magic angle spinning
DCC	N,N’-dicyclohexylcarbodiimide
DI	deionized
DIC	N,N’-diisopropylcarbodiimide
DMAP	4-(N,N-dimethylamino)pyridine
ee	enantiomeric excess
EPR	electron paramagnetic resonance
ESI	electrospray ionization
FAU	faujasite zeolite structure
FID	flame ionization detector
FT	Fourier transform

g	gram
GC	gas chromatography
GPC	gel permeation chromatography
h	hours
HCl	hydrochloric acid
HKR	hydrolytic kinetic resolution
IR	infrared
K	Kelvin
kHz	kilohertz
LA	Lewis acid
LB	Lewis base
m	multiplet (NMR)
M	molar (moles/liter)
m^2/g	square meters/gram
MAP	4-(methylamino)pyridine
MCM-41	Mobil mesoporous silica material
mg	milligram
MHz	megahertz
min	minute
mL	milliliter
mm	millimeter
mmol	millimole
Mn	number average molecular weight
mol%	mole percent
MS	mass spectrometry

N_2	nitrogen
NMR	nuclear magnetic resonance
PDI	polydispersity index
PO	propylene oxide
ppm	parts per million
s	seconds or singlet (NMR)
SBA-15	Santa Barbara mesoporous silica material
TEOS	tetraethyl orthosilicate
TGA	thermogravimetric analysis
THF	tetrahydrofuran
U.S.	United States
μs	microsecond
UV-Vis	ultraviolet-visible
$VO(OiPr)_3$	vanadium(V) oxytriisopropoxide
wt%	weight percent
XRD	X-ray diffraction

SUMMARY

Catalysis is an important field of study in chemical engineering and chemistry due to its application in a vast number of chemical transformations. Traditionally, catalysts have been developed as homogeneous molecular species or as heterogeneous insoluble materials. While homogeneous catalysts are typically very active and selective, they are difficult to recover. Conversely, heterogeneous catalysts are easy to recover and reuse, but they generally are less selective. To address these issues, the immobilization of homogeneous catalyst analogs onto solid supports has been a subject of research for the past few decades. Nonetheless, the effects of immobilization are still not completely predictable, and so continued effort is required to develop new immobilized catalysts as well as to develop a better understanding of how different parameters affect catalytic behavior.

This dissertation presents the synthesis, characterization, and evaluation of new immobilized catalysts for different applications. First, a solid base catalyst supported on silica was developed and studied in the synthesis of cyclic carbonates from epoxides and carbon dioxide. Next, polymer and silica supported vanadium Schiff base catalysts were developed and evaluated for use in the oxidative kinetic resolution of α-hydroxy esters, an enantioselective reaction. Lastly, salen catalyst analogs with amine reactive functional groups were synthesized and characterized for grafting onto aminosilicas with different degrees of amine group isolation. The grafted catalysts were then tested to determine how catalyst spacing on the surface affects their behavior. Throughout the presentation of these results, comparisons are made amongst the new supported catalysts and relevant

existing catalysts to discern general trends which could be applied to a wider range of immobilized catalysts. Finally, research opportunities for further improvements in these areas are suggested.

CHAPTER 1

INTRODUCTION

1.1. Immobilized Catalysts

The field of catalysis is extensive and diverse due to its ubiquitous use in all types of chemical and biological transformations. While catalysis in biological systems is predominantly governed by enzymes, catalysis in non-biological systems has focused on reactive solid materials, transition metal catalysts with or without organic ligands, and acid/base catalysts to name a few. Even though this field is vast, its development can be loosely divided into two parallel paths. The first path follows the progress of traditional heterogeneous catalysis, wherein the catalytically active site (metal, acid, or base) is directly attached to or incorporated in a solid material. The second path follows the advancement of homogeneous catalysis, which utilizes soluble molecular species whose active sites are often modified with complex ligand structures.

Each of these classes of catalysis has advantages that historically have been difficult for the other to achieve. On the heterogeneous side, the catalyst lends itself nicely to use in continuous flow reactor systems, and it is often more easily recovered from the product mixture. This can be particularly advantageous if there are concerns with product contamination or if there is a desire to reuse the catalyst without complex recovery and regeneration procedures. However, achieving high selectivity, particularly enantioselectivity, with heterogeneous catalysts is often not possible. Since the active site is directly linked to the solid surface, multiple types of active site/surface interactions may exist on the material. If these multiple types of catalytic sites interact with the reactant in different ways, selectivity can be decreased. Also, because of the limited

nature of active sites which can exist on these types of catalysts, the scope of reactions for which they can be applied is also restricted.[1]

In homogeneous catalysis, high activity and high selectivity are two significant advantages. Here, the model for this behavior is found in nature in enzymatic catalysis, which is exceptionally efficient and extremely selective.[2] The main reason for the high level of enzyme selectivity is the very controlled manner in which the substrate molecule interacts with the catalytic site – the substrate configuration must match with particular enzyme configurations for the binding and reaction to occur. This type of site-specificity is possible in non-biological homogeneous catalysis due to the vast range of organic synthesis methodologies available to design a catalyst to possess a single, specific chemical environment around the active site. However, recovery of homogeneous catalysts is typically difficult or expensive due to the need for high temperature distillations, high volume extractions, or other labor or energy intensive processes.

Over the past few decades, significant research efforts have focused on combining the best properties of both of these fields through the immobilization of homogeneous catalyst analogs onto insoluble supports.[1,3-9] Specifically, the goal has been to create catalysts that have the single-site nature of homogeneous catalysts and the ease of recovery and reuse of heterogeneous catalysts (Figure 1.1). Numerous immobilization techniques, support structures, catalyst analogs, and reactions have been investigated with varied degrees of success for developing highly active, selective, recoverable, and recyclable catalysts.

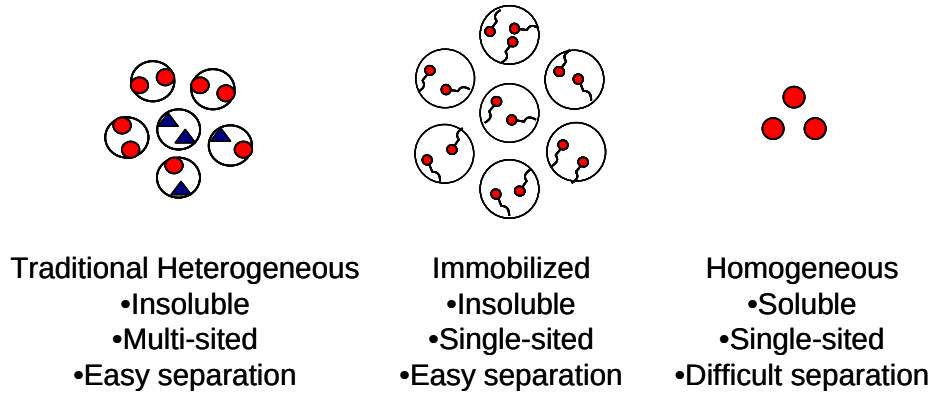

Figure 1.1. Representation of traditional heterogeneous catalysts, immobilized catalysts, and homogeneous catalysts.

The focus of this dissertation is the synthesis, characterization, and evaluation of new immobilized catalysts for three specific applications, with the broader goal of using the information learned from these systems to contribute to the on-going development of design criteria that may be applied to many immobilized catalyst systems. Each of the three systems detailed in this work is of increasing complexity in terms of synthesis and sensitivity to immobilization method, and each offers additional parameters for consideration in determining design criteria. Therefore, this dissertation demonstrates both an expansion in the available immobilized catalysts as well as an enhanced understanding of how immobilization parameters (support material, point of attachment, order of synthesis, etc.) effect catalytic activity and selectivity.

1.2. Immobilization Methods

As mentioned above, a number of immobilization methods have been employed in the development of new catalysts over the past few decades. Typically, most methods fall into one of four general categories: 1) adsorption of the catalytic species onto the

support, 2) encapsulation of the catalytic species inside cavities in the support structure, 3) grafting of a close analog of the catalytic species onto a solid support, and 4) direct incorporation of the catalytic species into the final insoluble material (Figure 1.2).[1,5,10] Each method finds use in different applications, and each method can be highly effective in appropriate reaction conditions.

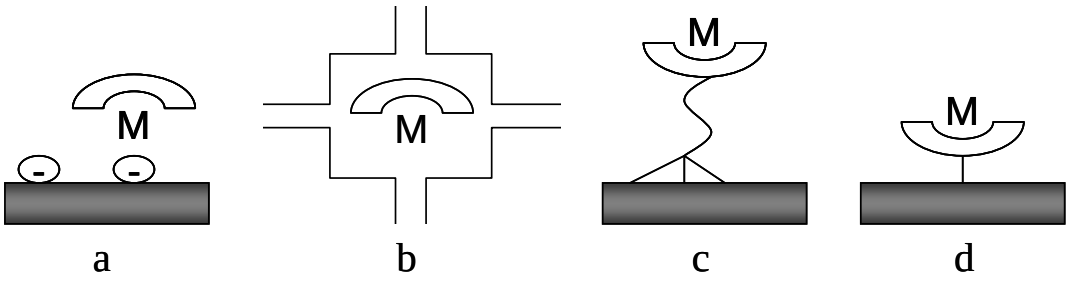

Figure 1.2. Immobilization methods: a) adsorption, b) encapsulation, c) grafting, d) direct incorporation.

Adsorption of the catalyst onto a solid support is attractive due to the fact that the desired catalyst is simply brought into contact with the support material to produce the immobilized catalyst. In this case, the synthetic procedure is very simple, and the catalyst need not be modified from its homogeneous configuration in many cases. However, the stability of the immobilized catalyst is highly dependent on interactions between the catalyst or surface and the reactants or solvents involved in the reaction. Therefore, the right combination of components must be used for this method to be suitable.[10]

Encapsulation is also a highly efficient immobilization method which utilizes a straightforward synthetic approach. This method is the only one which does not require

any interaction between the support structure and the catalyst.[5] Much like a ship-in-a-bottle, the individual components of the catalyst are diffused into cages in a support material where they assemble together. Once assembled, the catalyst is unable to diffuse back out of the pore channels as its size is now larger than the size of the pore. This method is most often used with zeolites since their frameworks have small diameter pore channels that interconnect larger cage structures (Figure 1.3). The drawbacks of encapsulation are that the sizes of the reactants one can use with this method are limited by the pore diameter of the channel, and diffusion effects can significantly influence reaction rates.

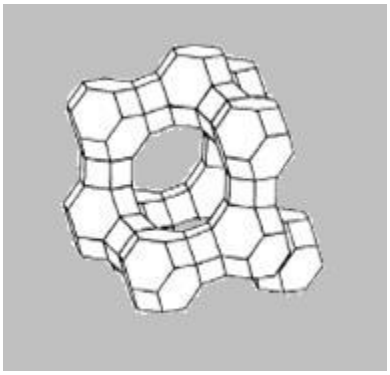

Figure 1.3. Zeolite structure FAU with smaller diameter pores leading into a larger cage structure.

The last two methods, grafting and direct incorporation, offer the greatest flexibility in terms of catalyst analog and reactant size. Additionally, the covalent nature of the attachment can be exploited to increase the catalyst's stability. For these reasons, these methods find the broadest application, and they will be used throughout this work.

1.2.1. Catalyst immobilization through grafting

Grafting is one of the most common methods of catalyst immobilization.[4,11] One of the reasons for this is that there is a large degree of flexibility in selecting the support material. The support material may be an inorganic material such as a zeolite, a mesoporous silica, an alumina, or a clay, or it may be an organic polymeric material such as a cross-linked resin or any polymer backbone bearing reactive functional groups. The only significant restraints on the support material are that: 1) it has functional groups on its surface that are able to react with a catalyst analog, and 2) the reactive surface groups are accessible to the catalyst which is being immobilized. Clearly there are other parameters which must also be considered when selecting an appropriate support material, but they are determined more by the particular application of the catalyst than by limitations of the method.

There are two main approaches to catalyst grafting.[4,12] The first is the step-wise grafting of the desired functionality onto the support material (Figure 1.4). The synthetic procedure is typically very straightforward, as one can take advantage of well-established solid-phase synthesis procedures.[9] With this approach, the selected support is stirred with the first component in the catalyst synthesis (along with any other reactants required to complete the surface reaction), filtered, and washed. Then each additional component is added individually, and the material is stirred, filtered, and washed until all of the components required to synthesize the complete catalyst analog have been added. The considerable disadvantage of this approach, however, is that characterization of the resulting material is limited.[4] Since the amount of functionalization on the surface is relatively small at each step relative to the amount of support material, most solid state

analytical techniques lack the resolution to detect unintended side products. This makes the appropriate assignment of catalytic properties imprecise and the ability to create a single-sited solid catalyst challenging.

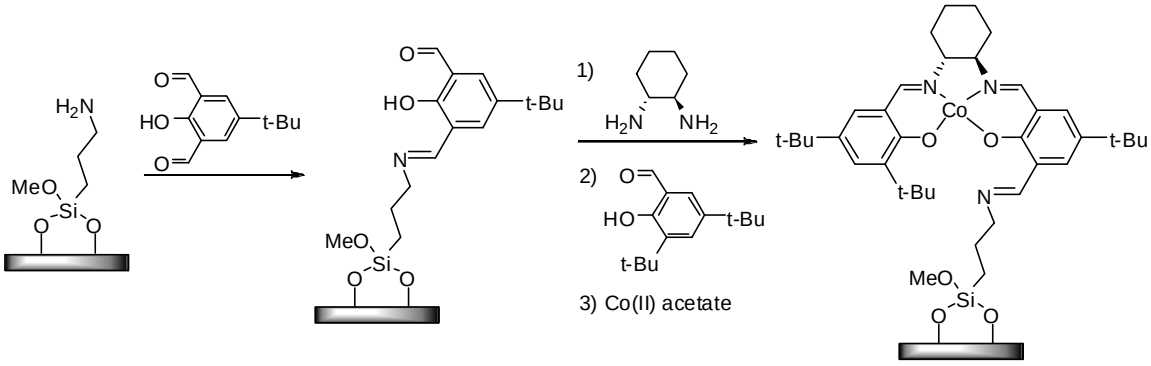

Figure 1.4. Step-wise grafting approach for anchoring a cobalt salen catalyst to a solid support.

The second approach to grafting is the preassembly and characterization of the catalyst analog before reacting it with the surface (Figure 1.5).[4] In this case, anchoring the complex to the surface is the last step in the synthetic protocol. This allows for the purification and characterization of the catalyst analog using standard quantitative solution techniques, but it is also more synthetically challenging than the step-wise grafting approach. Efficiently synthesizing and purifying the desired product at each step often requires great effort. If the catalyst is grafted onto silica, there also is always the possibility that the catalytic species may interact with silanols on the surface. However, this approach minimizes the opportunity to create undesired side products on the support's surface, especially when compared with the step-wise grafting approach.

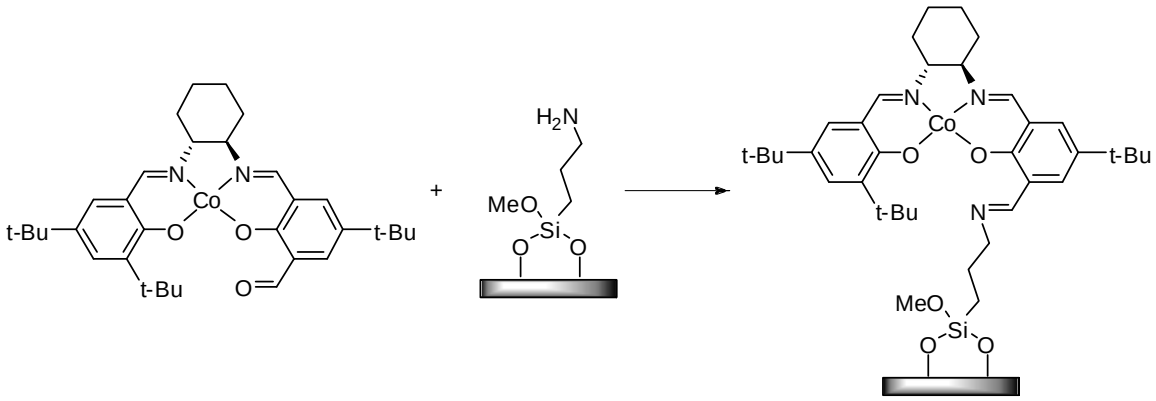

Figure 1.5. Grafting of a preassembled cobalt salen catalyst to a solid support.

Of course, not all grafting procedures must fall on either extreme of this synthetic spectrum. Preassembly of some portion of the catalyst analog followed by solid phase synthesis of the remaining portions is also possible. For example, the catalyst ligand structure might be preassembled and anchored to the surface, followed by metalation of the ligand. Regardless of the approach taken, thorough characterization of the solid catalyst is critical for the proper assignment of catalytic activity.

1.2.2. Catalyst immobilization through direct incorporation

Another method by which a homogeneous catalyst can be made heterogeneous is through direct incorporation of the catalytic species during the synthesis of the solid composite material.[13,14] This process differs from grafting in that the catalytic functionality is introduced before the support framework has formed. It is generally used when the desired support is an inorganic mesoporous silica or an organic polymer.

For incorporation in mesoporous silica, the desired catalytic species is functionalized with a trialkoxysilane. This compound is then co-condensed with a tetraalkoxysilane, usually tetraethyl orthosilicate or tetramethyl orthosilicate, in the

presence of structure directing agents (Figure 1.6).[15] These agents form ordered micelles in the synthesis solution, and the silica and catalyst functionalities co-condense around the micelles to form ordered materials. The structure directing agents are then extracted from the solid material, which leaves the catalytic species projecting into the pores of the support. This method generally produces a more regular distribution of the catalytic species throughout the material than grafting, but the concentration of functionalized catalyst that can be added before disturbing the ordering of the final material is limited.[13] Also, the catalytic functionality being incorporated must not interfere with either the co-condensation reaction or the formation of the solid material around the ordered micelles.

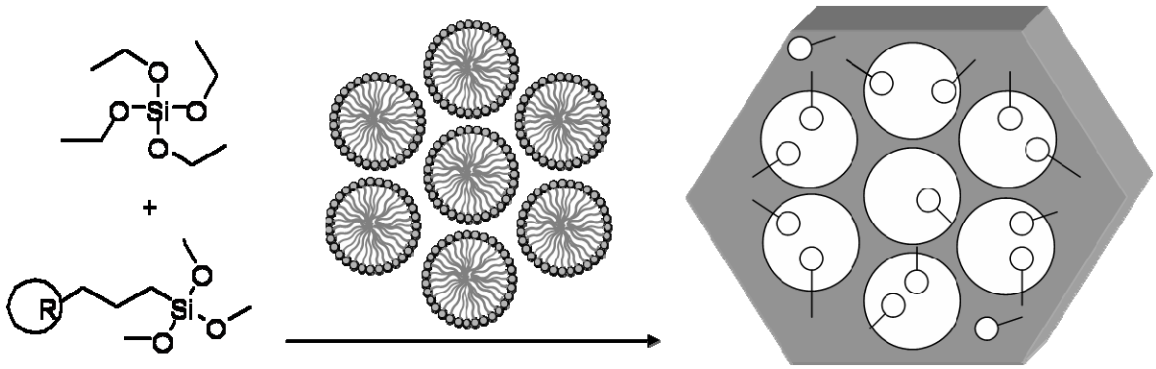

Figure 1.6. Direct incorporation of catalyst functionality into silica through co-condensation.

Direct incorporation of the catalytic species may also be used with organic polymer supports.[14] Here, the catalyst analog is synthesized in such a way that it is in itself a monomer capable of being polymerized, either alone or with a co-monomer (Figure 1.7). This allows for greater control over the architecture of the final material

than does the use of structure directing agents in the silica co-condensation process. In principle, the physical (and catalytic) properties of the polymer can be tuned with the appropriate selection of polymer backbone, degree of co-polymerization, and degree of cross-linking. As with silica co-condensation, polymerization of catalyst monomers can also provide a more uniform distribution of catalytic sites in the final material than when grafting onto polymer supports is used. Direct polymerization also allows a high degree of characterization to be completed on the monomeric catalyst prior to its immobilization.

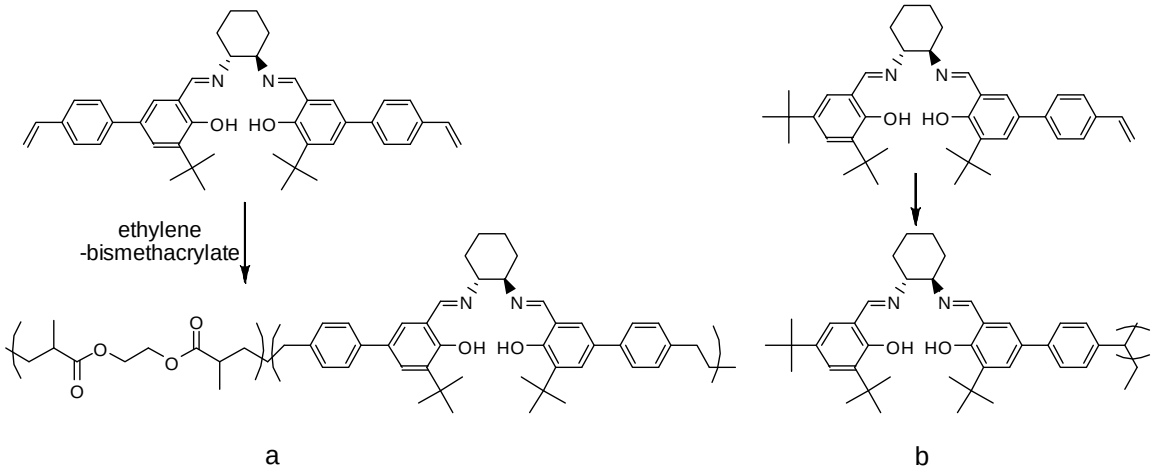

Figure 1.7. Direct incorporation of catalyst functionality through polymerization of analog monomers: a) catalyst in backbone, b) catalyst as pendant.

There are two main ways in which catalyst analogs are functionalized with polymerizable groups. The first is functionalization of the catalyst ligand with multiple polymerizable groups such that the catalyst becomes part of the polymer backbone (Figure 1.7a).[16-18] The synthesis of these monomers can be more straightforward, and having the catalytic site in the backbone can restrict its mobility and conformation. The

alternative is to functionalize the catalyst analog with only one polymerizable group such that the catalyst is attached in a pendant manner to the backbone, and only a portion of the modified ligand is incorporated into the polymer backbone (Figure 1.7b).[19,20] This method allows for greater mobility of the active site.

1.3. Support Materials

As previously stated, there are many support materials that are used for catalyst immobilization. Any number of parameters may be considered when selecting the ideal support for a given application. These include the support's porosity, thermal stability, swellability, chemical inertness, surface shape (flat, concave, convex), surface area, and density of reactive surface groups. When investigating how catalyst immobilization affects the catalytic behavior, a few of these parameters become particularly important. First, the support should be inert toward the chemical transformations for which the catalyst will be used as well as inert toward the solvent in which the reaction will take place. Second, the support must be stable over the temperature and pressure ranges under which the catalyst will be tested. Third, the support material should be well-defined. Given that cause and effect relationships are sought, broad ranges of support properties such as pore size are not desired as these can complicate the analysis of the catalytic data. Lastly, the support material must have reactive functional groups that allow the catalyst to be reacted to the surface, or the catalyst analog must have reactive functional groups that allow the formation of the solid structure. In this work, two types of support structures are used: 1) mesoporous, ordered silica and 2) organic polymers.

1.3.1. Mesoporous, ordered silica supports

Silica materials possess all of the desired properties listed for ideal immobilized catalyst supports, and as such have been widely employed in the synthesis of immobilized catalysts.[1,6,8,11,21,22] They are typically inert toward most chemical transformations, particularly if the surface silanol groups are capped after the desired catalyst is grafted. They show very high thermal stability, withstand wide pressure ranges, and do not swell in solvents. They also have high surface areas and a high density of surface silanol groups which are easily reacted with organic molecules.

Amorphous silica materials possess these traits, but the disordered nature of the material complicates the analysis of the catalytic behavior of the immobilized catalyst. Specifically, amorphous materials have wide distributions of pore diameters. Since some catalytic sites may be anchored inside very small pores while other sites are anchored in larger pores, the diffusion effects experienced at each site can be very different. At the other end of the spectrum, zeolites are crystalline silica materials with very small pore size distributions and very consistent properties. However, the use of zeolites is restrictive in terms of catalyst analog and reactant sizes due to the fact that the pore sizes are within the microporous region.

The discovery of the MCM-41 family of silica materials by Beck and co-workers in 1992 initiated an expansion in the investigation of immobilized catalysts because it extended the support pore size of ordered silica materials into the mesoporous range.[23] MCM materials are synthesized using quaternary ammonium surfactants. The surfactants form long, rod-shaped micelles in acidic solution, and then a silica source such as sodium silicate polymerizes around them (Figure 1.8). After synthesis, the surfactant is removed

by calcination to leave an ordered silica material. MCM-41 is an ordered material with a hexagonal array of unidirectional pores and a small pore size distribution. As an additional benefit, the average pore size is not restricted to one value, but can be tuned over a range of values by varying the alkyl chain length of the surfactant used in the synthesis (15-150 Å). These silica materials have high surface areas (>700 m^2/g) and high densities of surface silanol groups. These traits are desirable because there is a large area on which to graft the desired catalytic species, thereby increasing the amount of catalyst loaded per gram of support material.

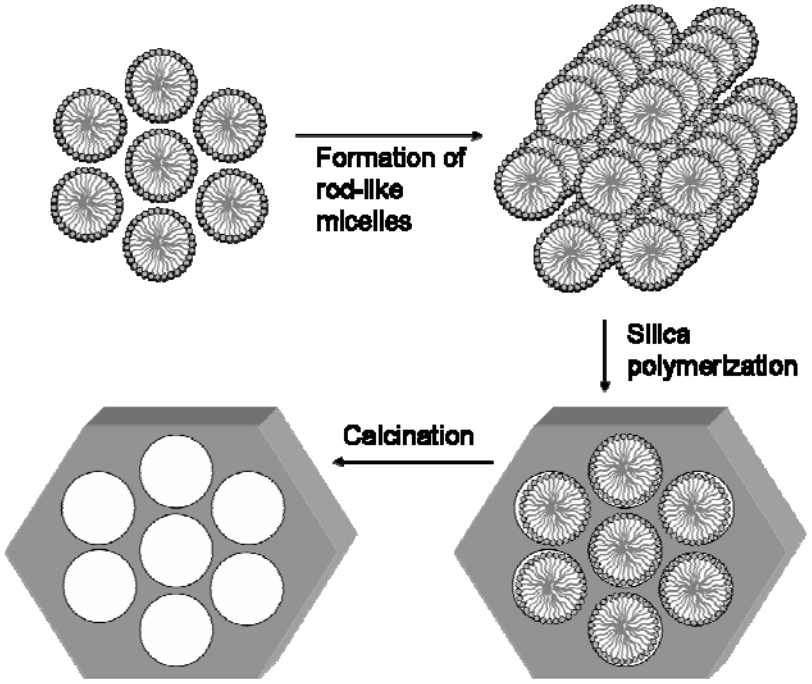

Figure 1.8. Synthesis of hexagonally ordered, mesoporous materials.

While MCM-41 offered many improvements in silica support structures for immobilized catalysts, the material did suffer from a lack of thermal stability due to its relatively thin pore walls. This issue was ameliorated with the development of the SBA-15 family of materials by Zhao and co-workers in 1998.[24] SBA-15 is synthesized similarly to MCM-41, but its synthesis uses a triblock poly(ethylene oxide)-poly(propylene oxide)-poly(ethylene oxide) copolymer template instead of quaternary ammonium surfactants. SBA-15 is also an ordered mesoporous material with unidirectional pores which are arranged in a hexagonal array. The pore sizes can be adjusted from 35-150 Å in a very simple manner, and the surface areas are >800 m^2/g. Because it is a well-defined, thermally stable, and extensively characterized material, it is used throughout this work for all of the silica supported catalysts.

As alluded to earlier, grafting onto silica materials occurs through reaction with the surface silanol groups. The silanol groups may be isolated, geminal, or vicinal (Figure 1.9). Siloxane bridges found on the surface may also be reacted with organic species. The most common method of grafting onto the silica surface is by the reaction of silanols with a trialkoxysilane that also possesses a desired functionality. This may be a preassembled catalyst analog that has been modified with a trialkoxysilane, or it may be another functional group capable of further reaction later with the desired catalyst analog. Depending on the proximity of the silanol groups, the trialkoxysilane can react to form one, two, or three anchoring points (Figure 1.10).

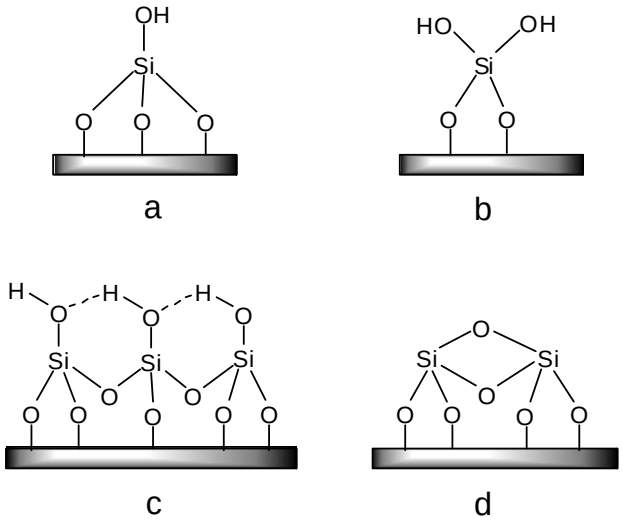

Figure 1.9. Surface silanol groups: a) isolated, b) geminal, c) vicinal, d) siloxane bridge.

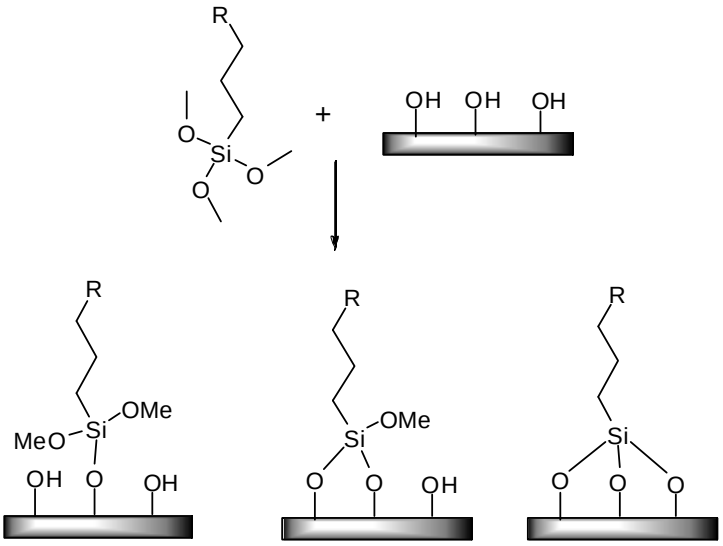

Figure 1.10. Reaction of a trialkoxysilane with a silica surface.

1.3.2. Polymer supports

Organic polymer supports also find wide application in catalyst immobilization. This is in spite of the fact that they do not have all of the attributes cited previously as desirable in support materials. In particular, they are not as thermally stable as silica materials, and they may exhibit swelling in some solvents. However, polymer supports offer some advantageous qualities that are simply not available with silica materials. For instance, the physical properties of the polymer may be tuned through the use of co-polymerization or cross-linking. Also, the degree of separation between active sites is more easily controlled with the use of a properly selected co-polymer than it can be controlled with standard silica grafting methods. Additionally, very high "loadings" of active sites are possible per gram of material when the direct incorporation method is used to homopolymerize the catalyst analog.

An additional benefit of polymer supports is that they may be designed to more closely bridge the gap between heterogeneous and homogeneous catalysis. In some cases, polymeric catalysts can be designed so that they are soluble under the reaction conditions but easily precipitated at the reaction's completion so that they may be easily recovered and reused.[25] This, in many ways, is truly the best of both worlds, but developing such a catalyst is not trivial. Many polymers, such as polystyrene, polyvinyl alcohol, polyacrylic acid, polyacrylamide, polyethylene imine, and others have good solubilities in common solvents. However, it is not always easy to predict how the solubility will be affected once the polymer is functionalized with the catalyst ligand structure. Furthermore, metalation of the catalyst can change the polymer's solubility as well. Since little

information is available *a priori* in regard to how these modifications effect the solubility of the new catalyst, some trial and error is often required.

1.4. Catalyst Systems Studied

1.4.1. Solid base catalysts

Many chemical transformations are promoted by acid or base catalysis. It was reported in 1999 that on an industrial scale, there were 127 types of processes using 180 different solid acid, solid base, or solid acid-base catalysts.[26] The motivations for the use of solid acids and bases in place of liquid acids and bases are both economical and environmental. From an economic viewpoint, the solid catalysts can be recovered and reused much more easily than their liquid phase counterparts, decreasing both catalyst and separation costs. From an environmental standpoint, the ability to reuse the catalyst instead of adding a corrosive material to a waste stream is a definite benefit. Thus, significant research efforts have centered on the development of these catalysts. While the majority of these efforts have focused on solid acid catalysts due to their extensive use in the petroleum refining industry, solid bases are also an important area of research.

Most of the initial research on solid base catalysis used materials such as zeolites, alkaline earth oxides, alkali metals on supports, and hydrotalcites.[27,28] These materials can catalyze such reactions as hydrogenations, aminations, alkylations, Knoevenagel condensations, aldol additions, transesterifications, Michael additions, and many more.[27,29] While this is a very broad range of applications, there are some constraints put on the catalyst design due to the nature of the solid materials. For instance, the pore sizes of zeolites limit both the size of the base functionality as well as the size of suitable reactants and products. Most of the early solid base catalysts incorporated ionic

functionalities onto or into the support, but the creation of catalysts with complex ligand structures was almost, if not completely absent. Additionally, the use of organic polymeric materials as supports was not possible.

Solid materials, both inorganic and polymeric, functionalized with organic bases have also been studied and offer considerable opportunities for the development of catalysts for new applications.[4,7,30] First, very strongly acidic and basic materials are often so reactive that they are not selective toward only the desired reaction, forming a mixture of products that must be separated. Additionally, such high reactivity can lead to coking of the catalyst.[26] The functionalized organic bases however, tend to be more weakly basic, and therefore often show high selectivity of the desired product. Also, as the field of catalyst immobilization expands and is more thoroughly understood, the combinations of ligand structures and support materials available to be tailored to specific reactions becomes vast.

In Chapter 2, an organic base catalyst is grafted onto a mesoporous silica support and evaluated for the addition of carbon dioxide (CO_2) to propylene oxide (Figure 1.11). It is compared with a commercially available catalyst which has a similar base functionality immobilized on a polymer support. This comparison allows insight to be obtained into how the support structure can effect the catalytic behavior. This work also highlights the important role a co-catalyst may play in a reaction; in fact, the "co-catalyst" here can be the only catalyst under certain reaction conditions.

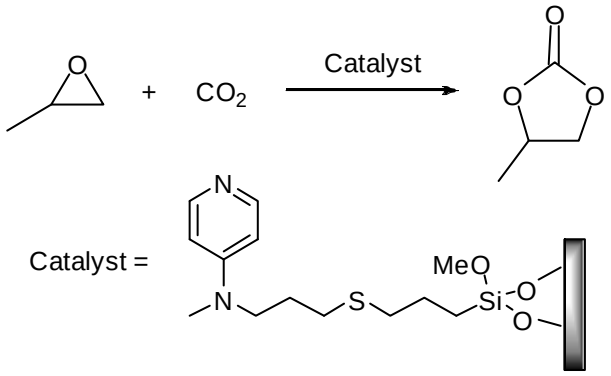

Figure 1.11. Reaction of propylene oxide with CO_2 using an immobilized base.

1.4.2. Schiff base catalysts

There are many catalysts whose ligand structures contain one or more Schiff bases.[31] A Schiff base is an imine group which has been created from the reaction of an aldehyde, or less frequently in this context a ketone, with a primary amine (Figure 1.12). Schiff base catalysts promote reactions such as oxidations, epoxidations, ketone reductions, olefin polymerizations, ring-opening polymerizations, hydrosilations, Michael additions, cyclopropanations, as well as many others. They are appropriate choices in the formation of metal complexes because of the basicity of the sp^2-hybridized lone pair on the imine nitrogen.[32,33] This basicity is why Schiff bases form complexes with almost all metal ions.[31] Additionally, this accounts for the increased stability of the metal complexed Schiff base, even though the un-complexed imine is prone to acid-catalyzed hydrolysis in the presence of water.

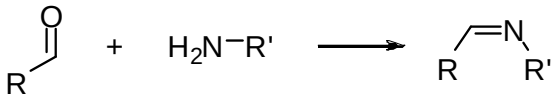

Figure 1.12. Reaction of an aldehyde with a primary amine to form a Schiff base.

The vast majority of Schiff bases in catalytic ligands are conjugated with aromatic rings. Additionally, the ligand structure almost always has at least one other heteroatom (usually oxygen, nitrogen, or sulfur) in close enough proximity to the imine that it will also coordinate with the metal. Often, the synthesis of the Schiff base is accomplished from the reaction of a diamine with a salicylaldehyde, which necessarily imparts the compound with the above mentioned characteristics (Figure 1.13). The number and nature of coordination sites, however, are tailored to the specific catalytic application, with mono-, bi-, tri-, and multi-dentate complexes all being employed. For example, many bi-dentate ruthenium Schiff base catalysts have one metal coordination with the imine nitrogen and one metal coordination with a phenolate oxygen.[34] This is because the phenolate oxygen is a hard donor which stabilizes the higher oxidation states of the ruthenium, whereas the imine nitrogen is a softer donor which stabilizes the lower oxidation states of the ruthenium.

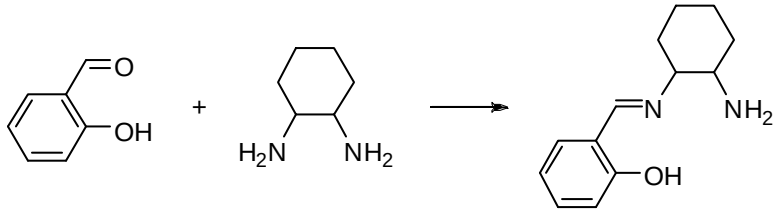

Figure 1.13. Reaction of salicylaldehyde with 1,2-cyclohexanediamine.

Another attractive feature of Schiff base ligands is that they are very amenable to enantioselective reactions. The ligands may be easily synthesized to generate a chiral center in the ligand (Figure 1.14), and this catalyst chirality can introduce enantioselectivity to the catalytic reaction. Interest in enantioselective reactions greatly increased when the U. S. Food and Drug Administration issued a statement in 1992 outlining a new policy for the development of pharmaceuticals with one or more chiral centers. This statement indicated that either enantiomerically pure compounds must be developed and tested, or individual enantiomers must be isolated and tested separately for their pharmacokinetic effects *in vivo*.[35] As development and testing of multiple enantiomers is generally more expensive than the additional cost of synthesizing only the desired enantiomer, developing catalysts which promote enantioselective reactions has become an intense area of research.[36]

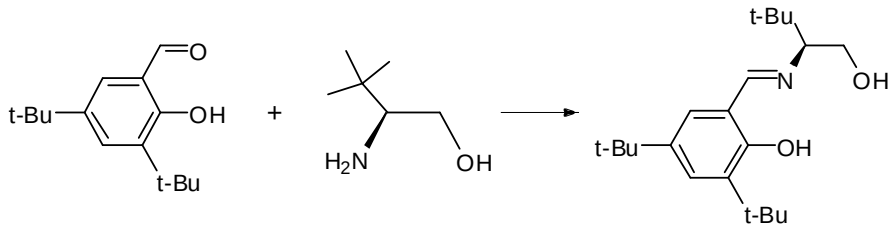

Figure 1.14. Reaction of a salicylaldehyde with S-*tert*-leucinol to form a chiral Schiff base ligand.

Sigman and Jacobsen have reported the use of a tridentate metal-free Schiff base catalyst for asymmetric Strecker reactions.[37] The reasons the tridentate ligand was selected were that its synthetic procedure was not overly complicated and that the

attachment of the ligand to a support still allowed a high degree of access to the catalytic center. There are also reports of transition metal, tridentate Schiff base catalysts for oxidation reactions. These catalysts use titanium, vanadium, copper, or zinc for various asymmetric oxidation reactions.[31,38-40]

In Chapter 3, three immobilized tridentate vanadium Schiff base catalysts are evaluated in the oxidative kinetic resolution of ethyl mandelate (Figure 1.15). Homogeneous catalyst analogs have been immobilized onto both polymeric (homopolymer and copolymer) and silica supports. The effects of support structure, solvent, and synthesis procedure are discussed.

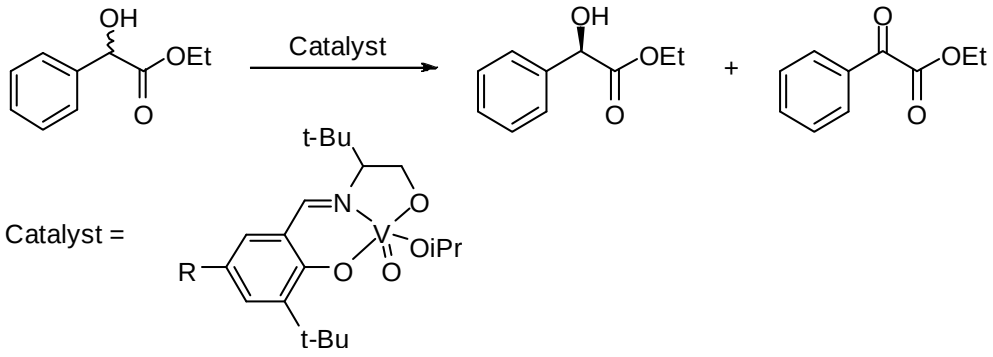

Figure 1.15. Oxidative kinetic resolution of ethyl mandelate using a vanadium Schiff base catalyst.

1.4.3. Salen catalysts

One of the most extensively studied Schiff base containing catalysts in contemporary research is the salen catalyst. This is due to its broad applicability in many different reactions and its high degree of enantiomeric control. The term salen is

generally applied to describe a family of tetradentate bisimine compounds derived from N,N'-bis(salicylidene)ethylenediamine (Figure 1.16).[32] The ligand may be metalated with any number of metals, including both transition metals and non-transition metals, and the resulting catalysts are active in numerous reactions including addition of carbon dioxide to epoxides, hydrolytic kinetic resolution of epoxides, oxidation of alkenes to form epoxides, hetero-Diels-Alder, and addition of cyanide to α,β-unsaturated imides. Homogeneous and heterogeneous salen catalysts are the subject of many reviews.[31,32,41,42]

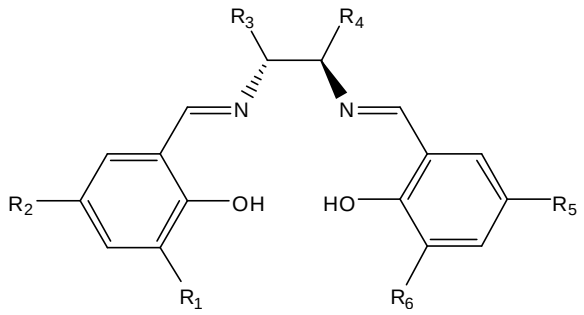

Figure 1.16. Structure of N,N'-bis(salicylidene)ethylenediamine.

Although salen catalysts are extensively studied for use in many reactions, two enantioselective reactions have garnered a particularly large amount of interest. The first of these is the asymmetric epoxidation of alkenes using manganese(III) salen complexes (Figure 1.17). Jacobsen and co-workers and Katsuki and co-workers first developed efficient catalysts for this reaction, although the Jacobsen catalyst imparted higher asymmetric induction (up to 98% enantiomeric excess depending on the substrate).[43,44] The Jacobsen catalyst is composed of di-*tert*-butyl substituted salicylaldehydes in its

homogeneous form. This reaction is reported to proceed through a monometallic mechanism, where only one active site is involved per catalytic cycle. Many immobilized forms of this catalyst have been studied, although often the enantiomeric induction is reduced on both the polymer and silica supported catalysts.[8,12,32,42]

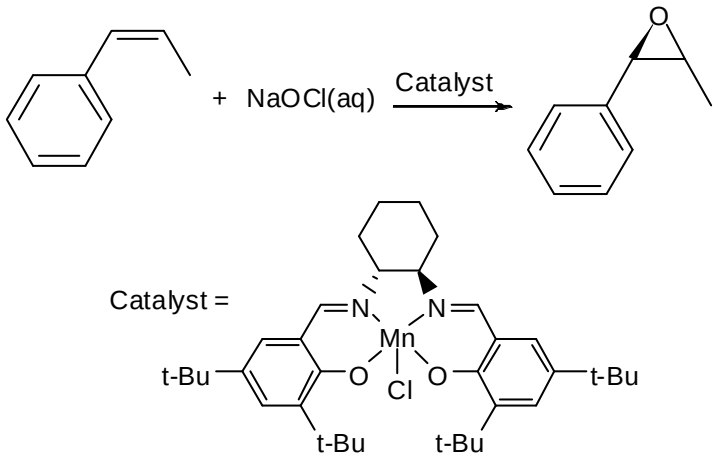

Figure 1.17. Asymmetric epoxidation of alkenes with a Mn(III) salen catalyst.

The second salen catalyzed reaction which is widely studied is the hydrolytic kinetic resolution of epoxides (Figure 1.18). During the Jacobsen group's work on the asymmetric epoxidation of alkenes, they postulated a reaction mechanism where the alkene attacked the oxygen atom on the metal in a side-on fashion.[41] The transition state in this reaction appeared to closely mimic that of ground state epoxides complexed with similar metal complexes.[45] This led to interest in general epoxide ring-opening reactions, and eventually to the development of the salen catalyzed hydrolytic kinetic resolution reaction for epoxides.[46] In this reaction, a cobalt(III) salen complex is used as the most

active catalyst, and it resolves terminal epoxides with high conversions and enantiomeric excesses. This reaction, unlike the epoxidation reaction, is bimetallic in nature, requiring two active sites to complete the catalytic cycle.[46,47] Again, many immobilized forms of this catalyst have been studied, but in this case, some immobilized catalysts actually exceed the activity and selectivity of the homogeneous catalyst.[19,20,32,47-49]

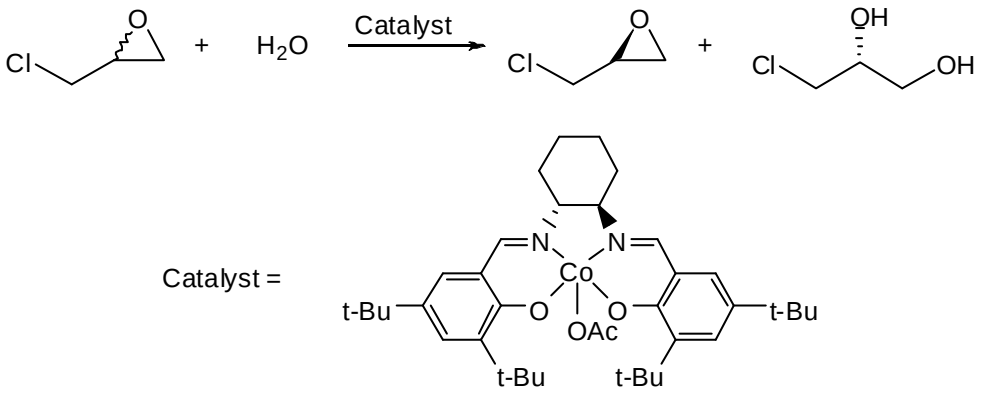

Figure 1.18. Hydrolytic kinetic resolution of epoxides with a Co(III) salen catalyst.

In Chapter 4, the immobilization of salen catalysts onto amine functionalized silica materials, or aminosilicas, is studied. The aminosilicas which are used exhibit different degrees of spacing between the amine groups. The role that this spacing plays in the catalytic behavior of the immobilized catalyst is investigated, specifically in regard to the hydrolytic kinetic resolution of epichlorohydrin. Synthetic challenges of immobilizing salen ligands onto amine groups are also discussed.

While the reports of immobilized catalysts grow at a faster rate each year, there are still many aspects of this field that are not clearly understood. Overarching design

parameters that allow the scientist to specifically design immobilized catalysts for new reactions with high success rates are still not well developed. In a small number of cases, parameters do exist. For instance, since the hydrolytic kinetic resolution of epoxides proceeds through a bimetallic mechanism, it is known that immobilization methods which allow two catalytic sites to come together easily will be more successful than those which do not force the sites to be close together. A recent study even reported optimized spacing and linker flexibility.[48] However, this type of information is typically not known for most systems, and so on-going research is required to generate these parameters for more systems, with the hope of discovering trends which can be widely applied.

This dissertation presents just that. It is an evaluation of new immobilized catalysts for two applications, as well as the evaluation of new support scaffolds as tools for designing better catalysts. In each case consideration is given to how the findings might be generalized. Finally, the conclusion brings together some key findings from these results as well as those of colleagues to provide direction for the design of future catalyst systems.

1.5. REFERENCES

[1] Wight, A. P., and Davis, M. E., *Chem. Rev.* 102 (2002) 3589.

[2] Breslow, R., *Science* 218 (1982) 532.

[3] Yermakov, Y. I., Kuznetsov, B. N., and Zakharov, V. A., *Studies in Surface Science and Catalysis,Vol. 8: Catalysis by Supported Complexes* Elsevier Scientific Publishing Company, New York, NY, (1981).

[4] Corma, A., and Garcia, H., *Adv. Synth. Catal.* 348 (2006) 1391.

[5] McMorn, P., and Hutchings, G. J., *Chem. Soc. Rev.* 33 (2004) 108.

[6] Thomas, J. M., and Raja, R., *J. Organomet. Chem.* 689 (2004) 4110.

[7] Benaglia, M., Puglisi, A., and Cozzi, F., *Chem. Rev.* 103 (2003) 3401.

[8] Song, C. E., and Lee, S.-G., *Chem. Rev.* 102 (2002) 3495.

[9] Clapham, B., Reger, T. S., and Janda, K. D., *Tetrahedron* 57 (2001) 4637.

[10] Jones, C. W., McKittrick, M. W., Nguyen, J. V., and Yu, K., *Topics in Catalysis* 34 (2005) 67.

[11] Clark, J. H., and Macquarrie, D. J., *Chem. Commun.* (1998) 853.

[12] Leadbeater, N. E., and Marco, M., *Chem. Rev.* 102 (2002) 3217.

[13] Hoffmann, F., Cornelius, M., Morell, J., and Froba, M., *Angew. Chem. Int. Ed.* 45 (2006) 3216.

[14] Mastrorilli, P., and Nobile, C. F., *Coord. Chem. Rev.* 248 (2004) 377.

[15] Burkett, S. L., Sims, S. D., and Mann, S., *Chem. Commun.* (1996) 1367.

[16] Alvaro, M., Baleizao, C., Carbonell, E., Ghoul, M. E., Garcia, H., and Gigante, B., *Tetrahedron* 61 (2005) 12131.

[17] Welbes, L. L., Scarrow, R. C., and Borovik, A. S., *Chem. Commun,* (2004) 2544.

[18] De, B. B., Lohray, B. B., Sivaram, S., and Dhal, P. K., *Macromolecules* 27 (1994) 1291.

[19] Zheng, X., Jones, C. W., and Weck, M., *Chem. Eur. J.* 12 (2006) 576.

[20] Zheng, X., Jones, C. W., and Weck, M., *J. Am. Chem. Soc.* 129 (2007) 1105.

[21] De Vos, D. E., Dams, M., Sels, B. F., and Jacobs, P. A., *Chem. Rev.* 102 (2002) 3615.

[22] Moller, K., and Bein, T., *Chem. Mater.* 10 (1998) 2950.

[23] Beck, J. S., Vartuli, J. C., Roth, W. J., Leonowicz, M. E., Kresge, C. T., Schmitt, K. D., Chu, C. T.-W., Olson, D. H., Sheppard, E. W., McCullen, S. B., Higgins, J. B., and Schlenker, J. L., *J. Am. Chem. Soc.* 114 (1992) 10834.

[24] Zhao, D., Huo, Q., Feng, J., Chmelka, B. F., and Stucky, G. D., *J. Am. Chem. Soc.* 120 (1998) 6024.

[25] Gravert, D. J., and Janda, K. D., *Chem. Rev.* 97 (1997) 489.

[26] Tanabe, K., and Holderich, W. F., *Appl. Catal. A* 181 (1999) 399.

[27] Hattori, H., *Chem. Rev.* 95 (1995) 537.

[28] Ono, Y., and Baba, T., *Catal. Today* 38 (1997) 321.

[29] Figueras, F., Kantam, M. L., and Choudary, B. M., *Current Org. Chem.* 10 (2006) 1627.

[30] Brunel, D., *Micropor. Mesopor. Mater.* 27 (1999) 329.

[31] Gupta, K. C., and Sutar, A. K., *Coord. Chem. Rev.* (2007) in press.

[32] Baleizao, C., and Garcia, H., *Chem. Rev.* 106 (2006) 3987.

[33] Smith, M. B., and March, J., *March's Advanced Organic Chemistry: Reactions, Mechanisms, and Structure* Wiley, New York, (2000).

[34] Drozdzak, R., Allaert, B., Ledoux, N., Dragutan, I., Dragutan, V., and Verpoort, F., *Coord. Chem. Rev.* 249 (2005) 3055.

[35] *FDA's policy statement for the development of new stereoisomeric drugs*, http://www.fda.gov/cder/guidance/stereo.htm, (1992).

[36] Farina, V., Reeves, J. T., Senanayake, C. H., and Song, J. J., *Chem. Rev.* 106 (2006) 2734.

[37] Sigman, M. S., and Jacobsen, E. N., *J. Am. Chem. Soc.* 120 (1998) 4901.

[38] Radosevich, A. T., Musich, C., and Toste, F. D., *J. Am. Chem. Soc.* 127 (2005) 1090.

[39] Weng, S.-S., Shen, M.-W., Kao, J.-Q., Munot, Y. S., and Chen, C.-T., *PNAS* 103 (2006) 3522.

[40] Chen, C.-T., Bettigeri, S., Weng, S.-S., Pawar, V. D., Lin, Y.-H., Liu, C.-Y., and Lee, W.-Z., *J. Org. Chem.* 72 (2007) 8175.

[41] Jacobsen, E. N., *Acc. Chem. Res.* 33 (2000) 421.

[42] Canali, L., and Sherrington, D. C., *Chem. Soc. Rev.* 28 (1999) 85.

[43] Zhang, W., Loebach, J. L., Wilson, S. R., and Jacobsen, E. N., *J. Am. Chem. Soc.* 112 (1990) 2801.

[44] Irie, R., Noda, K., Ito, Y., Matsumoto, N., and Katsuki, T., *Tetrahedron Lett.* 31 (1990) 7345.

[45] Groves, J. T., Han, Y., and Van Engen, D. V., *J. Chem. Soc., Chem. Commun.* (1990) 436.

[46] Tokunaga, M., Larrow, J. F., Kakiuchi, F., and Jacobsen, E. N., *Science* 277 (1997) 936.

[47] Annis, D. A., and Jacobsen, E. N., *J. Am. Chem. Soc.* 121 (1999) 4147.

[48] Zheng, X., Jones, C. W., and Weck, M., *Adv. Synth. Catal.* 350 (2008) 255.

[49] Breinbauer, R., and Jacobsen, E. N., *Angew. Chem. Int. Ed.* 39 (2000) 3604.

CHAPTER 2

HOMOGENEOUS AND HETEROGENEOUS 4-(N,N-DIALKYLAMINO)PYRIDINES AS EFFECTIVE SINGLE COMPONENT CATALYSTS IN THE SYNTHESIS OF PROPYLENE CARBONATE[†]

2.1. Introduction

Solid acid and solid base catalysts are used widely on an industrial scale for many chemical transformations.[1] Within this area, solid materials functionalized with organic bases have been attractive catalysts for study, largely owing to their frequently higher selectivities than more traditional solid base catalysts.[2-4] Additionally, functionalization of solid materials affords the opportunity for more types of organic base groups to be employed heterogeneously. One relevant reaction which utilizes organic base catalysis, typically in combination with Lewis acid catalysis, is the coupling of carbon dioxide (CO_2) with epoxides to form cyclic carbonates.

The synthesis of cyclic carbonates is of continuing interest for two principal reasons.[5-9] First, cyclic carbonates are useful molecules as precursors in fine chemical and pharmaceutical syntheses due to their cyclic and chiral nature.[10] Second, these compounds find application as specialty polar solvents, as precursors to 1,2-diols, as curing agents, and in electrolytic formulations for high-energy density batteries.[11] Cyclic

---

[†] Reproduced in part with permission from Journal of Molecular Catalysis: A Chemical 261 (2007) 160-166. Copyright 2007 Elsevier.

carbonates are also interesting from an environmental standpoint due to the consumption of CO_2 in their synthesis (Figure 2.1).

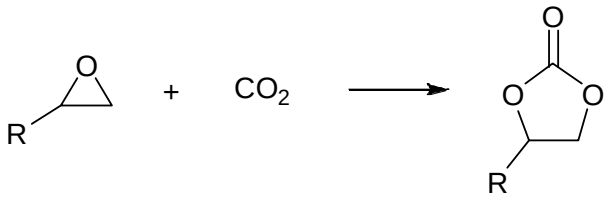

Figure 2.1.Synthesis of cyclic carbonates from epoxides and CO_2.

Many bi-functional solid catalysts possessing both acidic and basic sites have been reported for the synthesis of cyclic carbonates, including alkali-loaded zeolites, mixed oxides, and amine-functionalized oxide materials.[9,12-18] In many of these cases, it is suggested that the basic sites activate the CO_2 molecule and the acidic sites activate the epoxide. Homogeneous systems combining Lewis acids and Lewis bases also have been reported for this reaction.[19] Another common catalytic system used for cyclic carbonate production combines a transition metal compound, often a salen complex, which acts as a Lewis acid with a Lewis base co-catalyst. Both heterogeneous and homogeneous versions of this system have been studied.[20-35] In these cases, the most frequently proposed mechanism involves the metal species activating the epoxide and the base opening the epoxide ring (Figure 2.2). A final type of catalyst that commonly has been employed for the synthesis of cyclic carbonates is quaternary onium salts. These catalysts have been used as single component catalysts in either homogeneous or heterogeneous forms, although it has been reported that reaction rates can be substantially increased by

combining the onium salt with a weak Brønsted acid such as silanols on silica surfaces.[36-41] These reports indicate that the reaction mechanism is not clearly understood.

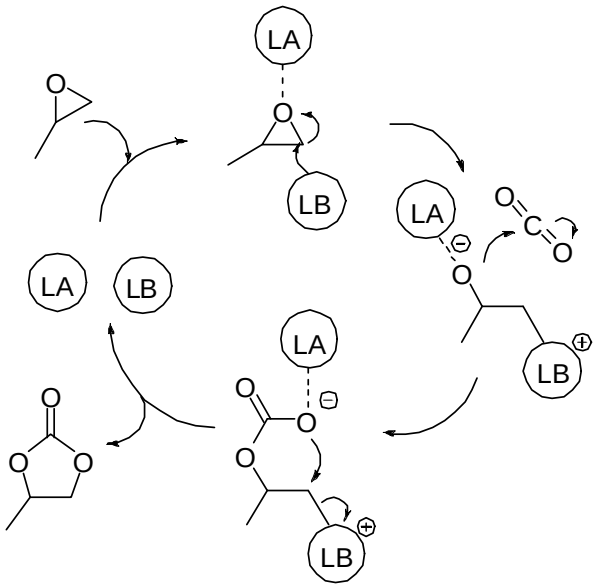

Figure 2.2. Frequently suggested mechanism for cyclic carbonate synthesis using Lewis acid/ Lewis base catalysis.

One particular aspect of the cyclic carbonate reaction mechanism about which there are many conflicting reports is the role of the Lewis basic co-catalyst. One report by Du and coworkers suggests that a single Lewis basic component may be able to promote the coupling of epoxides and CO_2.[38] They studied polymer resins with primary, secondary, and tertiary amine groups as single component catalysts for the synthesis of propylene carbonate and found all of these materials to be active at 80 bar CO_2 pressure and 100 °C. In contrast, Zhang and coworkers found that a silica supported strong tertiary amine base, 1,5,7-triazabicyclo[4,4,0]dec-5-ene, was completely inactive at 20 bar CO_2

pressure and 150 °C when the surface silanols, hypothesized to be co-catalysts, were rendered unreactive via a capping reaction.[18] Another example of conflicting data concerns the use of 4-(N,N-dimethylamino)pyridine (DMAP) as a single component catalyst. Shen and coworkers report that DMAP is inactive as a single component catalyst at 36 bar CO_2 pressure and 120 °C.[19] In contrast, Sankar found that DMAP was an active catalyst under the relatively mild conditions of 4 bar CO_2 pressure and 120-140 °C.[20] In bi-functional metal complex/DMAP systems, it is often assumed that both components are needed to effect catalysis, but even here there are conflicting views as to the role each component plays in the catalytic cycle (see Appendix A). The above examples showing the activity of the Lewis base alone, however, suggest that there may not be a need for bi-functional catalysis. In agreement with the work reported by Sankar, this chapter also demonstrates the use of DMAP as a single component catalyst in the non-enantioselective synthesis of propylene carbonate.

One drawback to the use of DMAP as a homogeneous catalyst in the synthesis of cyclic carbonates is that it can be expensive to separate the pure carbonate from the catalyst after the reaction. Since cyclic carbonates have high boiling points, purification by distillation can engender significant energy costs as well as thermally degrade the catalyst. Therefore, an equally productive and selective heterogeneous catalyst that could be recovered from the product without the need for high temperature separation is an important goal. As supporting analogs of selective and active homogeneous catalysts on solid supports has been an active area of research for quite some time, there are reports of numerous silica-supported organic base hybrid catalysts used for cyclic carbonate synthesis.[9,16-18,38,41] Similarly, there are reports of DMAP type functionalities

immobilized on organic and inorganic supports including polymers and sol-gels, although they are not believed to have been evaluated for cyclic carbonate synthesis.[3,21,42-46] Building on these precedents, this chapter presents the synthesis of a new DMAP analog tethered to an SBA-15 support. This supported catalyst exhibits comparable productivity to the homogeneous catalyst under the reaction conditions studied, and it can be easily separated from the product by filtration.

2.2. Experimental

2.2.1. Materials

4-(Dimethylamino)pyridine (DMAP) (Acros), 4-methylaminopyridine (MAP) (Aldrich), and 2,2'-azo-bis(isobutyronitrile) (AIBN) (Aldrich) were dried under vacuum and stored in a nitrogen dry box. 3-Mercaptopropyltrimethoxysilane (Alfa-Aesar), n-butyllithium 1.6 M in hexanes (Aldrich), tetraethyl orthosilicate (TEOS) (Aldrich), poly(ethylene glycol)-block-poly(propylene glycol)-block-poly(ethylene glycol) (Aldrich), 'Dimethylaminopyridine' on polystyrene (~3 mmol/g) (Fluka), and 99.999% pure research grade carbon dioxide (<3 ppm water) (Airgas) were used as received. Phenol (Acros) was used as received except where otherwise indicated. Propylene oxide (PO) (Aldrich) and dichloromethane (Fisher) were dried over calcium hydride and distilled; chloroform (Aldrich) was dried with 4 Å molecular sieves and distilled; allyl bromide (Acros) was dried over magnesium sulfate and distilled. Tetrahydrofuran (THF) and toluene were used after purification and drying via a packed bed solvent system made of copper oxide and alumina columns in the case of THF and dual alumina columns in the case of toluene.[47]

2.2.2. Characterization methods

Solid state cross-polarization magic angle spinning (CP-MAS) NMR analyses were conducted on a Bruker DSX 300-MHz spectrometer with samples packed in 7-mm zirconia rotors. For ^{13}C CP-MAS samples, the following parameters were used: 5 kHz spin rate, 16000 scans, 90° pulse length of 5μs, and repetition time between scans of 4 s. For ^{29}Si CP-MAS samples, the following parameters were used: 5 kHz spin rate, 18000 scans, 90° pulse length of 5 μs, and repetition time between scans of 5 s. Solution NMR was conducted on a Varian Mercury Vx 400 spectrometer. FT-Raman spectra were collected on a Bruker FRA-106. Three thousand scans were collected with a resolution of 2-4 cm^{-1}. Thermogravimetric analyses (TGA) were performed on a Netzsch STA409. Samples, under an air blanket, were heated from 30 °C to 900 °C at a rate of 10 °C/min. The organic loading was determined from the weight loss between 200 °C and 700 °C. Nitrogen physisorption measurements were taken on a Micromeritics ASAP 2010 at 77 K. Prior to analysis, SBA-15 samples were degassed at 150 °C under vacuum overnight, and DMAP-SBA samples were degassed at 50 °C under vacuum overnight. X-ray diffraction (XRD) patterns were taken using Cu Kα radiation on a PAN analytical X'Pert Pro powder X-ray diffractometer equipped with a PW3011 proportional detector with a parallel plate collimator. Gas chromatography was conducted on a Shimadzu GC 17-A equipped with a flame-ionization detector and an HP-5 column (length = 30 m, inner diameter = 0.32 mm, and film thickness = 0.25 μm). The temperature profile was as follows: heat to 50 °C, wait 2 min, ramp to 140 °C at a rate of 30 °C/min, ramp to 300 °C at 40 °C/min, and hold for 2 min.

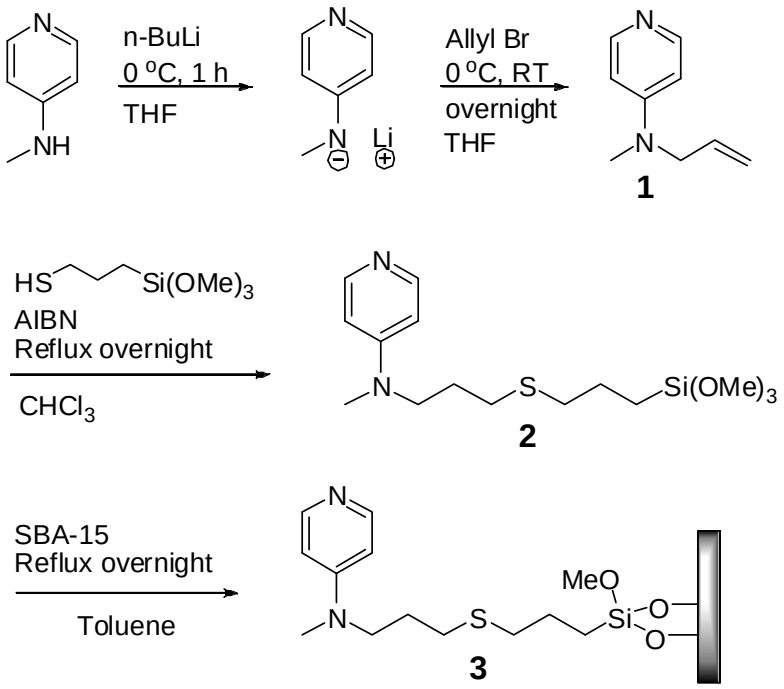

Figure 2.3. Synthesis of supported DMAP analog on SBA-15.

2.2.3. Synthesis of 4-(*N*-allyl-*N*-methylamino)pyridine (1)

A solution of 4-(methylamino)pyridine (MAP) (2.0 g, 18.5 mmol) in THF was prepared in a nitrogen dry box and then stirred under argon at 0 °C for 2 h (Figure 2.3). n-Butyllithium (13 ml of 1.6 M in hexanes, 21 mmol) was added via syringe to the MAP/THF mixture while under an argon purge and stirred for an additional 1 h at 0 °C. Dry allyl bromide (3.4 g, 28.1 mmol) in THF was added via syringe, and the mixture was allowed to warm to room temperature overnight while being stirred. Excess n-butyllithium was quenched with DI water, and the volatile components were removed under vacuum. Compound **1** was recovered as a dark yellow oil by extraction from dichloromethane/DI water and was dried.

1: Yield 72 %. ^{1}H NMR (400 MHz, $CDCl_3$): δ 3.00 (s, 3H), δ 3.94-3.98 (b, 2H), δ 5.08-5.21 (m, 2H), δ 5.74-5.85 (m, 1H), δ 6.51 (d, J = 6.36 Hz, 2H), δ 8.20 (d, J = 6.04 Hz, 2H). ^{13}C NMR (101 MHz, $CDCl_3$): δ 37.4, 53.9, 106.8, 116.8, 132.1, 150.1, 153.7.

2.2.4. Synthesis of 4-[N-methyl-N-(3'-(3'-(trimethoxysilyl)propylthio)propyl) amino]pyridine (2)

A solution of **1** (2.0 g, 13.5 mmol) in chloroform was prepared in a nitrogen dry box. 3-Mercaptopropyltrimethoxysilane (12 g, 61 mmol) was added to the solution along with AIBN (150 mg, 0.9 mmol) (Figure 2.3). The reaction mixture was then stirred at reflux conditions under an argon blanket overnight. The solvent was removed under vacuum, and excess 3-mercaptopropyltrimethoxysilane was distilled off at 110 °C under vacuum to isolate compound **2** as a brown oil.

2: Yield 95%. ^{1}H NMR (400 MHz, $CDCl_3$): δ 0.71 (m, 2H), δ 1.66 (m, 2H), δ 1.82 (m, 2H), δ 2.49 (m, 4H), δ 2.93 (s, 3H), δ 3.42 (t, 2H), δ 3.52 (s, 9H), δ 6.47 (d, J = 6.56 Hz, 2H), δ 8.16 (d, J = 6.48 Hz, 2H). ^{13}C NMR (101 MHz, $CDCl_3$): δ 8.6, 22.9, 26.4, 29.1, 35.2, 37.5, 50.0, 50.5, 106.4, 149.8, 153.3. MS (ESI): *m/z* 345.2 $[M + H]^+$. Accurate mass: calcd., for $C_{15}H_{29}N_2O_3SSi$, 345.1663; found, 345.1647.

2.2.5. Synthesis of SBA-15

SBA-15 was synthesized according to literature procedures.[48] In a typical batch, the poly(ethylene glycol)-block-poly(propylene glycol)-block-poly(ethylene glycol) copolymer template (18 g) was dissolved in HCl (103.5 g) and DI water (477 g). Tetraethyl orthosilicate (TEOS) (38.4 g) was added to the solution which was stirred for 20 h at 35 °C. Then, the solution was heated to 80 °C and maintained at that temperature

for 24 h. The reaction was quenched with DI water, filtered, and washed with several portions of DI water to remove excess copolymer and give SBA-15 as a white powder. The SBA-15 was dried for 3 h at 50 °C and then calcined according to the following temperature program: 1) ramp to 200 °C at 1.2 °C/min, 2) hold at 200 °C for 1 h, 3) ramp to 550 °C at 1.2 °C/min, and 4) hold at 550 °C for 6 h. Finally, the calcined SBA-15 was heated under vacuum at 200 °C for 3 h and stored in a nitrogen dry box. The procedure yielded approximately 12 g of SBA-15.

2.2.6. Synthesis of 4-[N-methyl-N-(3'-(3'-(trimethoxysilyl)propylthio)propyl) amino]pyridine supported on SBA-15 (DMAP-SBA, 3)

Compound **2** (1.0 g, 2.9 mmol) was added drop-wise to a solution of calcined SBA-15 (1.5 g) in dry toluene in a nitrogen dry box (Figure 2.3). The solution was stirred at reflux conditions under an argon blanket overnight. The functionalized DMAP-SBA was then filtered in the dry box and washed with toluene and hexanes. Finally, material **3** was dried overnight under vacuum to give a pale brown powder. The procedure yielded approximately 2 g of **3**.

2.2.7. Catalytic reactions

In a representative reaction, DMAP or an immobilized analog (0.36 mmol), propylene oxide (PO) (5.20 g, 89.5 mmol), and dichloromethane (1.33 g, 15.7 mmol) were charged into a 50 ml Parr stainless steel reactor and sealed inside a nitrogen dry box. The reactor was then removed from the dry box and connected to a supply of 3.4 bar of CO_2 for 10 min with no heating. Next, the reactor was heated to 120 °C, and the CO_2 supply pressure was increased to 17.2 bar. The contents were maintained at these conditions for the length of the reaction, and the reaction was quenched by placing the

reactor in an ice bath. Excess pressure was released, and the reactor contents were transferred into a round-bottom flask. Un-reacted propylene oxide and dichloromethane were removed under vacuum, and the yield of propylene carbonate was determined from the residual weight after subtracting the weight of the catalyst that had been added.[26] Production of propylene carbonate was verified by GC through comparison with a known standard of propylene carbonate (99.5% purity, Acros) and by ^{1}H and ^{13}C NMR.

2.3. Results and Discussion

2.3.1. Carbonate reactions with the homogeneous catalyst(s)

This investigation into the catalytic role of DMAP in cyclic carbonate reactions initially began with the use of a co-catalyst system of phenol and DMAP which was reported by Shen and coworkers.[19] It should be noted that the majority of the experiments in this work were conducted at greatly reduced CO_2 pressure compared to their original work (35.7 bar in their work vs. 17.2 bar in this work). Reaction results from the catalytic systems that were examined are shown in Table 2.1. For the phenol and DMAP co-catalyst system, each catalyst was added at a loading of 4 mmol/mol propylene oxide (PO), and an 86% conversion of the epoxide was achieved. In this case, propylene carbonate was the only product as verified by GC and ^{1}H NMR. As a control experiment, PO and CO_2 were reacted under the same conditions with no catalysts, and a conversion of PO of approximately 50% was observed. However, in this case, there were two product peaks in the GC trace. One peak was the desired cyclic carbonate, and the other peak was identified as propylene glycol by comparison with a known standard. Postulating that the presence of water could cause the formation of the glycol, all reagents and catalysts were rigorously dried and charged and sealed in the reactor in a

nitrogen dry box. After this careful exclusion of water, no conversion was seen for the reaction of PO and CO_2 without any catalyst at these conditions. This result suggests that water can act as a catalyst if the system is not rigorously dried.

Table 2.1. Cyclic carbonate reaction results.[a]

Entry	Catalyst	Conversion[b]	# Products[c]
1	Phenol, homogeneous DMAP	86 %	1
2	none (ambient conditions)	48 %	2
3	none (anhydrous conditions)	0 %	0
4	Homogeneous DMAP	85 %	1
5	Homogeneous DMAP[d]	92 %	1
6	DMAP-SBA **3**	81 %	1
7	DMAP-SBA **3** recycle	49 %	1
8	Poly(styrene) supported DMAP	82 %	1
9	Poly(styrene) supported DMAP recycle	30 %	1
10	3-Aminopropyl functionalized SBA	0 %	0
11	3-Mercaptopropyl functionalized SBA	0 %	0
12	Capped DMAP-SBA **3**	81 %	1

[a] Reaction conditions: Propylene oxide (89.5 mmol), methylene chloride (15.7 mmol), and catalyst (0.36 mmol) were stirred at 120 °C and 17.2 bar CO_2 pressure for 4 hours. [b] Conversion determined by residual weight after removing volatile components and subtracting catalyst weight. [c] Determined by GC-FID and NMR. [d] CO_2 pressure was 34 bar in this case.

The next system that was examined was DMAP alone without the presence of phenol. The loading of DMAP was again 4 mmol/mol PO. Using the reaction conditions of Shen (120 °C and 35.7 bar), yields of 92% were unexpectedly observed, with propylene carbonate as the only product as verified by GC and ^{1}H NMR. At the same temperature and only 17.2 bar CO_2 pressure, yields of 85% were observed. To further explore the effect of pressure, additional experiments at 120 °C and various pressures were performed. These results suggest that once a sufficiently high pressure is employed, a further increase in CO_2 pressure does not significantly increase the yield (Figure 2.4). With the experimental set-up used, it was difficult to determine the minimum pressure required for the reaction to take place. If the initial pressure was set at 3.4 bar, the reactor would pressurize beyond this value as it was heated. If the initial pressure was set lower than 3.4 bar, the epoxide and solvent would vaporize as the reactor was heated, and the catalyst would char onto the bottom of the reactor.

The effect of the reaction time on the yield was also studied (Figure 2.5). These results indicate that the homogeneously catalyzed reaction has reached its maximum conversion after approximately 2 h. This conversion was not observed to increase even after 24 h. It also should be noted that if the temperature was decreased to 100 °C for reactions run for 2 h at 17.2 bar, only 30% yield was attained versus the 85% yield attained at 120 °C. In the case of DMAP alone, just as in the case of the control reaction with no added catalysts, it was observed that if the reactor was charged in ambient atmosphere, propylene glycol was occasionally obtained as a side product. Again, the glycol was not seen if the reaction conditions were kept dry.

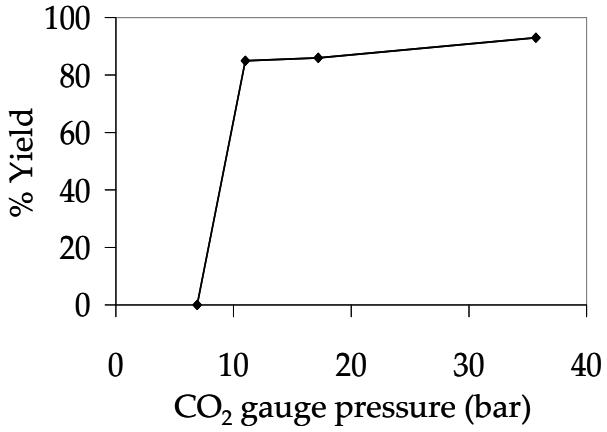

Figure 2.4 Yield of propylene carbonate versus CO_2 pressure with 0.4 mol% DMAP catalyst after 4 h at 120 °C.

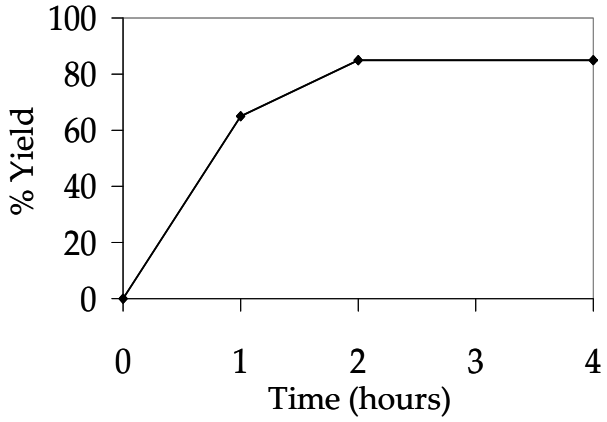

Figure 2.5. Yield of propylene carbonate versus time with 0.4 mol% DMAP catalyst at 17.2 bar CO_2 and 120 °C.

Previously reported mechanisms for this reaction involve both a Lewis acid and Lewis base site for the catalytic cycle as discussed in the introduction (Figure 2.2). For most of these suggested mechanisms, a lone pair of electrons from the Lewis base attacks the least hindered carbon of the epoxide ring. Since DMAP is known to be a strong base, and in light of the data shown here suggesting that DMAP promotes the reaction without the addition of another catalyst, we have proposed a mechanism which may be operating for this system when the reaction is conducted under anhydrous conditions (Figure 2.6). This mechanism involves the lone pair on the pyridyl nitrogen from a single DMAP molecule attacking the epoxide ring with subsequent addition of CO_2 to the opened epoxide. It should be noted that a related mechanism involving two DMAP molecules working in concert might also be reasonable.[20] To ensure that trace acid impurities from the dichloromethane used as the reaction solvent were not added to the system, dichloromethane treated with base and dichloromethane distilled from calcium hydride were used in reactions. In both cases, the reaction results were the same as those reported above. Additionally, the use of rigorously dry solvents, gases and techniques suggests that traces of water likely do not play a co-catalytic role.[†]

[†] As nearly all cyclic carbonate syntheses that are carried out at high temperatures are conducted in autoclaves, one cannot conclusively rule out the presence and possible importance of traces of dissolved transition metal species in solution that may leach from the reactor walls.

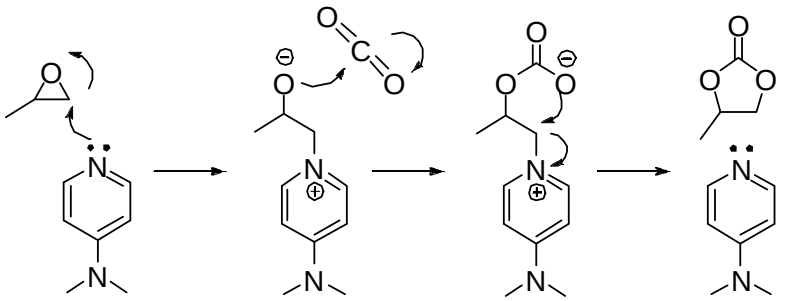

Figure 2.6. Proposed mechanism for cyclic carbonate synthesis using only DMAP as a catalyst.

An alternate mechanism for those reactions not conducted under anhydrous conditions is additionally proposed (Figure 2.7). This mechanism is based on the observations of seeing two products in the reaction of PO and CO_2 conducted in ambient atmosphere with no added catalyst and of seeing no products in the reaction of PO and CO_2 conducted under anhydrous conditions with no added catalyst. In this mechanism, a water molecule attacks the least hindered carbon of the epoxide ring and opens it. Once the epoxide is in the ring opened form, it may undergo proton transfer to yield propylene glycol, or it may undergo carbon dioxide insertion and cyclization to produce propylene carbonate.

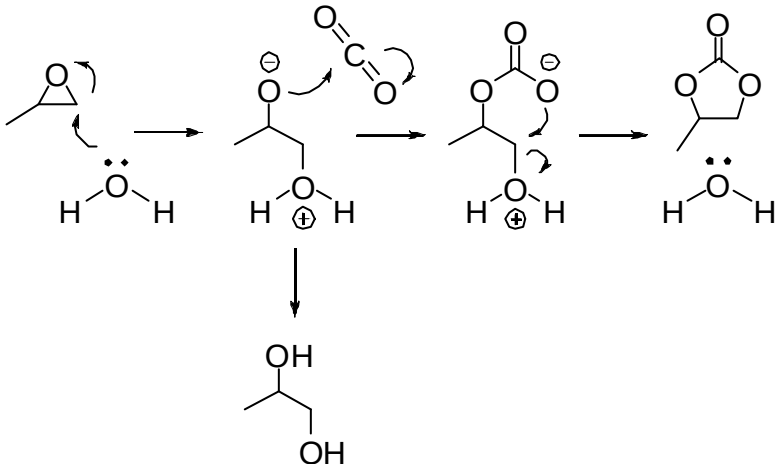

Figure 2.7. Proposed mechanism for cyclic carbonate synthesis with water as a catalyst/reactant.

2.3.2. Characterization of DMAP-SBA (3)

One of the main goals of this study was to develop a well-defined, effective, silica supported catalyst that could be easily separated from the product without the use of distillation. Therefore, after attaining good yields with homogeneous DMAP as the catalyst, the effectiveness of an immobilized DMAP analog supported on mesoporous SBA-15 was tested (Figure 2.3). In order to better understand the properties of the immobilized catalyst **3**, it was extensively characterized to confirm the covalent nature of the immobilization as well as to confirm the nature of the organic functionality on the surface.

The solid state ^{13}C CP-MAS NMR spectrum of **3** exhibited peaks corresponding to those present in the solution ^{13}C NMR spectrum of ligand **2** prior to tethering (Figure 2.8). Also, the solid state ^{29}Si CP-MAS NMR spectrum showed the Q^2, Q^3, and Q^4 silicon resonances between -90 and -110 ppm associated with the silica framework and T^1, T^2,

and T^3 resonances between -40 and -60 ppm corresponding to one, two, and three methoxy groups from the silane reacting with the surface.[49] These results suggest the organic moiety is covalently bound to the silica surface.

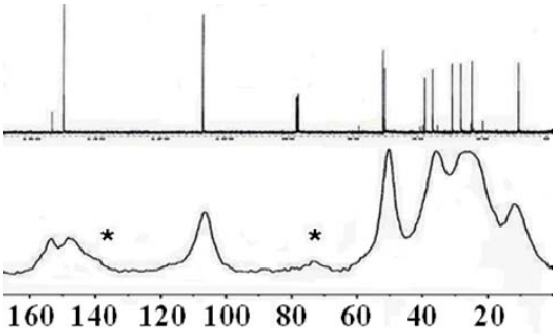

Carbon	δ	Carbon	δ
1	149.8	6	26.4
2	106.4	7	29.1
3	153.3	8	35.2
4	37.5	9	22.9
5,11	50.0, 50.5	10	8.6

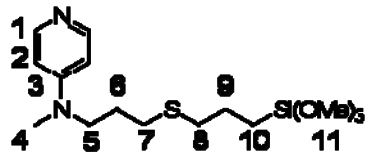

Figure 2.8. Solution ^{13}C NMR of **2** and solid state ^{13}C CP-MAS NMR of **3**.

FT-Raman spectroscopy was also conducted on **3** to further confirm the nature of the organic species on the surface. The spectrum is shown in Figure 2.9 along with the resonances of interest.[50] This analysis further suggests that the DMAP analog has in fact been immobilized onto the SBA-15 support.

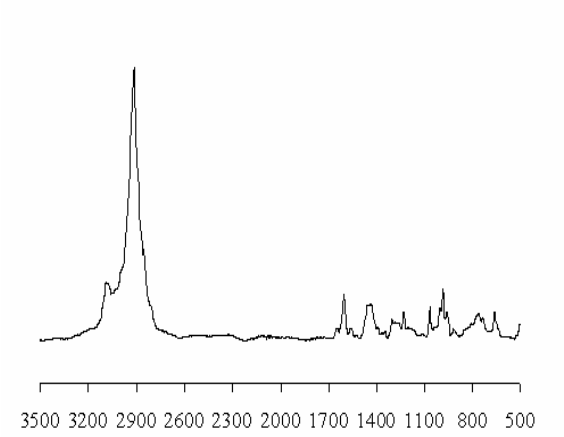

Assignment	cm^{-1}
aromatic C-H (ν_{C-H})	3075
aromatic C=C ($\nu_{C=C}$)	1600
aromatic-N-R_2 (ν_{C-N})	1380
4-monosubstituted pyridine ($\nu_{skeletal}$)	985
aliphatic tether (ν_{CH2} as)	2915
CH_2-S in tether(δ_{CH2-S} and ϖ_{CH2-S})	1440, 1260

Figure 2.9. FT-Raman spectrum of DMAP-SBA with peak assignments.

Thermogravimetric analysis (TGA) was preformed to determine the amount of catalyst loaded onto the silica surface. This measurement indicated a loading of 1.77 mmol catalyst/g SiO_2. This value was used to determine the amount of solid added in the propylene carbonate reactions conducted with the silica immobilized catalyst.

Nitrogen physisorption provided further evidence that the catalyst was in fact immobilized onto the silica support material. Both bare SBA-15 and DMAP-SBA

demonstrate a type IV isotherm with hysteresis. Bare SBA-15 exhibited a BJH average adsorption pore diameter of 67 Å, whereas DMAP-SBA exhibited a BJH average adsorption pore diameter of 41 Å. This suggests that the catalyst is in fact inside the mesopores of the SBA-15. Also, the BET surface area for the silica material decreased from 964 m^2/g before functionalization to 201 m^2/g after functionalization. This can be explained by the fact that organic loading inside the pores blocks access to the micropores that are known to exist in SBA-15, and thus much or all of the microporous surface area is no longer included in the total surface area calculation.[51]

Finally, to ensure that the immobilization procedure did not alter the ordered structure of the SBA-15 support material, X-ray diffraction (XRD) patterns were analyzed for bare SBA-15 and DMAP-SBA (Figure 2.10). In the diffraction pattern for bare SBA-15, three peaks corresponding to the (1 0 0), (1 1 0), and (2 0 0) reflections were seen. These peaks are ascribed to an ordered mesoporous structure with 2-d hexagonal (*p*6*mm*) symmetry.[48] In the diffraction pattern for DMAP-SBA prior to use, the same three peaks are still present. These results indicate that the ordered nature of the SBA-15 support material persists after functionalization with ligand **2**. Additionally, the XRD pattern for DMAP-SBA after reaction indicates that the ordered nature of the support material is maintained during use.

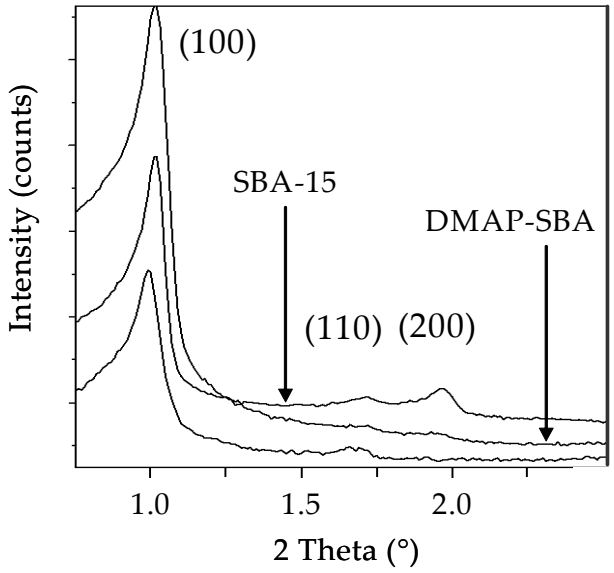

Figure 2.10. XRD patterns for bare SBA-15 (top line on right-hand side) and DMAP-SBA (middle line is prior to reaction, bottom line is after reaction).

2.3.3. Carbonate reactions with the immobilized catalyst (3)

Under the same reaction conditions used with the homogeneous catalyst, the silica immobilized catalyst **3** produced propylene carbonate yields of 81%, which is remarkably close to the homogeneous result (Table 2.1). Also, catalyst **3** could be efficiently separated from the product by simple filtration, leaving behind pure propylene carbonate as the filtrate since excess PO and CO_2 were removed under vacuum prior to filtration as described in Section 2.2.7. When the catalyst was recycled, the propylene carbonate product was again generated, although the yield was decreased relative to the fresh supported catalyst (49% versus 81%). The lower yield on recycle could be due to several factors including pore clogging, degradation of the DMAP functionality, leaching, or others. It should be noted that it was not conclusively determined if traces of the DMAP functionality leached from the surface, although NMR and GC of the propylene

carbonate product did not detect any catalyst species. In addition, FT-Raman and FTIR spectroscopy both confirmed that the DMAP moiety was still present on the surface after its use in reactions.

To provide insight on the effect of the support structure, DMAP-SBA **(3)** was compared with a commercially available DMAP analog supported on poly(styrene). When the polymer catalyst was tested, the activity in the initial run was virtually the same as the silica supported DMAP (Table 2.1). However, when the catalysts were recycled, the DMAP-SBA retained more of its initial activity than did the polymer supported catalyst (49% versus 30%). This suggests that degradation of the catalyst is more severe for the polymer supported catalyst, indicating the high temperatures and pressures used in this reaction may require more stable supports such as inorganic silica materials.

Control experiments were also conducted to confirm that it was the DMAP functionality on the SBA-15 and not some other portion of the immobilized ligand that was performing the catalysis. The reactivities of 3-aminopropyl functionalized SBA-15 and 3-mercaptopropyl functionalized SBA-15, neither with DMAP, were tested, and no conversion of the epoxide was observed.[52-54] Additionally, catalyst **3** was treated with 1,1,1,3,3,3-hexamethyldisilazane (HMDS) to cap the accessible surface silanols and was tested, and the capped material produced the same yield of propylene carbonate as the uncapped material. These results plus the observed productivity of soluble DMAP without the addition of another catalyst suggest that DMAP can behave as a single component catalyst. Thus, although DMAP is not the most productive catalyst available, it is noteworthy that it can behave as a single component catalyst under the conditions reported here in either a homogeneous or heterogeneous state.

2.4. Conclusions

This chapter has provided evidence that homogeneous 4-(N,N-dimethylamino) pyridine, DMAP, can catalyze the reaction of propylene oxide with carbon dioxide giving propylene carbonate yields of 85% without the addition of a co-catalyst under the given reaction conditions. Furthermore, the reaction forms only propylene carbonate when conducted under anhydrous conditions. A new immobilized DMAP analog was synthesized which produced propylene carbonate yields of 81% at the same conditions and could be easily separated from the product by filtration. Additionally, the recycle performance of the silica immobilized catalyst was better than the recycle performance of a poly(styrene) supported DMAP, indicating the inorganic silica support may be more robust toward the high reaction temperatures and pressures. Although most of the literature concerning CO_2 fixation to epoxides to form cyclic carbonates suggests the need for bi-functional catalytic systems, the results presented in this chapter indicate that multiple reaction mechanisms, including those utilizing only one catalytic component, are likely possible depending on the reaction conditions.

2.5. REFERENCES

[1] Tanabe, K., and Holderich, W. F., *Appl. Catal. A* 181 (1999) 399.

[2] Corma, A., and Garcia, H., *Adv. Synth. Catal.* 348 (2006) 1391.

[3] Benaglia, M., Puglisi, A., and Cozzi, F., *Chem. Rev.* 103 (2003) 3401.

[4] Brunel, D., *Micropor. Mesopor. Mater.* 27 (1999) 329.

[5] Darensbourg, D., and Holtcamp, M. W., *Coord. Chem. Rev.* 153 (1996) 155.

[6] Yamaguchi, K., Ebitani, K., Yoshida, T., Yoshida, H., and Kaneda, K., *J. Am. Chem. Soc.* 121 (1999) 4526.

[7] Nomura, R., Ninagawa, A., and Matsuda, H., *J. Org. Chem.* 45 (1980) 3735.

[8] Yoshida, M., and Ihara, M., *Chem. Eur. J.* 10 (2004) 2886.

[9] Srivastava, R., Srinivas, D., and Ratnasamy, P., *J. Catal.* 233 (2005) 1.

[10] Biggadike, K., Angell, R. M., Burgess, C. M., Farrell, R. M., Hancock, A. P., Harker, A. J., Irving, W. R., Ioannou, C., Procopiou, P. A., Shaw, R. E., Solanke, Y. E., Singh, O. M. P., Snowden, M. A., Stubbs, R. J., Walton, S., and Weston, H. E., *J. Med. Chem.* 43 (2000) 19.

[11] Shaikh, A. G., and Sivaram, S., *Chem. Rev.* 96 (1996) 951.

[12] Davis, R. J., *J. Catal.* 216 (2003) 396.

[13] Tu, M., and Davis, R. J., *J. Catal.* 199 (2001) 85.

[14] Doskocil, E. J., Bordawekar, S. B., Kaye, B. G., and Davis, R. J., *J. Phys. Chem. B* 103 (1999) 6277.

[15] Yasuda, H., He, L.-N., Takahashi, T., and Sakakura, T., *Appl. Catal. A* 298 (2006) 177.

[16] Barbarini, A., Maggi, R., Mazzacani, A., Mori, G., Sartori, G., and Sartorio, R., *Tetrahedron Lett.* 44 (2003) 2931.

[17] Srivastava, R., Srinivas, D., and Ratnasamy, P., *Micropor. Mesopor. Mater.* 90 (2006) 314.

[18] Zhang, X., Zhao, N., Wei, W., and Sun, Y., *Catal. Today* 115 (2006) 102.

[19] Shen, Y.-M., Duan, W.-L., and Shi, M., *Eur. J. Org. Chem.* (2004) 3080.

[20] Sankar, M., Tarte, N. H., and Manikandan, P., *Appl. Catal. A* 276 (2004) 217.

[21] Alvaro, M., Baleizao, C., Carbonell, E., Ghoul, M. E., Garcia, H., and Gigante, B., *Tetrahedron* 61 (2005) 12131.

[22] Mori, K., Mitani, Y., Hara, T., Mizugaki, T., Ebitani, K., and Kaneda, K., *Chem. Commun.* 26 (2005) 3331.

[23] Alvaro, M., Baleizao, C., Das, D., Carbonell, E., and Garcia, H., *J. Catal.* 228 (2004) 254.

[24] Ramin, M., Jutz, F., Grunwaldt, J.-D., and Baiker, A., *J. Mol. Catal. A: Chem.* 242 (2005) 32.

[25] Paddock, R., and Nguyen, S.-B. T., *J. Am. Chem. Soc.* 123 (2001) 11498.

[26] Jing, H., Edulji, S. K., Gibbs, J. M., Stern, C. L., Zhou, H., and Nguyen, S.-B. T., *Inorg. Chem.* 43 (2004) 4315.

[27] Eberhardt, R., Allmendinger, M., and Riger, B., *Macromol. Rapid Commun.* 24 (2003) 194.

[28] Shen, Y.-M., Duan, W.-L., and Shi, M., *J. Org. Chem.* 68 (2003) 1559.

[29] Paddock, R., and Nguyen, S.-B. T., *Chem. Commun.* (2004) 1622.

[30] Darensbourg, D. J., Fang, C. C., and Rogers, J. L., *Organometallics* 23 (2004) 924.

[31] Tanaka, H., Kitaichi, Y., Sato, M., Ikeno, T., and Yamada, T., *Chem. Lett.* 33 (2004) 676.

[32] Lu, X.-B., Zhang, Y.-J., Jin, K., Luo, L.-M., and Wang, H., *J. Catal.* 227 (2004) 537.

[33] Lu, X.-B., Feng, X.-J., and He, R., *Appl. Catal. A* 234 (2002) 25.

[34] Lu, X.-B., He, R., and Bai, C.-X., *J. Mol. Catal. A: Chem.* 186 (2002) 1.

[35] Srivastava, R., Bennur, T. H., and Srinivas, D., *J. Mol. Catal. A: Chem.* 226 (2005) 199.

[36] Sit, W. N., Ng, S. M., Kwong, K. Y., and Lau, C. P., *J. Org. Chem.* 70 (2005) 8583.

[37] Nishikubo, T., Kameyama, A., Yamashita, J., Tomoi, M., and Fukuda, W., *J. Polym. Sci. Part A* 31 (1993) 939.

[38] Du, Y., Cai, F., Kong, D.-L., and He, L.-N., *Green Chem.* 7 (2005) 518.

[39] Du, Y., Wang, J.-Q., Chen, J.-Y., Cai, F., Tian, J.-S., Kong, D.-L., and He, L.-N., *Tetrahedron Lett.* 47 (2006) 1271.

[40] Takahashi, T., Watahiki, T., Kitazume, S., Yasuda, H., and Sakakura, T., *Chem. Commun.* (2006) 1664.

[41] Xie, H., Duan, H., Li, S., and Zhang, S., *New J. Chem.* 29 (2005) 1199.

[42] Corma, A., and Garcia, H., *Chem. Rev.* 102 (2002) 3837.

[43] Corma, A., Garcia, H., Moussaif, A., Sabater, M. J., Zniber, R., and Redouane, A., *Chem. Commun.* 10 (2002) 1058.

[44] McMorn, P., and Hutchings, G. J., *Chem. Soc. Rev.* 33 (2004) 108.

[45] Rubinsztajn, S., Zeldin, M., and Fife, W., *Macromolecules* 23 (1990) 4026.

[46] Chen, H.-T., Huh, S., Wiench, J. W., Pruski, M., and Lin, V. S.-Y., *J. Am. Chem. Soc.* 127 (2005) 13305.

[47] Pangborn, A. B., Giardello, M. A., Grubbs, R. H., Rosen, R. K., and Timmers, F. J., *Organometallics* 15 (1996) 1518.

[48] Zhao, D., Huo, Q., Feng, J., Chmelka, B. F., and Stucky, G. D., *J. Am. Chem. Soc.* 120 (1998) 6024.

[49] Sindorf, D. W., and Maciel, G. E., *J. Am. Chem. Soc.* 105 (1983) 3767.

[50] Baranska, Labudzinska, and Terpinski, *Ellis Horwood Series in Analytical Chemistry,Vol. Laser Raman Spectroscopy: Analytical Applications* John Wiley & Sons, New York, (1987).

[51] Miyazawa, K., and Inagaki, S., *Chem. Commun,* (2000) 2121.

[52] Stein, A., Melde, B., and Schroden, R., *Adv. Mater.* 12 (2000) 1403.

[53] Kallury, K. M. R., Macdonald, P. M., and Thompson, M., *Langmuir* 10 (1994) 492.

[54] Kang, T., Park, Y., and Yi, J., *Ind. Eng. Chem. Res.* 43 (2004) 1478.

CHAPTER 3

POLYMER AND SILICA SUPPORTED TRIDENTATE SCHIFF BASE VANADIUM CATALYSTS FOR THE ASYMMETRIC OXIDATION OF ETHYL MANDELATE

3.1. Introduction

The ability to synthesize enantiomerically pure α-hydroxy esters is a significant topic of interest since these compounds are useful building blocks for chiral syntheses in the pharmaceutical and fine chemical industries.[1] A great deal of research has been devoted to discovering catalytic systems that can efficiently generate enantiomerically pure α-hydroxy esters and other secondary alcohols,[2-4] and an important subset of these systems exploit the kinetic resolution of racemic substrates through the appropriate selection of catalyst and reaction conditions.[5-10] One such system that effectively utilizes kinetic resolution to yield enantiomerically pure alcohols from racemic mixtures involves the application of vanadium complexes with Schiff base ligands for selective oxidation with molecular oxygen. Specifically, tridentate Schiff base vanadium catalysts derived from salicylaldehydes and *tert*-leucinol or *tert*-leucine have been shown to promote the oxidative kinetic resolution of racemic α-hydroxy esters by the selective oxidation of only one enantiomer (Figure 3.1).[11-13] This reactions is particularly attractive not only due to the high enantioselectivity it imparts but also due to the use of molecular oxygen at atmospheric pressure as the primary oxidant. Molecular oxygen is highly abundant, low in cost, and non-toxic, which make it more attractive than other oxidants, particularly

inorganic oxidants, which can be expensive and potentially hazardous to dispose of after use.

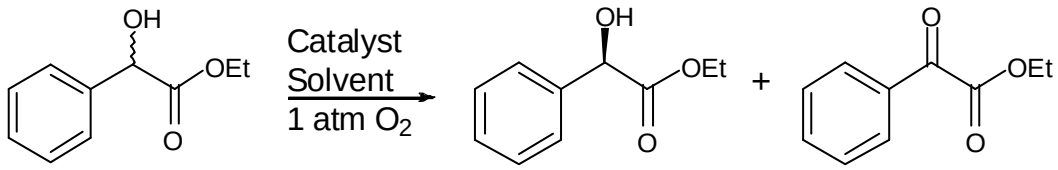

Figure 3.1. Oxidative kinetic resolution of an α-hydroxy ester.

Previous research efforts in our group have investigated the immobilization of enantioselective homogeneous catalysts to improve catalyst performance, with the key parameters by which performance is judged being productivity, selectivity, ease of recovery, and recyclability. This research, up to now, predominantly has focused on the immobilization of cobalt salen catalysts for application in the hydrolytic kinetic resolution (HKR) of epoxides, and a number of successful polymer supported catalysts have resulted from these efforts.[14-16]

Since the tridentate Schiff base vanadium catalysts used in the oxidative kinetic resolution reaction resemble "half" salen functionalities, it was desired to apply the knowledge gained from the immobilization of the cobalt salen HKR catalysts to the development of immobilized vanadium oxidative kinetic resolution catalysts. Even though the activities of homogeneous catalysts are well-established, there are no found reports of analogous immobilized catalysts derived from salicylaldehydes and *tert*-leucinol for the resolution reaction. The development of active and selective immobilized

catalysts for this reaction, therefore, is attractive for a few reasons. First, it provides data as to how immobilization effects the catalytic properties. Also, it creates the opportunity for easier recovery of the metal catalyst from the product, which is important due to economic, environmental, and product quality issues. This chapter describes the immobilization of these vanadium catalysts on both insoluble polymers as well as SBA-15 mesoporous silica, and it demonstrates the new catalysts' utilities in the oxidative kinetic resolution of ethyl mandelate.

3.2. Experimental

3.2.1. Materials

3,5-Di-*tert*-butyl-2-hydroxybenzaldehyde (Aldrich), (S)-*tert*-leucinol (Aldrich), 3-isocyanatopropyltrimethoxysilane (Gelest), anhydrous methanol (EMD Chemicals), and vanadium(V) oxytriisopropoxide ($VO(OiPr)_3$) (Aldrich) were used as received. 2,2'-Azo-bis(isobutyronitrile) (AIBN) (Aldrich) was dried under vacuum and stored in a nitrogen dry box. Styrene was distilled and stored in a nitrogen dry box. Dichloromethane and acetonitrile were dried over calcium hydride and distilled; chlorobenzene was dried with 4 Å molecular sieves and distilled under vacuum; acetone was dried over anhydrous calcium sulfate and distilled. Toluene and THF were used after purification and drying via a packed bed solvent system made of dual alumina columns.[17]

3.2.2. Characterization methods

Solution ^{1}H and ^{13}C NMR spectroscopy was conducted on a Varian Mercury Vx 400 spectrometer. FT-IR spectroscopy was conducted on a Bruker Equinox 55 using disks made from solid catalyst samples dispersed in potassium bromide (KBr). The

samples were analyzed using 1024 scans with a resolution of 4 cm^{-1}. Nitrogen physisorption measurements were taken on a Micromeritics ASAP 2010 at 77 K. Prior to analysis, SBA-15 was degassed with heating at 150 °C under vacuum overnight, and the functionalized SBA-15 sample was degassed with heating at 50 °C under vacuum overnight. Gas chromatography was used to monitor the reaction progress and was conducted on a Shimadzu GC 17-A equipped with a flame-ionization detector and a Chiraldex γ-TA column (length = 40 m, inner diameter = 0.25 mm, and film thickness = 0.25 μm). The following temperature profile was used: heat to 90 °C, ramp to 140 °C at a rate of 6 °C per minute, and hold for 11 minutes.

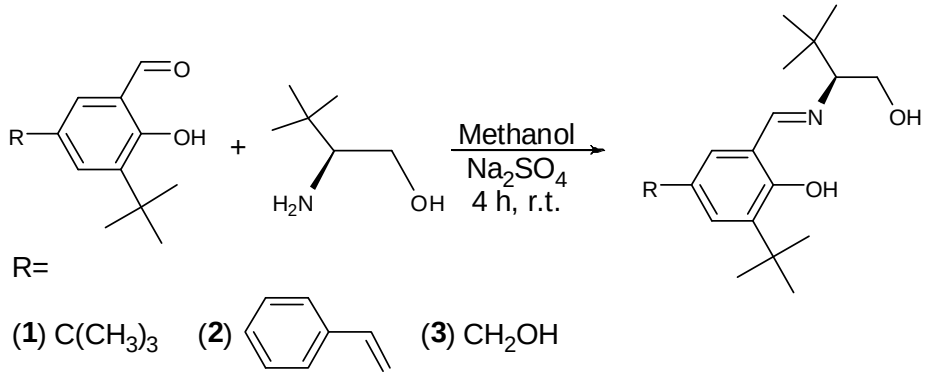

Figure 3.2. Synthesis procedure for catalyst ligands.

3.2.3. Synthesis of homogeneous Schiff base ligand (1)

The homogeneous Schiff base ligand (**1**) was synthesized according to literature procedures (Figure 3.2).[11,18] 3,5-Di-*tert*-butyl-2-hydroxybenzaldehyde (4 g, 17 mmol) was dissolved in anhydrous methanol. Then, sodium sulfate (12.2 g) and (S)-*tert*-leucinol

(2 g, 17 mmol) were added, and the mixture was stirred at room temperature for 4 h. The solution was filtered through Celite, the solvent was removed, and the product was dried under vacuum. The synthesis produced a yellow solid which was used without further purification.

1: Yield 98 %. ^{1}H NMR (400 MHz, $CDCl_3$): δ 0.96 (s, 9H), δ 1.30 (s, 9H), δ 1.44 (s, 9H), δ 2.91 (dd, J = 9.48 and 2.72 Hz, 1H), δ 3.73 (m, 1H), δ 3.90 (m, 1H), δ 7.13 (d, J = 2.36 Hz, 1H), δ 7.39 (d, J = 2.32 Hz, 1H), δ 8.35 (s, 1H), δ 13.60 (s, 1H). ^{13}C NMR (101 MHz, $CDCl_3$): δ 27.4, 29.7, 31.7, 33.5, 34.4, 35.3, 62.8, 81.7, 117.9, 126.4, 127.4, 137.0, 140.4, 158.4, 167.4. Elemental analysis calcd. (%) for $C_{21}H_{35}NO_2$: C 75.63, H 10.58, N 4.20, Found: C 75.39, H 10.64, N 4.24. Accurate mass calcd., 333.2668; found, 333.2656.

3.2.4. Synthesis of styryl functionalized Schiff base monomer (2)

The styryl functionalized Schiff base monomer was prepared similarly to the homogeneous ligand **1** (Figure 3.2). 3-*tert*-Butyl-2-hydroxy-5-(4'-vinylphenyl) benzaldehyde was synthesized according to published literature procedures.[14,19] This styryl aldehyde (1.5 g, 5.35 mmol) was dissolved in anhydrous methanol. Then, sodium sulfate (4 g) and (S)-*tert*-leucinol (0.627g, 5.35 mmol) were added, and the mixture was stirred at room temperature for 4 h. The solution was filtered through Celite, the solvent was removed, and the product was dried under vacuum. The synthesis produced a yellow solid which was used without further purification.

2: Yield 98%. ^{1}H NMR (400 MHz, $CDCl_3$): δ 0.98 (s, 9H), δ 1.48 (s, 9H), δ 2.95 (dd, J = 9.44 and 2.60 Hz, 1H), δ 3.76 (m, 1H), δ 3.96 (m, 1H), δ 5.25 (d, J = 10.88 Hz, 1H), δ 5.77 (d, J = 17.60 Hz, 1H), δ 6.74 (dd, J = 17.60 and 10.88 Hz, 1H), δ 7.37 (d, J = 2.12

Hz, 1H), δ 7.48 (m, 4H), δ 7.58 (d, J = 2.12 Hz, 1H), δ 8.42 (s, 1H), δ 13.94 (s, 1H). ^{13}C NMR (101MHz, $CDCl_3$): δ 27.4, 29.6, 33.5, 35.3, 62.8, 81.6, 113.8, 118.8, 126.90, 126.95, 128.4, 128.7, 130.8, 136.2, 136.7, 138.1, 140.7, 160.4, 167.0. Elemental analysis calcd. (%) for $C_{25}H_{33}NO_2$: C 79.11, H 8.76, N 3.69, Found: C 79.12, H 8.42, N 3.63. Accurate mass calcd., 379.2511; found, 379.2505.

3.2.5. Synthesis of Schiff base homopolymer ligand (2a)

The styryl functionalized Schiff base monomer (**2)** was polymerized to form the homopolymer ligand (**2a)** (Figure 3.3). In a typical preparation, monomer (0.25 g, 0.66 mmol) was added to a 15 ml pressure tube reaction vessel in a nitrogen dry box. Then, approximately 3 ml of dry, degassed chlorobenzene was added along with AIBN (11 mg, 0.067 mmol). The pressure tube was sealed and placed in an 80 °C oil bath and was allowed to stir for 48 h. The reaction mixture was then cooled to room temperature and precipitated into cold hexanes. The precipitated polymer was filtered from the solution, washed with hexanes, and dried under vacuum to give a yellow solid.

2a: Yield 76%. Mn: 5,330. PDI: 2.16.

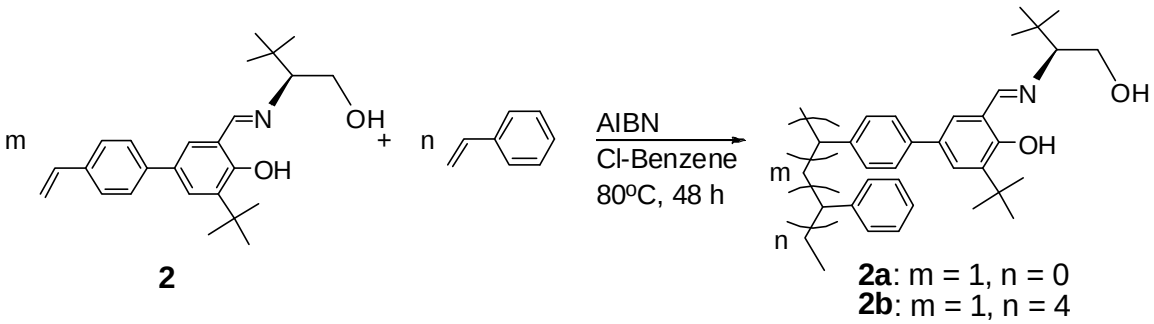

Figure 3.3. Synthesis of polymeric ligands.

3.2.6. Synthesis of Schiff base copolymer ligand (2b)

The styryl functionalized Schiff base monomer (**2**) was copolymerized with styrene to form the copolymer ligand (**2b)** (Figure 3.3). In a typical preparation, one equivalent of styryl Schiff base monomer (152 mg, 0.4 mmol) and four equivalents of styrene (167 mg, 1.6 mmol) were added to a 15 ml pressure tube reaction vessel in a nitrogen dry box. Then, approximately 3 ml of dry, degassed chlorobenzene was added along with AIBN (8.2 mg, 0.05 mmol). The pressure tube was sealed and placed in an 80°C oil bath and was allowed to stir for 48 h. The reaction mixture was then cooled to room temperature and precipitated into cold hexanes. The precipitated polymer was filtered from the solution, washed with hexanes, and dried under vacuum to give a yellow solid.

2b: Yield 63%. Mn: 8,439. PDI: 2.01.

3.2.7. Synthesis of hydroxyl functionalized ligand (3)

3-*tert*-Butyl-5-chloromethyl-2-hydroxybenzaldehyde was synthesized according to published literature procedures.[20] This compound was then converted to 3-*tert*-butyl-2-hydroxy-5-(hydroxymethyl)benzaldehyde.[21] The 5-hydroxymethyl aldehyde (2.08 g, 10 mmol) was dissolved in anhydrous methanol. Then, sodium sulfate (6 g) and (S)-*tert*-leucinol (1.17 g, 10 mmol) were added, and the mixture was stirred at room temperature for 4 h (Figure 3.2). The solution was filtered through Celite, the solvent was removed, and the product was dried. The product was purified via column chromatography (1:1 hexanes: ethyl acetate) and then recrystallized from methanol to produce a pure, pale yellow solid.

3: Yield 79%. ^{1}H NMR (400 MHz, $CDCl_3$): δ 0.96 (s, 9H), δ 1.42 (s, 9H), δ 1.55 (s, 2H), δ 2.92 (dd, J = 9.48 and 2.76 Hz, 1H), δ 3.75 (m, 1H), δ 3.92 (m, 1H), δ 4.60 (d, J = 2.72 Hz, 2H), δ 7.16 (d, J = 1.84 Hz, 1H), δ 7.31 (d, J = 1.92 Hz, 1H), δ 8.34 (s, 1H), δ 13.85 (s, 1H). ^{13}C NMR (101 MHz, $CDCl_3$): δ 27.3, 29.6, 33.5, 35.1, 62.7, 65.6, 81.6, 118.5, 129.1, 129.3, 130.3, 138.0, 160.4, 166.8. Elemental analysis calcd. (%) for $C_{18}H_{29}NO_3$: C 70.32, H 9.51, N 4.56, Found: C 70.26, H 9.59, N 4.51. Accurate mass calcd., 307.2147; found, 307.2116.

3.2.8. Synthesis of SBA-15 supported catalyst (3a)

The SBA-15 silica support material was synthesized and calcined according to literature procedures, dried under vacuum at 200 °C for 3 hours, and stored in a nitrogen dry box prior to use.[22,23] The hydroxyl functionalized ligand (**3)** (0.25 g, 0.81 mmol) was first reacted with $VO(OiPr)_3$ (188 mg, 0.77 mmol) by stirring the compounds in dry acetone under an oxygen blanket for 30 minutes. The acetone was removed under vacuum, and the metal complex was re-dissolved in dried tetrahydrofuran. Then, 3-isocyanatopropyltrimethoxysilane (183 mg, 0.89 mmol) was added to the THF solution in a nitrogen dry box along with triethylamine (90 mg, 0.89 mmol), and the solution was stirred at reflux conditions overnight (Figure 3.4).[24,25] The solvent was again removed, and the compound was dried under vacuum. The silane functionalized catalyst was dissolved in a small amount of toluene and added to a solution of calcined SBA-15 (0.45 g) in toluene in a nitrogen dry box. This slurry was stirred at reflux conditions overnight. The functionalized silica catalyst was filtered in the dry box and washed with copious amounts of toluene, hexanes, and acetone until each solvent ran clear. Catalyst **3a** was dried overnight under vacuum to give a light brown/maroon powder. The procedure

yielded approximately 0.4 g of compound **3a**. Elemental analysis indicated a vanadium loading on the silica of 2 wt%.

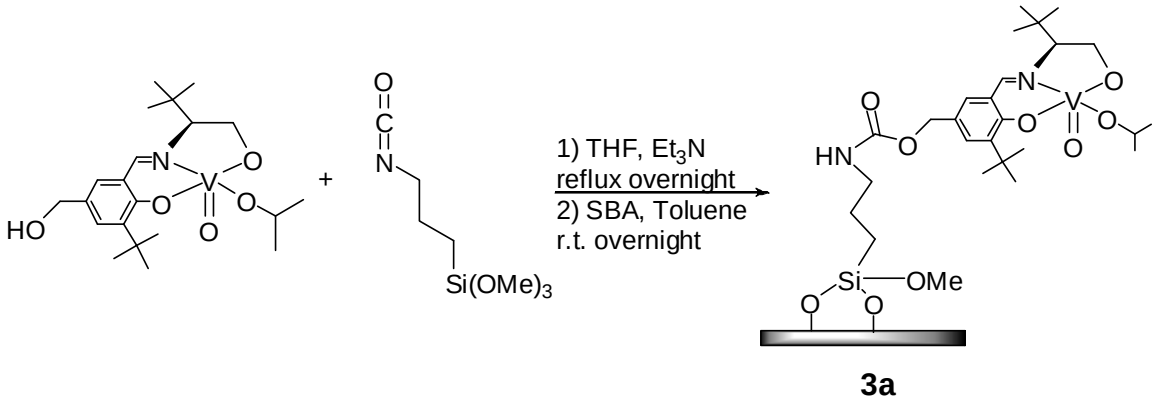

Figure 3.4. Synthesis of silica supported vanadium Schiff base catalyst **3a**.

3.2.9. Catalytic reactions with *in situ* metalation (Method 1)

Oxidative kinetic resolution reactions were preformed via two methods. In the first method, the ligand was metalated *in situ* just prior to the reaction. The selected ligand (**1**, **2a**, or **2b**) (0.0825 mmol, 5.5 mol %) was added to the reaction flask, followed by 3.5 ml of solvent. Once the ligand was completely dissolved, $VO(OiPr)_3$ (17.5 μl, 0.075 mmol, 5 mol %) was added to the flask. The mixture was allowed to stir under an oxygen blanket for 15 minutes. At the completion of this time, a solution of ethyl mandelate (270.3 mg, 1.5 mmol) and hexamethylbenzene (12.5 mg as an internal standard) in 4 ml of solvent was added to the reaction flask, and 100 μl samples were

taken periodically to monitor the extent of the reaction. An oxygen blanket was maintained in the flask throughout the course of the reaction.

3.2.10. Catalytic reactions with pre-metalated ligands (Method 2)

In the second method, the selected ligand was metalated and isolated prior to reaction. For the polymer catalysts (**2a** and **2b**), the polymerized ligand first was dissolved in dry acetone. $VO(OiPr)_3$ (0.9 equivalents) was added, and the solution was stirred under an oxygen blanket for 1 ½ h. During this time, the metalated catalyst precipitated from the solution for both the homopolymer and the copolymer. Then, stirring was ceased, the solid catalyst was allowed to settle, and the liquid layer was decanted. Fresh dry acetone was added, and the catalyst was stirred for 20 minutes. Again, the catalyst was allowed to settle, and the liquid layer was decanted. This wash procedure was repeated two additional times. The metalated polymers were then dried under vacuum overnight. Silica catalyst **3a** was always tested with Method 2 and was never metalated after the ligand was anchored to the silica surface.

For the oxidative kinetic resolution, the selected metalated catalyst (**2a**, **2b**, or **3a**) was added to the reaction flask at a 5 mol% vanadium loading (determined from elemental analysis) with 3.5 ml of solvent, and it was allowed to stir under an oxygen blanket for 15 minutes. At the completion of this time, a solution of ethyl mandelate (270.3 mg, 1.5 mmol) and hexamethylbenzene (12.5 mg as an internal standard) in 4 ml of solvent was added to the reaction flask, and 100 μl samples were taken periodically to monitor the extent of the reaction. An oxygen blanket was maintained in the flask throughout the course of the reaction.

3.3. Results and discussion

3.3.1. Oxidative kinetic resolution using the homogeneous catalyst

In order to provide a benchmark for the heterogeneous catalysts, experiments with both the homogeneous catalyst and unligated $VO(OiPr)_3$ were conducted to determine their reactivities in the oxidation of ethyl mandelate. The reactivity of the homogeneous catalyst was tested in dry acetone, dry acetonitrile, and dry methylene chloride in the manner described in Section 3.2.9. The results showed acetone to be the best solvent for the reaction, providing > 99% conversion of S-ethyl mandelate and 99% enantiomeric excess (ee) of R-ethyl mandelate in less than 4 h (Figure 3.5) (total conversion S + R: 54%). Acetonitrile was also a suitable solvent, providing > 99% conversion of S-ethyl mandelate and 99% ee of R-ethyl mandelate in 5 hours (total conversion S + R: 50%). However, the resolution reaction was significantly slower in methylene chloride, reaching only 85% conversion of S-ethyl mandelate and 79% ee of R-ethyl mandelate after 7 h. This trend is similar to that reported by Radosevich, although the reaction times found in this work are different than those for their system.[11]

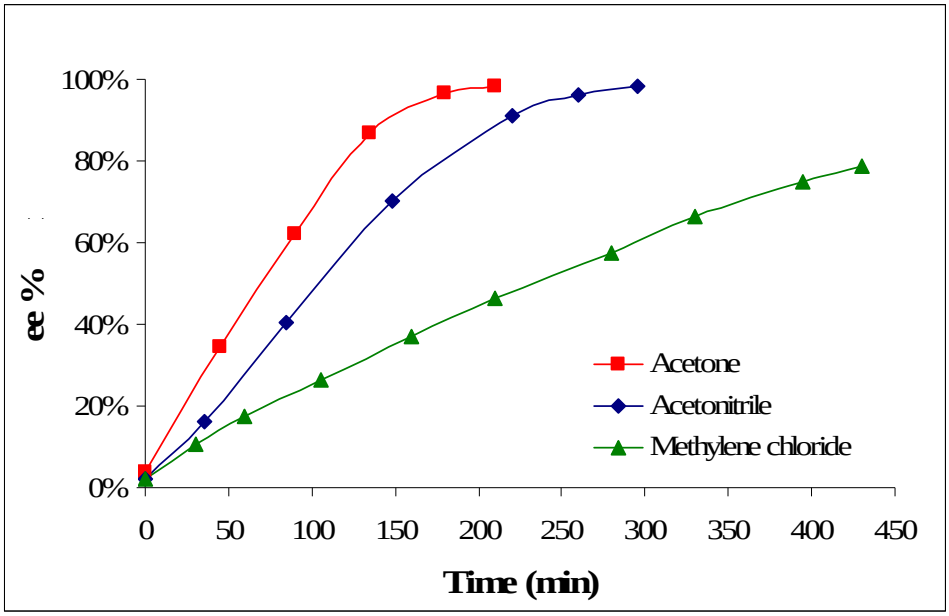

Figure 3.5. Enantiomeric excess of R-ethyl mandelate vs. time for homogeneous catalyst **1** in various solvents.

Since the homogeneous catalyst is metalated *in situ* prior to reaction, the catalytic activity of $VO(OiPr)_3$ alone was probed to determine if this compound plays a part in the oxidation of ethyl mandelate if it is not fully ligated by the Schiff base ligand. Test reactions were conducted in both dry acetone and dry acetonitrile and were allowed to run for 23 h. At the end of this period, the reaction in acetone yielded a total ethyl mandelate conversion of only 7% with no increase in ee. The reaction in acetonitrile gave a total ethyl mandelate conversion of 5% with no increase in ee. These results suggest that any catalytic contribution from free $VO(OiPr)_3$ in solution can be neglected relative to the contribution from the metalated ligand.

3.3.2. Polymer catalyst syntheses and characterization (2a, 2b)

With the homogeneous benchmark established, polymer immobilized catalysts derived from salicylaldehydes and *tert*-leucinol were synthesized and investigated. Generally, researchers employ one of two strategies when creating immobilized polymer catalysts. The first strategy involves grafting the desired catalyst functionality onto an insoluble polymeric support such as a resin. This is an efficient way to create a heterogeneous catalyst, but if the procedure is performed in a step-wise manner or if the surface reaction is not quantitative, multiple types of species can exist on the resin surface. In order to circumvent this issue, the second strategy for immobilization is the direct polymerization of monomers containing the desired catalyst functionality. Since previous research in our group utilized the second method to synthesize polymeric salen catalysts for the hydrolytic kinetic resolution of epoxides with great success, this approach was taken in this work as well.[14-16]

By employing the synthesis described in Section 3.2.4, a monomer bearing both the desired ligand functionality and a styryl group capable of being polymerized was created (**2**). Corresponding polymers were then easily prepared by the AIBN initiated free-radical homopolymerization of the styryl monomer (**2a**) or copolymerization of the styryl monomer with styrene (**2b**). ^{1}H NMR spectroscopy of the polymers exhibited the typical broadening features that are expected for macromolecules (Figure 3.6). Also, the peaks associated with the vinyl protons in the monomer spectrum (δ 5.0-6.0) were absent in the polymer spectra, which indicated that residual monomer was removed during the isolation of the polymers. Using gel-permeation chromatography (GPC) in THF with poly(styrene) standards, the number average molecular weight (Mn) of the homopolymer

was determined to be 5,330 with a polydispersity index (PDI) of 2.16. This corresponds to an average of 14 repeat units in the polymer chain. The Mn of the copolymer was determined to be 8,439 with a PDI of 2.01. This corresponds to an average of 11 repeat units in the polymer chain with a 2:5 ligand to styrene ratio (determined from ^{1}H NMR). These data are summarized in Table 3.1.

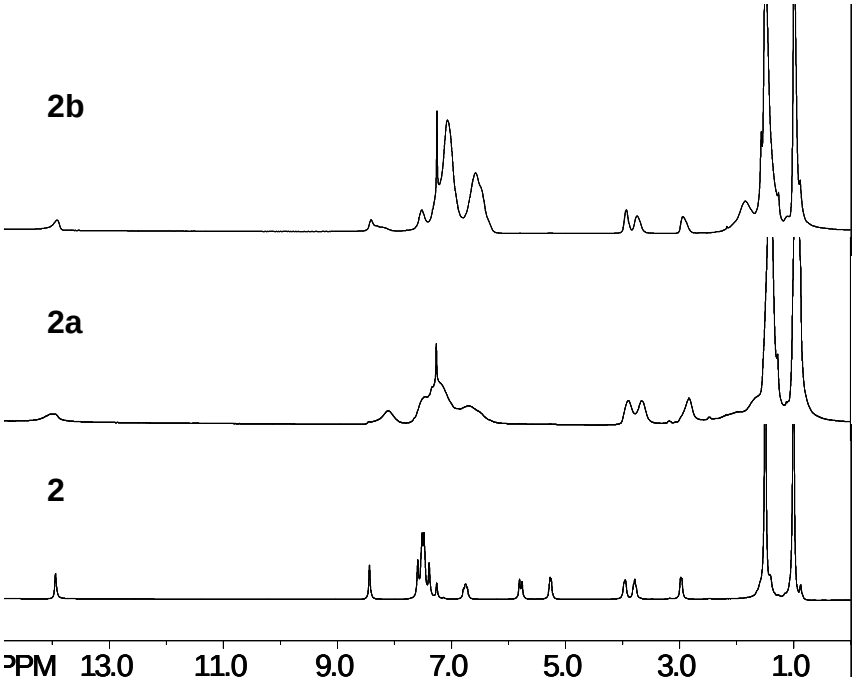

Figure 3.6. ^{1}H NMR spectra of the styryl functionalized monomer **2**, homopolymer **2a**, and copolymer **2b**.

Table 3.1. Polymeric ligand characterization.

Polymer	AIBN loading (mol%)	Mn[a]	PDI[a]	m,n actual[b]
2a	10 %	5,330	2.16	14, 0
2b	2.5 %	8,439	2.01	11, 28

a: From GPC in THF with poly(styrene) standards; b: Calculated from Mn and ^{1}H NMR.

In order to establish the heterogeneous nature of these catalysts, the solubilities of the homopolymer and copolymer were tested. The homopolymer ligand was soluble in acetone, ethanol, methylene chloride and THF, and the copolymer ligand was soluble in acetone and THF. However, both the homopolymer and the copolymer were insoluble in a range of solvents including acetone, acetonitrile, hexanes, THF, methylene chloride, ethanol, and water after metalation with $VO(OiPr)_3$.

The vanadium content of the metalated polymers was determined by elemental analysis. In the case of homopolymer **2a**, the vanadium loading was 10.3 wt% (2.02 mmol/g), which corresponds to roughly 87% of the Schiff base ligands being metalated. For copolymer **2b**, the vanadium loading was 6.0 wt% (1.18 mmol/g), which corresponds to roughly 83% of the Schiff base ligands being metalated.

Lastly, the metalated polymers were characterized by Fourier transform infrared spectroscopy (FT-IR) (Figure 3.7). The spectra for homopolymer **2a** and copolymer **2b** closely resemble one another, and both exhibit the expected peaks that indicate the presence of the immobilized catalyst functionality (Table 3.2). Particularly noteworthy is the strong C=N stretch located at 1617 cm^{-1} which is indicative of the coordination of the imine nitrogen with the vanadium. This stretch would be expected to appear around 1630 cm^{-1} for the uncoordinated ligand.[26] Also, the V=O stretch is seen at 986 cm^{-1} in the homopolymer and 984 cm^{-1} in the copolymer, and these values are in line with literature reports as well.[13,26-28]

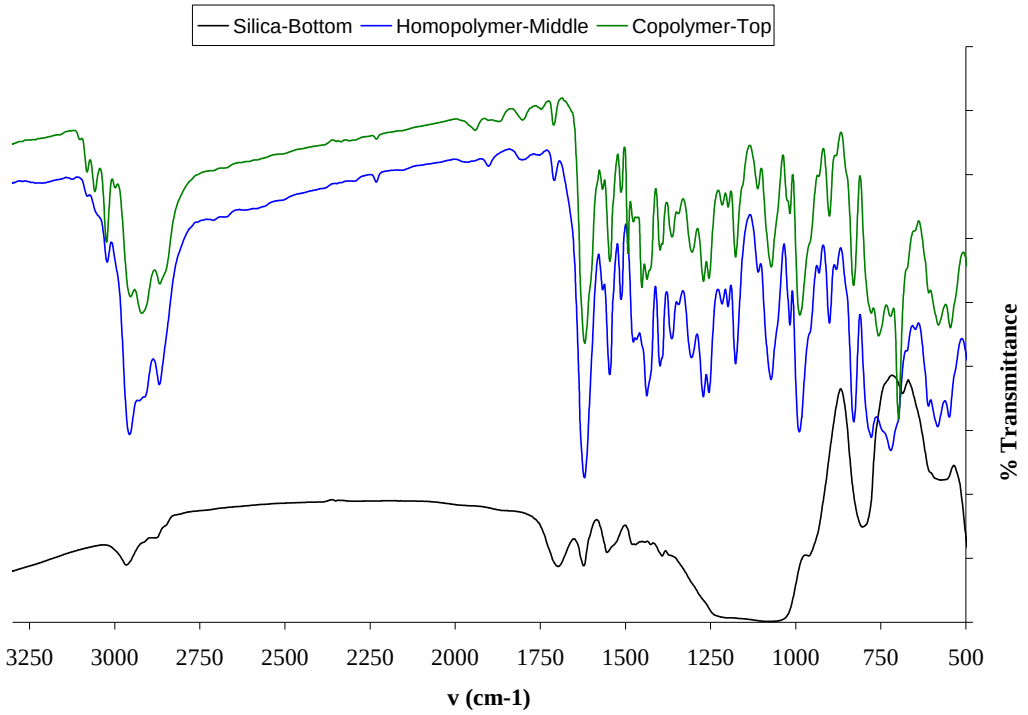

Figure 3.7. FT-IR spectra of copolymer catalyst **2b** (top), homopolymer catalyst **2a** (middle), and silica catalyst **3a** (bottom).

Table 3.2. FT-IR data (KBr disk) for metalated polymeric catalysts **2a** and **2b.**

	ν cm^{-1} Homopolymer **2a**	ν cm^{-1} Copolymer **2b**
C-H aromatic and aliphatic stretches	3020, 2953, 2908, 2867	3055, 3021, 2948, 2908, 2862
C=N	1617	1617
V=O	986	984

3.3.3. Oxidative kinetic resolution using polymeric catalysts (2a, 2b)

Since acetone was the most effective solvent for the oxidative kinetic resolution of ethyl mandelate with the homogeneous catalyst, all reactions using the polymeric catalysts were conducted in acetone. As stated in the experimental section, two catalyst preparation methods were used to investigate the activity of the polymer catalysts: *in situ* metalation (Method 1) and metalation and isolation prior to reaction (Method 2).

First, homopolymer catalyst **2a** was assessed using Method 1. Although the metalated polymer becomes insoluble once it precipitates, it should be noted that when the polymeric ligand was metalated *in situ*, the catalyst was initially soluble in the reaction solvent for a short period of time (less than one hour). Once the reaction commenced, the resolution of ethyl mandelate proceeded to 99% conversion of S-ethyl mandelate and 99% ee of R-ethyl mandelate in approximately 11 h (total conversion S + R: 57%) (Figure 3.8). To determine if the catalyst was still active, an additional portion of unresolved ethyl mandelate was added to the solution the following day. The reaction then proceeded to 89% conversion of S-ethyl mandelate and 86% ee R-ethyl mandelate after 10 h, compared with the initial resolution values of 95% conversion of S-ethyl mandelate and 90% ee of R-ethyl mandelate at 10 h, or approximately 94% of the initial efficiency. This may be explained by the fact that the partially soluble nature of the catalyst in the early stages of the initial run slightly increases the rate for that reaction. However, when the second portion of reactant is added, the catalyst is insoluble from time zero.

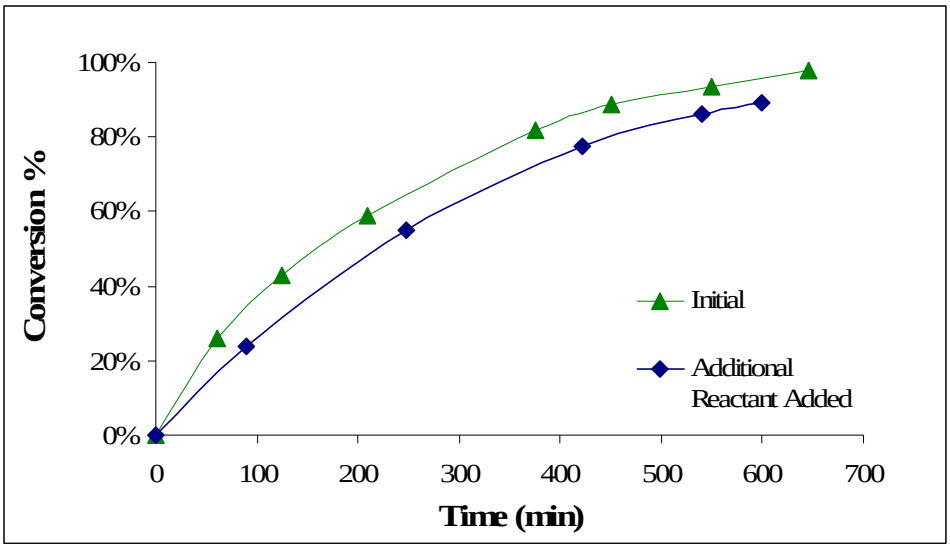

Figure 3.8 Conversion of S-ethyl mandelate vs. time for homopolymer catalyst **2a** with *in situ* metalation (Method 1).

The activity of homopolymer catalyst **2a** was also assessed using Method 2. Significant differences in reaction rates were observed between the two catalyst preparation methods (Figure 3.9). The homopolymer catalyst that was metalated and isolated prior to use (Method 2) was significantly less active than the homopolymer catalyst that was metalated *in situ* (Method 1). For instance, after 9 h of reaction, the Method 1 reaction had proceeded to 94% conversion of S-ethyl mandelate and 88% ee of R-ethyl mandelate, whereas the Method 2 reaction had only reached 61% conversion of S-ethyl mandelate and 42% ee of R-ethyl mandelate. This behavior is attributed to the semi-soluble nature of the *in situ* metalated catalyst in the early stages of the reaction. The continued activity of pre-metalated catalyst **2a** was not tested since the initial activity was so low.

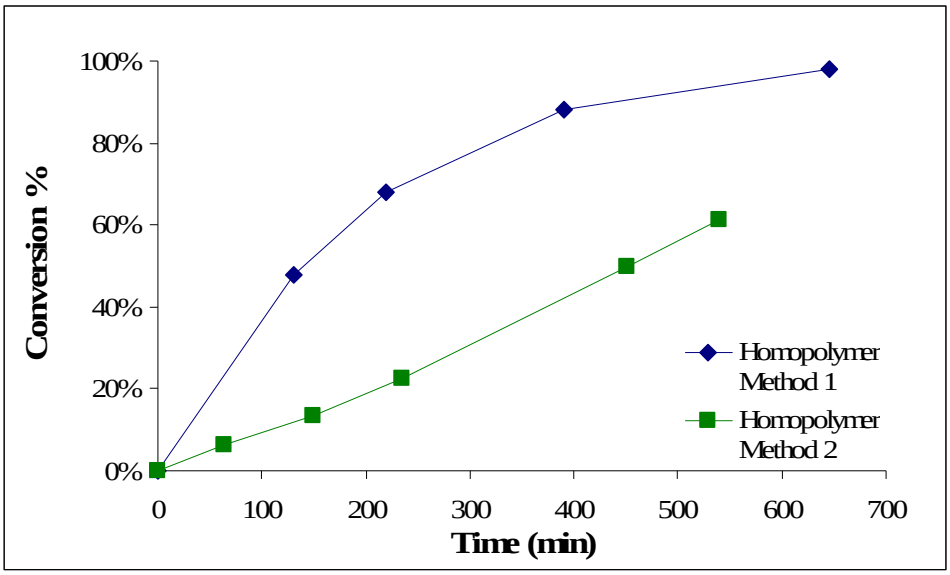

Figure 3.9. Conversion of S-ethyl mandelate vs. time for homopolymer catalyst **2a** with *in situ* metalation (Method 1) and metalation and isolation (Method 2).

Copolymer catalyst **2b** was also studied in the oxidative kinetic resolution of ethyl mandelate. Method 1 (*in situ* metalation) was examined first. In this case, it was observed that the metalated polymer precipitated out of the solution during the initial oxygen pre-treatment prior to reaction, unlike homopolymer catalyst **2a** which remained soluble for a short period of time. Copolymer catalyst **2b** successfully completed the resolution reaction, taking 9 ½ h to reach 99% conversion of S-ethyl mandelate with 98% ee of R-ethyl mandelate (total conversion S + R: 58%) (Figure 3.10). To determine if the catalyst was still active, another portion of unresolved ethyl mandelate was added to the reaction flask the following day. This reaction reached 99% conversion of S-ethyl mandelate in 10 ½ h with an ee of R-ethyl mandelate of 95%, indicating that the catalyst remained active after the initial reaction, although a slightly longer reaction time was required.

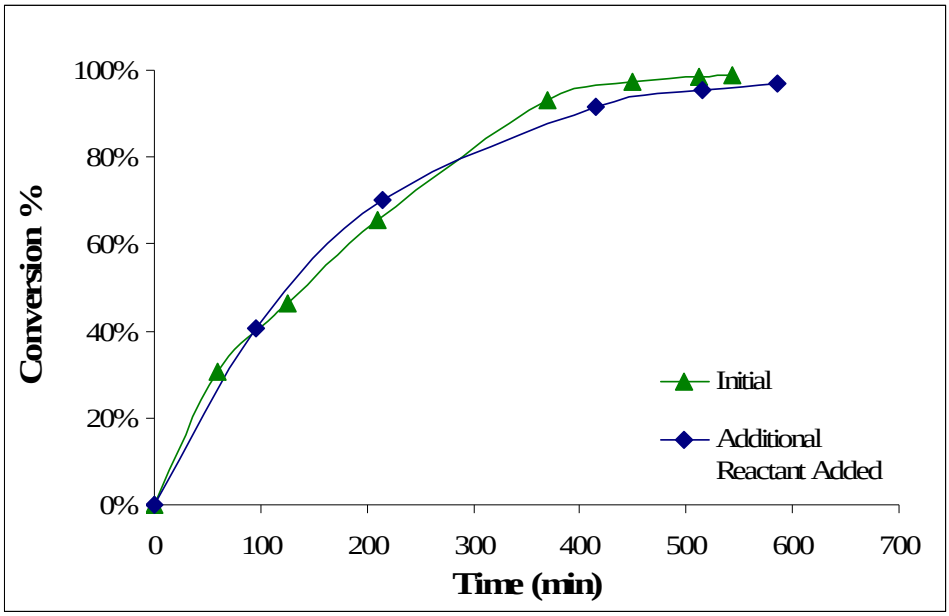

Figure 3.10. Conversion of S-ethyl mandelate vs. time for copolymer catalyst **2b** with *in situ* metalation (Method 1).

When Method 2 (metalation and isolation) was used with copolymer catalyst **2b**, the catalyst was able to reach 99% conversion of S-ethyl mandelate and 97% ee of R-ethyl mandelate in 8 h (total conversion S + R: 61%). This result is slightly faster than the result obtained using Method 1 (*in situ* metalation) for the copolymer catalyst (Figure 3.11). To test the continued activity of the catalyst, an additional portion of unresolved ethyl mandelate was added to the reaction flask, and the conversion of the S enantiomer was monitored (Figure 3.12). In the same 8 h reaction time, the conversion of the S enantiomer had reached 95% with an ee of R-ethyl mandelate of 94%, roughly 96% of the original efficiency.

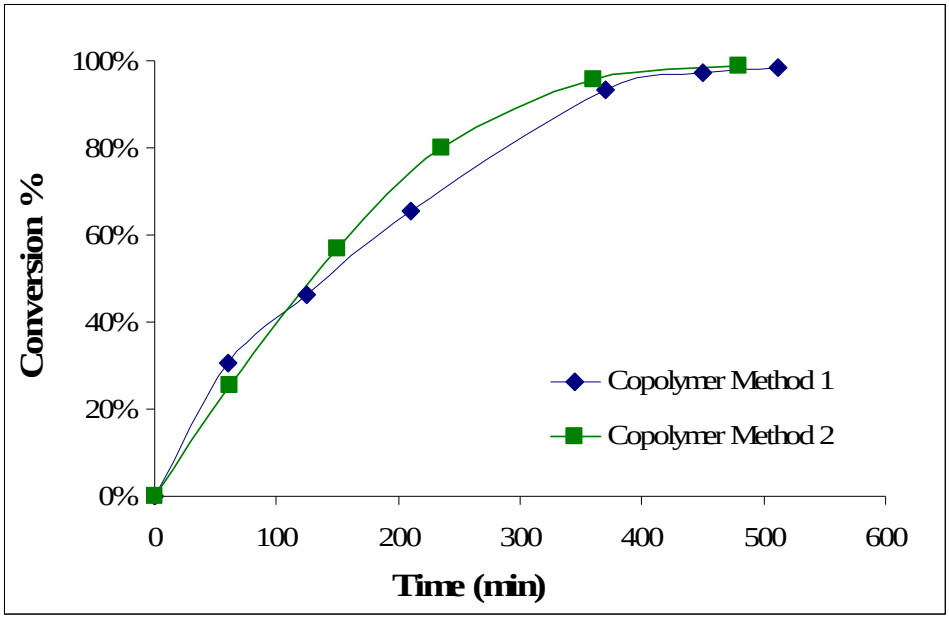

Figure 3.11. Conversion of S-ethyl mandelate vs. time for copolymer catalyst **2b** with *in situ* metalation (Method 1) and metalation and isolation (Method 2).

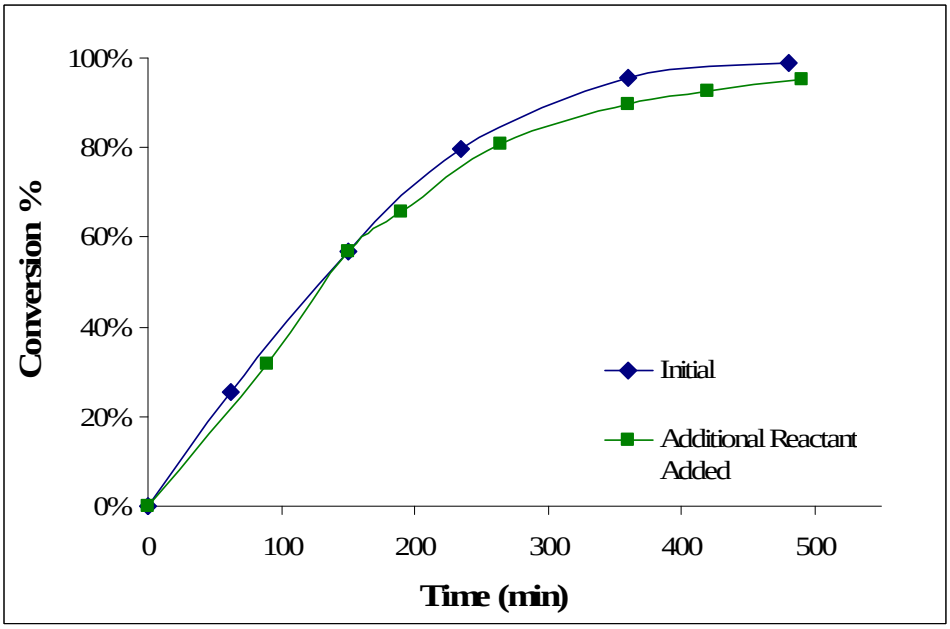

Figure 3.12. Conversion of S-ethyl mandelate vs. time for copolymer catalyst **2b** with metalation and isolation of catalyst prior to reaction (Method 2).

Comparing homopolymer **2a** and copolymer **2b** metalated by Method 1, it is observed that the copolymer is able to completely oxidize S-ethyl mandelate more rapidly than the homopolymer (9 h vs. 11 h), even though the homopolymer remains partially soluble during the early stages of the reaction (Figure 3.13). The copolymer is also much more efficient when metalation Method 2 is used (8 h vs. >15 h) (Figure 3.14). This may be due to the separation between the active sites in the copolymer which aids in the reactant's ability to access the active site or which prevents interactions between active vanadium sites. In summary, the results presented here indicate that the styrene copolymer **2b** is a more active catalyst for the oxidative kinetic resolution of ethyl mandelate than the catalyst homopolymer **2a**, and it shows a slightly shorter reaction time when metalated by Method 2 as compared with Method 1.

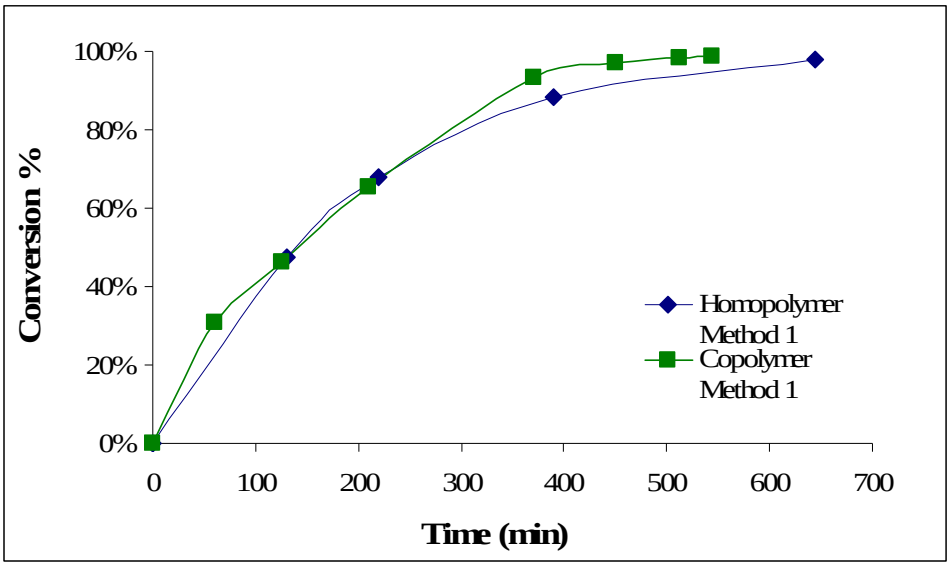

Figure 3.13. Conversion of S-ethyl mandelate vs. time for polymer catalysts **2a** and **2b** with *in situ* metalation (Method 1).

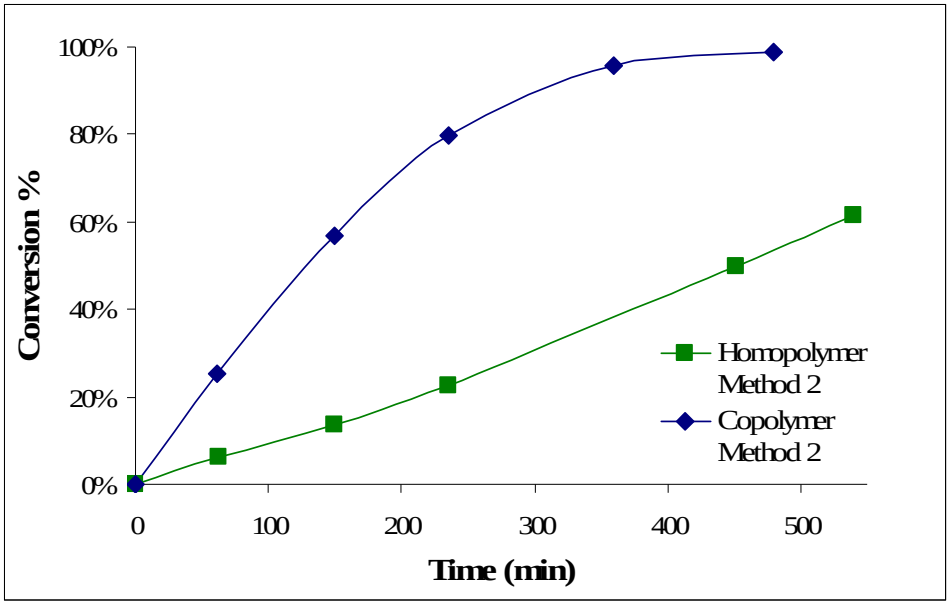

Figure 3.14. Conversion of S-ethyl mandelate vs. time for polymer catalysts **2a** and **2b** with metalation and isolation prior to reaction (Method 2).

3.3.4. Silica catalyst synthesis and characterization (3a)

A trialkoxysilane functionalized catalyst analog was synthesized as described in Sections 3.2.7 and 3.2.8 (Figure 3.4). This analog was then grafted onto SBA-15 silica, and supported catalyst **3a** was characterized. FT-IR spectroscopy was used to determine the nature of the organic species on the silica surface (Figure 3.7). The spectrum shows the anticipated peaks which indicate that the catalyst functionality is grafted to the silica surface (Table 3.3). Of particular interest are the C=N stretch at 1617 cm^{-1}, indicating the vanadium is coordinated with the imine nitrogen, and the V=O stretch at 955 cm^{-1}. These values are in line with those reported for similar materials.[26] These results suggest the desired catalytic functionality is on the silica surface.

Table 3.3. FT-IR data (KBr disk) for silica supported catalyst **3a.**

	ν cm^{-1}
C-H aromatic and aliphatic stretches	2956, 2871, 2845
C=N	1617
Si-O-Si	1060 (broad)
V=O	986

Nitrogen physisorption provided additional evidence that the catalyst was immobilized onto the silica. The SBA-15 prior to functionalization as well as after functionalization exhibits a type IV isotherm with hysteresis, which is indicative of its mesoporous nature. The bare SBA-15 had a BJH average adsorption pore diameter of 65 Å, whereas the vanadium functionalized material had a BJH average adsorption pore diameter of 62 Å. Also, the BET surface area for the SBA-15 material decreased from 858 m^2/g before functionalization to 325 m^2/g after functionalization. This is typical of what is observed when grafted organometallic or organic species block access to the micropores that are known to exist in SBA-15, and thus much or all of the microporous surface area is no longer included in the total surface area calculation.[23,29-31]

3.3.5. Oxidative kinetic resolution using the silica catalyst (3a)

Once characterized, silica catalyst **3a** was tested for the oxidative kinetic resolution of ethyl mandelate in both dry acetone and dry acetonitrile (Figure 3.15). For the reaction in acetone, the resolution was complete in 11 h, reaching 99% conversion of S-ethyl mandelate and 98% ee of R-ethyl mandelate (total conversion S + R: 49%). The reaction in acetonitrile proceeded at roughly the same rate, also taking 11 h to complete

the resolution. These results are similar to those found for homopolymer catalyst **2a** metalated *in situ* in an acetone solution, but slower than the results for copolymer **2b**.

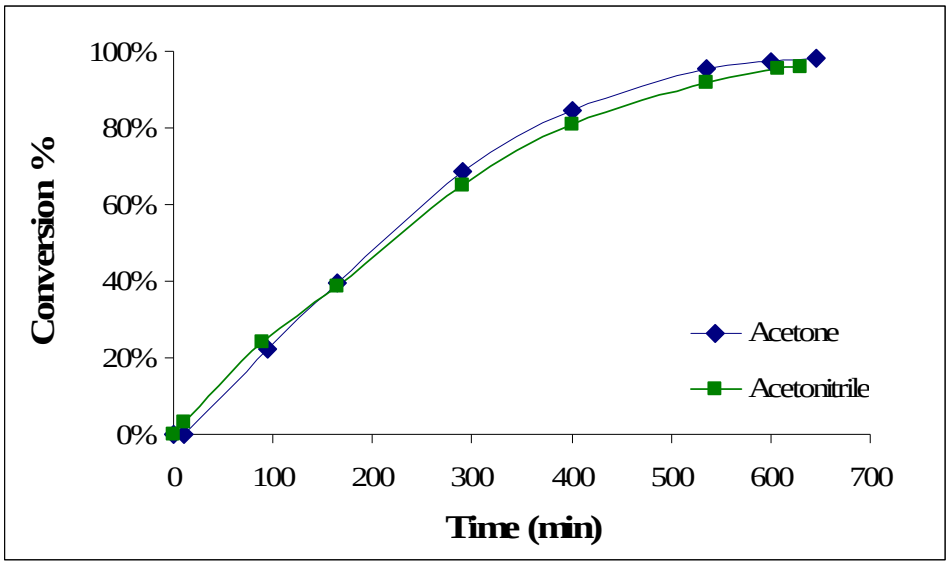

Figure 3.15. Conversion of S-ethyl mandelate vs. time for silica catalyst **3a** in acetone and acetonitrile.

In the initial synthesis procedure for the silica grafted catalyst, the metalated hydroxyl functionalized catalyst was stirred overnight in chloroform with 3-isocyanatopropyltrimethoxysilane to form a carbamate. The silane functionalized catalyst was subsequently reacted with the silica surface as in step 2 of Figure 3.4. When the resulting silica catalyst was tested for the resolution of ethyl mandelate in acetonitrile, the reaction rate was much faster than that reported above for catalyst **3a** (7 ½ h vs. 11 h). The same trend was seen when the reaction was performed in acetone. However, the extremely poor recycle performance of these materials (~25 % of the efficiency of the

fresh catalyst) led to the conclusion that the carbamate was not completely formed prior to adding the catalyst analog to the surface, which caused significant catalyst leaching from the surface. This conclusion was supported by experiments conducted with benzyl alcohol and the same silane. The addition of base and the use of reflux conditions were required to effectively form the carbamate. Therefore, the synthesis procedure was modified to incorporate these findings.

Silica catalyst **3a** was tested for its recycle performance in both acetone and acetonitrile, and it exhibited approximately 60-65% of the reactivity of the fresh catalyst. This result is significantly better than that obtained with the original silica materials. However, additional improvements would be required to make recyclability of this catalyst viable.

3.4. Conclusions

This chapter has presented the development of three new heterogeneous tridentate Schiff base vanadium catalysts for the oxidative kinetic resolution of ethyl mandelate. The ligands and metalated catalysts were characterized by a number of quantitative and qualitative techniques to ensure that the desired species were immobilized. Polymer and silica supported catalysts were created so that the effect of the support structure on the catalytic behavior could be determined. In this reaction, the copolymer supported catalyst proved to have the highest activity, perhaps due to its ability to isolate catalytic sites from one another.

The effect of reaction solvent was also investigated. It was found that the polar, aprotic solvents acetone and acetonitrile favored the reaction more so than

dichloromethane. This was the case for both the homogeneous catalyst and the silica supported catalyst.

Finally, the effect of the metalation protocol for the polymer catalysts was studied, and noticeable differences were observed. The copolymer catalyst was the most active regardless of whether it was metalated *in situ* or isolated prior to reaction, but the pre-metalation procedure increased its rate a small amount. The pre-metalated homopolymer catalyst, however, was the least active catalyst, taking significantly longer to complete the resolution than when the catalyst was metalated *in situ*. Overall, these results provide a nice basis from which to design the next generation of even more active catalysts for the oxidative kinetic resolution reaction.

3.5. REFERENCES

[1] Coppola, G. M., and Schuster, H. F., *α-Hydroxy Acids in Enantioselective Synthesis* VCH, Weinheim, Germany, (1997).

[2] Arterburn, J. B., *Tetrahedron* 52 (2001) 9765.

[3] Schultz, M. J., and Sigman, M. S., *Tetrahedron* 52 (2006) 8227.

[4] Irie, R., and Katsuki, T., *Chem. Rev.* 4 (2004) 96.

[5] Robinson, D. E. J. E., and Bull, S. D., *Tetrahedron: Asymmetry* 13 (2003) 1407.

[6] Sun, W., Wang, H., Xia, C., Li, J., and Zhao, P., *Angew. Chem., Int. Ed.* 42 (2003) 1042.

[7] Nishibayashi, Y., Yanauchi, A., Onodera, G., and Uemura, S., *J. Org. Chem.* 68 (2003) 5875.

[8] Jensen, D. R., Pugsley, J. S., and Sigman, M. S., *J. Am. Chem. Soc.* 123 (2001) 7475.

[9] Ferreira, E. M., and Stoltz, B. M., *J. Am. Chem. Soc.* 123 (2001) 7725.

[10] Sun, W., Wu, X., and Xia, C., *Helv. Chim. Acta* 90 (2007) 623.

[11] Radosevich, A. T., Musich, C., and Toste, F. D., *J. Am. Chem. Soc.* 127 (2005) 1090.

[12] Weng, S.-S., Shen, M.-W., Kao, J.-Q., Munot, Y. S., and Chen, C.-T., *PNAS* 103 (2006) 3522.

[13] Chen, C.-T., Bettigeri, S., Weng, S.-S., Pawar, V. D., Lin, Y.-H., Liu, C.-Y., and Lee, W.-Z., *J. Org. Chem.* 72 (2007) 8175.

[14] Zheng, X., Jones, C. W., and Weck, M., *Chem. Eur. J.* 12 (2006) 576.

[15] Zheng, X., Jones, C. W., and Weck, M., *J. Am. Chem. Soc.* 129 (2007) 1105.

[16] Zheng, X., Jones, C. W., and Weck, M., *Adv. Synth. Catal.* 350 (2008) 255.

[17] Pangborn, A. B., Giardello, M. A., Grubbs, R. H., Rosen, R. K., and Timmers, F. J., *Organometallics* 15 (1996) 1518.

[18] Liu, G., Cogan, D. A., and Ellman, J. A., *J. Am. Chem. Soc.* 119 (1997) 9913.

[19] Sellner, H., Karjalainen, J. K., and Seebach, D., *Chem. Eur. J.* 7 (2001) 2873.

[20] Canali, L., Cowan, E., Deleuze, H., Gibson, C. L., and Sherrington, D. C., *J. Chem. Soc., Perkin Trans. I* (2000) 2055.

[21] Holbach, M., Zheng, X., Burd, C., Jones, C. W., and Weck, M., *J. Org. Chem.* 71 (2006) 2903.

[22] Zhao, D., Huo, Q., Feng, J., Chmelka, B. F., and Stucky, G. D., *J. Am. Chem. Soc.* 120 (1998) 6024.

[23] Shiels, R. A., and Jones, C. W., *J. Mol. Catal. A: Chem.* 261 (2007) 160.

[24] Bellec, N., Lerouge, F., Jeannin, O., Cerveau, G., Corriu, R. J. P., and Lorcy, D., *J. Organomet. Chem.* 691 (2006) 5774.

[25] Chen, L., Cui, Y., Qian, G., and Wang, M., *Dyes and Pigments* 73 (2007) 338.

[26] Maurya, M. R., Kumar, U., Correia, I., Adao, P., and Pessoa, J. C., *Eur. J. Inorg. Chem.* (2008) 577.

[27] Clark, R. J. H., *The Chemistry of Titanium and Vanadium* Elsevier Publishing Company, Amsterdam, (1968).

[28] Hartung, J., Drees, S., Greb, M., Schmidt, P., Svoboda, I., Fuess, H., Murso, A., and Stalke, D., *Eur. J. Org. Chem.* 2003 (2003) 2388.

[29] Hicks, J. C., and Jones, C. W., *Langmuir* 22 (2006) 2676.

[30] Richardson, J. M., and Jones, C. W., *J. Catal.* 251 (2007) 80.

[31] Miyazawa, K., and Inagaki, S., *Chem. Commun*, (2000) 2121.

CHAPTER 4

METAL SALEN CATALYSTS SUPPORTED ON AMINOSILICAS

4.1. Introduction

As previously stated, silica materials are often selected as supports for immobilized catalysts due to their tunable pore sizes and surface areas, their thermal stability, and the ease with which the surfaces can be functionalized. One of the most studied functionalities that has been immobilized on silica surfaces is the amine group. Amine functionalized silica materials, or aminosilicas, can be used directly for many applications including adsorption,[1-3] separation,[4] and catalysis.[5] However, they can also be used as support structures on which to graft more complex molecules.[6-15]

Aminosilicas are most often synthesized by either co-condensation of an aminoalkoxysilane with a silica source to form the functionalized silica material,[16] or they are synthesized by grafting an aminoalkoxysilane onto an already synthesized solid silica surface.[17] This work utilizes only the second method, whereby the aminoalkoxysilane is grafted on the silica material after its synthesis and characterization. Traditionally, 3-(aminopropyl)trimethoxysilane is the most common aminoalkoxysilane used, and it is grafted to the surface by stirring the silane together with the silica material in a toluene solution at either room temperature or under reflux conditions (Figure 4.1).

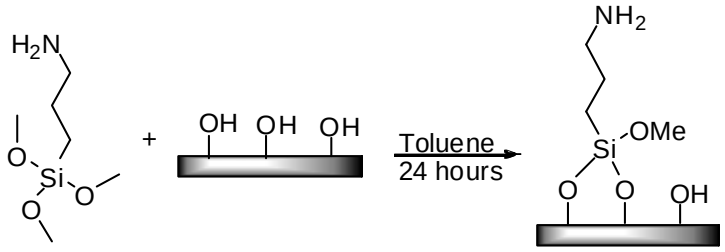

Figure 4.1. Traditional synthesis of amine functionalized silica material.

Previous research in our group has demonstrated that the traditional aminosilica synthesis leads to multiple types of amine environments on the surface.[6,18,19] Some amines may hydrogen bond with the surface, other amines may hydrogen bond with one another, and some amines may be isolated (Figure 4.2). The isolated amine groups are preferred as support structures, as they are the most accessible and the most reactive toward further modification. To prevent the formation of the hydrogen bonded amine groups on the surface, two techniques were developed to protect the amine groups during grafting and to isolate them on the silica surface.[6,18] The first technique uses a trityl aldehyde as a protecting group for the aminoalkoxysilane during grafting, and the second technique uses a benzyl aldehyde as a protecting group for the aminoalkoxysilane during grafting (Figure 4.3). Once the protected amines are grafted, the surface silanol functionalities are capped, and the protecting groups are cleaved to leave spaced, isolated amine groups. The degree of spacing is dependent on the size of the protecting group that was used in the synthesis.[19]

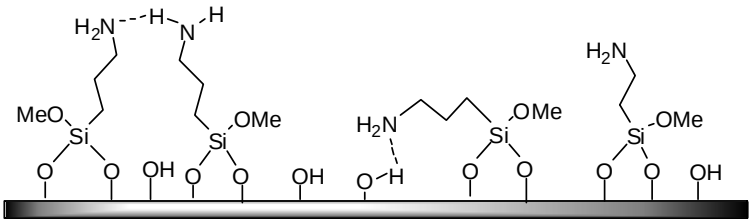

Figure 4.2. Multiple types of amine environments on traditionally grafted aminosilicas.

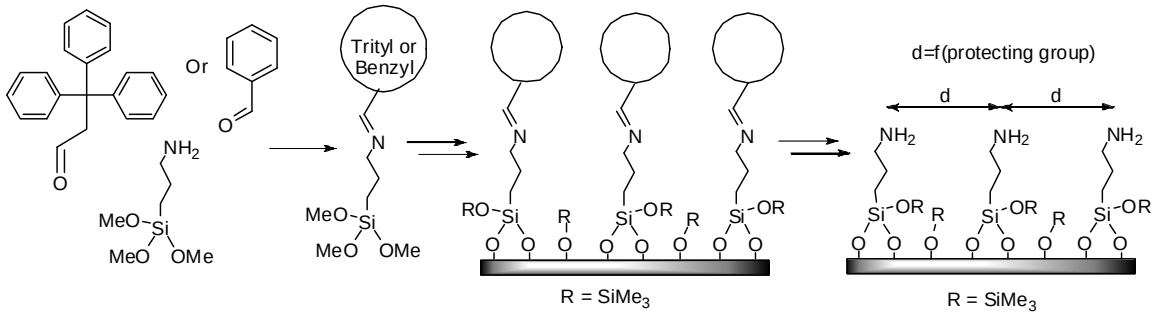

Figure 4.3. Synthesis of trityl de-protected and benzyl de-protected aminosilica materials to generate spaced, isolated amine groups.

One of the overarching goals of this dissertation is to examine how immobilization onto a solid support effects a catalyst's activity and selectivity, and so an important parameter to probe is the support scaffold onto which the catalyst is grafted. Since these aminosilica materials possess reactive functional groups with different degrees of isolation, or different surface environments, they seemed ideal for further examination in the study of immobilized metal salen catalysts to see how the starting scaffold might impact the catalytic properties. As previously mentioned, salen catalysts are widely studied because they find application in many different reactions including

alkene epoxidation, hydrolytic kinetic resolution of epoxides, addition of carbon dioxide to epoxides, cyanide addition to α,β-unsaturated imides, Hetero-Diels-Alder reactions, and many more.[20] Different metals are used in the salen ligand to modulate the reactivity toward the most active catalyst for the desired reaction. Because of the number of possible catalytic reactions and the variety of salen catalysts of interest, gaining insight into the effects of the support material could potentially find wide applicability in catalyst design.

Although salen catalysts promote these many reactions, the reaction mechanisms are not the same in all cases. It has been shown that some of the reactions proceed through the catalytic cycle utilizing only one metal center,[21,22] whereas other reactions require the presence of two metal salens to complete the catalytic cycle.[23,24] Therefore, it would be particularly desirable to use the isolated aminosilica materials mentioned above as well as traditionally grafted aminosilicas as supports for well-defined salen catalyst analogs because it might provide insight into what support will work best for a specific reaction mechanism. For instance, a reaction involving only one active site in the catalytic cycle might show decreased activity due to limiting reactant accessibility or one site deactivating another site if the catalytic sites can interact with one another. Likewise, if two catalytic sites are required and the sites on the surface are not close enough together, the reactivity would be decreased. Therefore, grafting the salen catalyst on the more isolated or spaced aminosilicas (trityl de-protected and benzyl de-protected) might allow catalytic sites to be isolated from one another thereby increasing reactivity for single-site reactions. Similarly, grafting the salen catalyst on the traditional or closely packed aminosilicas might allow the catalytic sites to come into close proximity to one

another more frequently thereby increasing reactivity for dual-site reactions. Finally, the aminosilica immobilized catalysts could provide an analytical tool to help elucidate the nature of a single-site vs. a dual-site cycle for a reaction of unknown mechanism. If the reactivity of the catalyst grafted to all three aminosilica materials was determined, a spacing-dependent trend could provide evidence for the nature of the cycle.

In order to utilize the aminosilica materials, a modified salen ligand with a functional group reactive toward surface amine groups is required. There have been previous reports in the literature of salen ligand analogs which can react with surface amine groups. The three main approaches that have been used are step-wise grafting using an aldehyde/amine coupling, or Schiff base reaction (Figure 4.4),[9-12] one-pot or single step grafting using a chloromethyl/amine coupling (Figure 4.5),[13-15,25] and grafting using a protected carboxylic acid/amine coupling (Figure 4.6).[26]

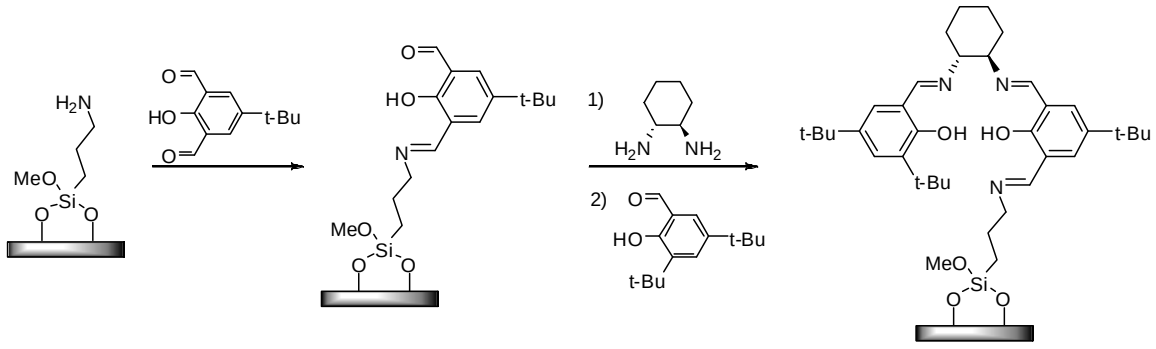

Figure 4.4. Step-wise grafting of a salen catalyst to an aminosilica surface using an aldehyde/amine or Schiff base reaction.

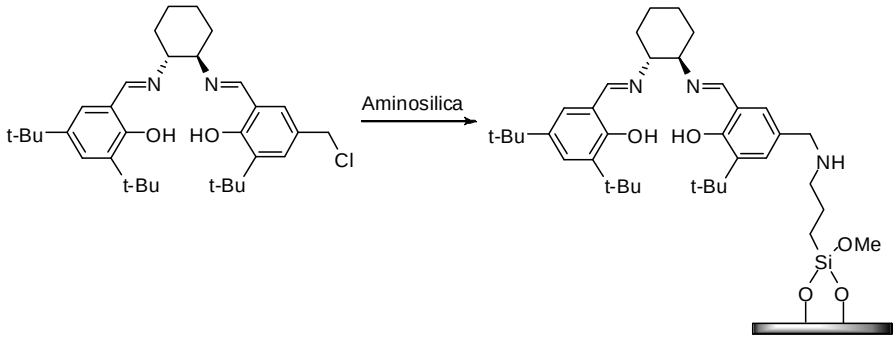

Figure 4.5. Grafting of a salen catalyst to an aminosilica surface using a chloromethyl/amine reaction.

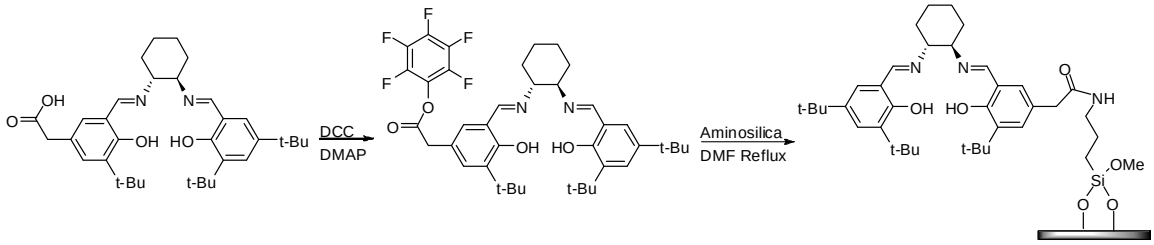

Figure 4.6. Grafting of a salen catalyst to an aminosilica surface using a protected carboxylic acid/amine reaction.

This chapter will outline my work toward grafting salen catalysts to traditional and spaced aminosilicas. The three approaches shown in Figures 4.4, 4.5, and 4.6 will be used as starting points, but they will be modified so as to create more well-defined surfaces. The grafted catalysts will then be probed for catalytic activity.

4.2. Experimental

4.2.1. Materials

3,5-di-*tert*-Butyl-2-hydroxybenzaldehyde (Aldrich), triethylamine (Alfa Aesar), 4-*tert*-butyl-2,6-diformylphenol (Aldrich), Florisil 60-100 mesh particle size (Aldrich), anhydrous ethanol, anhydrous methanol, and anhydrous diethyl ether were used as received. (1R,2R)-(-)-1,2-Diaminocyclohexane (Aldrich) was used as received and stored in a nitrogen dry box. Aminosilica materials were prepared on SBA-15 according to previously published procedures.[6,18,27] Anhydrous methylene chloride was further dried via a packed bed solvent system by passing the solvent through dual alumina columns.[28]

4.2.2. Characterization methods

Solution ^{1}H and ^{13}C NMR were conducted on a Varian Mercury Vx 400 spectrometer. Elemental analysis was performed by Desert Analytics, Tucson, AZ. FT-Raman spectra were collected on a Bruker FRA-106. Three thousand scans were collected with a resolution of 2-4 cm^{-1}. Thermogravimetric analyses (TGA) were performed on a Netzsch STA409. Samples, under an air blanket, were heated from 30 °C to 900 °C at a rate of 10 °C/min. The organic loading was determined from the weight loss between 200 °C and 700 °C. Gas chromatography for monitoring the hydrolytic kinetic resolution of epichlorohydrin was conducted on a Shimadzu GC 17-A equipped with a flame-ionization detector and a Chiraldex γ-TA column (length = 40 m, inner diameter = 0.25 mm, and film thickness = 0.25 μm). The temperature profile was as follows: heat to 65 °C, wait 15 minutes, ramp to 170 °C at a rate of 10 °C/min, and hold for 4.5 minutes.

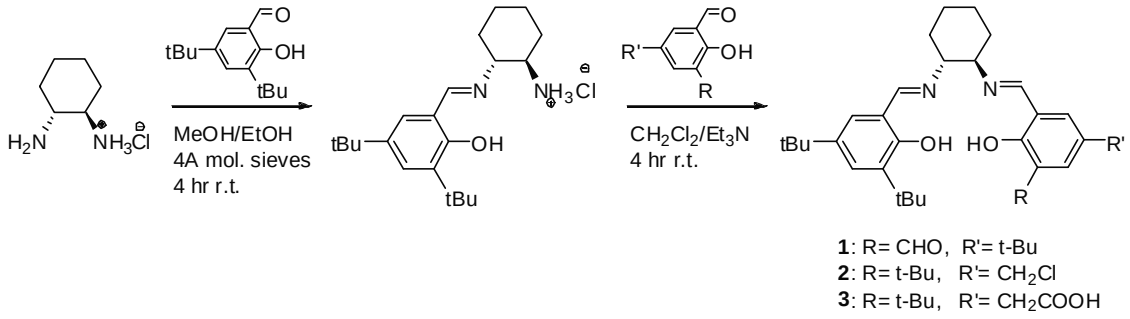

Figure 4.7. Synthesis of unsymmetrical functionalized salen ligands **1, 2**, and **3**.

4.2.3. Synthesis of aldehyde functionalized salen ligand (1)

Compound **1** was synthesized similarly to other reported literature procedures for unsymmetrical salen analogs (Figure 4.7).[29,30] A solution of (1R,2R)-1,2-diaminocyclohexane monohydrochloride salt (0.75 g, 5 mmol) and activated 4Å molecular sieves (2 g) was prepared in anhydrous ethanol (20 ml) and anhydrous methanol (20 ml). 3,5-di-*tert*-Butyl-2-hydroxybenzaldehyde (1.17 g, 5 mmol) was then added, and the solution was stirred at room temperature for 4 hours. At the end of this time period, a solution of 4-*tert*-butyl-2,6-diformylphenol (1.03 g, 5 mmol) in anhydrous methylene chloride (40 ml) was added to the reaction mixture. Triethylamine (1.4 ml, 10 mmol) was then slowly added to the solution, and the mixture was stirred for an additional 4 hours. The solution was filtered to remove the sieves, and then the solvents were removed. The residue was re-dissolved in methylene chloride (50 ml) and was washed with aqueous hydrochloric acid (1M, 25 ml) and deionized water (2 x 25 ml). The organic phase was then dried with magnesium sulfate. Flash chromatography of the

crude product over Florisil with ethyl acetate/hexanes (first 1:15 then followed by 1:10) gave compound **1** as a yellow solid.

1: Yield 44 %. ^{1}H NMR (400 MHz, $CDCl_3$): δ 1.24 (s, 9H), δ 1.24 (s, 9H), δ 1.41 (s, 9H), δ 1.45-1.53 (m, 2H), δ 1.66-1.82 (m, 2H), δ 1.84-2.04 (m, 4H), δ 3.26-3.44 (m, 2H), δ 7.00 (d, J = 2.20 Hz, 1H), δ 7.32 (d, J = 2.16 Hz, 1H), δ 7.38 (d, J = 2.44 Hz, 1H), δ 7.84 (d, J = 2.44 Hz, 1H), δ 8.29 (s, 1H), δ 8.35 (s, 1H), δ 10.48 (s, 1H), δ 13.60 (s, 1H), δ 14.41 (s, 1H). ^{13}C NMR (101 MHz, $CDCl_3$): δ 24.5, 24.6, 29.7, 31.4, 31.7, 33.1, 33.7, 34.3, 34.4, 35.3, 72.4, 72.7, 117.8, 119.4, 123.7, 126.1, 127.1, 128.5, 135.0, 136.5, 140.2, 140.9, 157.9, 163.1, 164.7, 166.0, 189.6. Elemental analysis calcd. (%) for $C_{33}H_{46}N_2O_3$: C 76.41, H 8.94, N 5.40, Found: C 76.36, H 8.96, N 5.39. MS (FAB): *m/z* 519.4 $[M + H]^+$. Accurate mass: calcd., 519.3587; found, 519.3515.

4.2.4. Synthesis of chloromethyl functionalized salen ligand (2)

Compound **2** was prepared similarly to compound **1** (Figure 4.7). A solution of (1R,2R)-1,2-diaminocyclohexane monohydrochloride salt (0.75 g, 5mmol) and activated 4Å molecular sieves was also prepared in anhydrous ethanol (20 ml) and anhydrous methanol (20 ml). 3,5-di-*tert*-Butyl-2-hydroxybenzaldehyde (1.17 g, 5 mmol) was then added and the solution was stirred at room temperature for 4 hours. At the end of this time period, a solution of 3-*tert*-butyl-5-(chloromethyl)-2-hydroxybenzaldehyde[31] (1.13 g, 5 mmol) in anhydrous methylene chloride (40 ml) was added to the reaction mixture. Triethylamine (1.4 ml, 10 mmol) was then slowly added to the solution, and the mixture was stirred for an additional 4 hours. The solution was filtered to remove the residual sieves, and then the solvents were removed. The residue was re-dissolved in methylene chloride (50 ml) and was washed with aqueous hydrochloric acid (1M, 25 ml) and

deionized water (2 x 25 ml). The organic phase was then dried with magnesium sulfate. Although compound **2** was verified to be in the crude product mixture and various purification methods were attempted, successful isolation of the pure product in reasonable yields was not achieved. Further information regarding the purification difficulties associated with this compound may be found in section 4.3.2.

4.2.5. Synthesis of carboxylic acid functionalized salen ligand (3)

2-(3-tert-Butyl-5-formyl-4-hydroxyphenyl)acetic acid (subsequently referred to as carboxylic acid functionalized aldehyde) was synthesized following literature procedures.[26] Synthesis of compound **3** was attempted using this carboxylic acid functionalized aldehyde as indicated in Figure 4.7. This did not produce a sufficiently pure salen catalyst for further studies. As an alternative, a self-protecting synthesis was evaluated following a literature report for similar compounds (Figure 4.8).[32] The carboxylic acid functionalized aldehyde (591 mg, 2.5 mmol) and (1R,2R)-1,2-diaminocyclohexane (285 mg, 2.5 mmol) were stirred under reflux conditions in methanol for 2 hours. The zwitterionic product was unable to be isolated. Further information regarding the difficulties associated with synthesizing compound **3** may be found in section 4.3.3.

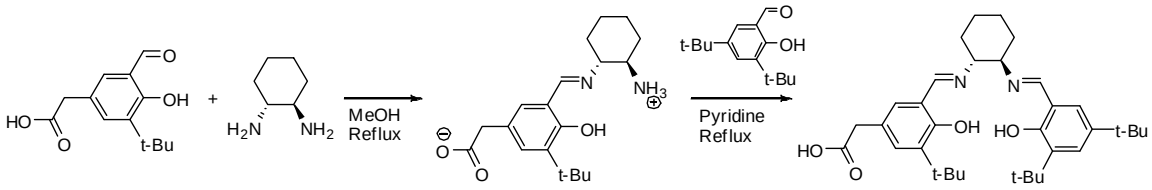

Figure 4.8. Synthesis of self-protecting carboxylic acid functionalized salen ligand.

4.3. Results and Discussion

4.3.1. Aldehyde functionalized salen ligand (1)

As mentioned in the introduction, the reports of using an aldehyde/amine reaction, or Schiff base reaction, as a method to graft salen ligands to aminosilica surfaces build the metal complexes in a stepwise manner off of the aminosilica surfaces. However, it is generally desired to have a well-defined immobilized catalyst so as to be able to properly assign catalytic behavior and more clearly understand the properties of the supported catalyst. For this reason, the stepwise grafting approach for the aldehyde functionalized salen has a number of disadvantages. Using this approach, undesirable side reactions can take place during the synthesis of the immobilized catalyst, particularly since excess reactant is often added during each grafting step.[9,10] Specifically, during the first grafting step in Figure 4.4, the di-aldehyde could react with two adjacent amine sites rendering it unreactive toward the remaining catalyst grafting steps (Figure 4.9 b). Likewise, during the addition of the cyclohexanediamine, two adjacent aldehyde functionalities could be linked (Figure 4.9 c). The result is an immobilized catalyst that is poorly defined with many different species on the surface.

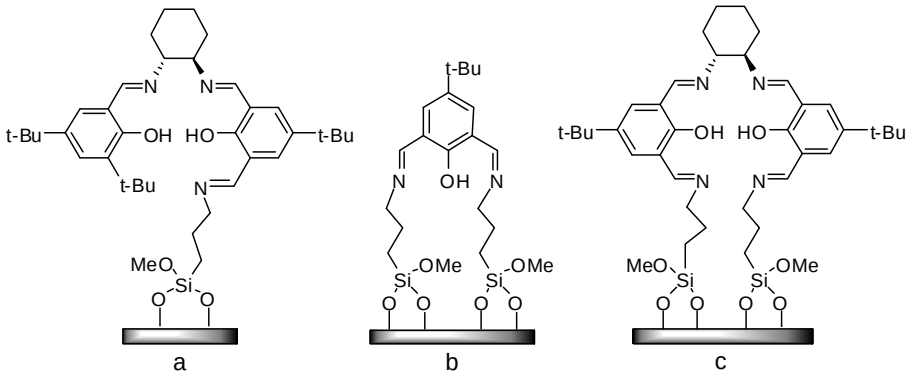

Figure 4.9. Possible products of step-wise grafting approach using a Schiff base linker, where (a) is the desired moiety and (b) and (c) are undesired side products.

To circumvent this problem and create a more well-defined surface, a synthesis was developed to generate an unsymmetrical salen ligand that could be preassembled prior to grafting but would still possess the aldehyde functionality for reaction with the surface. This ligand is shown in Figure 4.7 as compound **1**. After synthesis, this molecule was extensively characterized using ^{1}H and ^{13}C NMR spectroscopy, elemental analysis, and mass spectroscopy. Indeed, these techniques verified that the desired molecule was produced.

After synthesis and characterization, the ligand was metalated. This was accomplished by dissolving compound **1** in methylene chloride and then adding one equivalent of cobalt(II) acetate dissolved in methanol. The brick red solid product precipitated from solution and was recovered via filtration. The cobalt(II) salen was then oxidized to the cobalt(III) salen by stirring the compound with two equivalents of glacial acetic acid in toluene until the solution changed from brick red to dark brown in color. In these studies, cobalt was selected for the metal because cobalt salen catalysts are used

in the hydrolytic kinetic resolution of epoxides (Figure 4.10). This reaction is well-known to require two catalytic sites to promote the kinetic resolution, and therefore it could indicate if the spacing of the amine sites on the silica materials had an effect on the immobilized catalyst's reactivity. The trityl de-protected and the traditionally grafted aminosilicas were tested first.

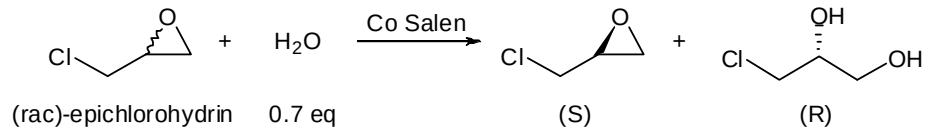

Figure 4.10. Hydrolytic kinetic resolution of epichlorohydrin using cobalt salen catalyst.

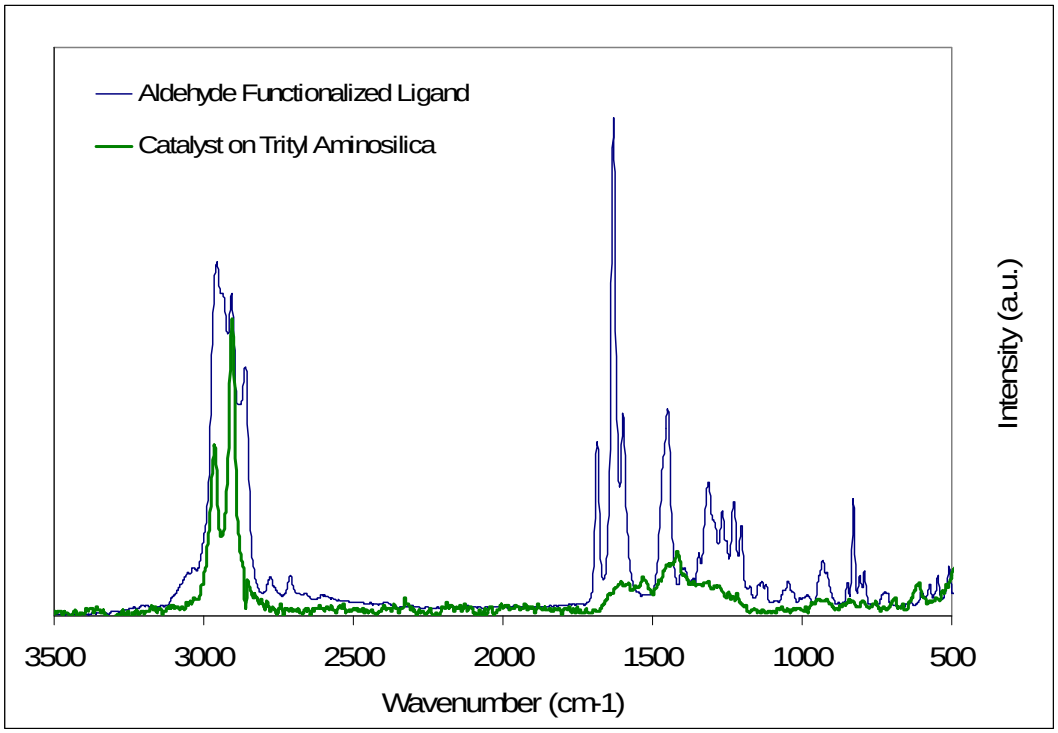

Figure 4.11. FT-Raman spectra for the aldehyde functionalized ligand **1** and the cobalt salen catalyst grafted to trityl de-protected aminosilica.

The metalated ligand was grafted to the surface by refluxing (using a Dean Stark trap) the metal complex and the desired aminosilica in toluene overnight. The solid materials were then filtered, washed, and dried, and the immobilized catalysts were characterized using FT-Raman spectroscopy. The results obtained for the ligand prior to grafting, compound **1**, and the cobalt salen catalyst grafted to the trityl de-protected aminosilica are shown above (Figure 4.11). It should be noted that the intensity of the spectrum of the immobilized catalyst is decreased because the sample contains mostly silica, whereas the other spectrum results from the pure organic compound. The main resonances of interest are the aliphatic and aromatic resonances from 2800-3100 cm^{-1} in both spectra, the aldehyde resonance at 1684 cm^{-1} in only the ligand prior to grafting, and

the imine resonance at 1630 cm^{-1} in both spectra. This data provides evidence that the desired catalyst is in fact grafted to the surface. Similar results were obtained for the catalyst grafted onto traditionally prepared aminosilica.

It was also noted that the efficiency of the catalyst loading onto the amine sites was much higher on the trityl de-protected aminosilica, showing more than 95% of the amines to be reacted with the cobalt catalyst (Table 4.1). In contrast, only 36% of the amines on the traditionally synthesized aminosilica had reacted with the catalyst. This result is expected as it previously has been shown that the de-protected aminosilicas display more uniform reactivity toward further functionalization.[33,34]

Table 4.1. Efficiency of catalyst loading onto aminosilicas.

Catalyst	Amine Loading[a]	Cobalt Loading[b]	% Amines Reacted
Cobalt(III) salen on trityl de-protected aminosilica	0.45 mmol NH_2/ g SiO_2	0.43 mmol Co/ g SiO_2	> 95%
Cobalt(III) salen on traditionally grafted aminosilica	2.02 mmol NH_2/ g SiO_2	0.73 mmol Co/ g SiO_2	36%

a – Determined by TGA. b – Determined by elemental analysis.

Once the cobalt loading was determined, the catalysts were tested in the hydrolytic kinetic resolution of epichlorohydrin. It was hypothesized that the catalyst immobilized on the trityl de-protected aminosilica should possess less reactivity since it would be less likely for two catalytic sites to be in close enough proximity to complete the reaction. Indeed, when this material was used in the HKR reaction, no activity was

observed. Conversely, the catalyst grafted onto the traditionally prepared aminosilica was expected to perform well in this reaction as the active sites should be in close proximity to one another. However, when this material was tested, it also showed no reactivity toward the HKR of epichlorohydrin.

Two main possibilities were seen as potential explanations for the absence of reactivity with this material. First, there could be some constraint or accessibility issue caused by the anchoring of the catalyst onto the solid surface. Otherwise, there could be active site blocking due to the proximity of the tethering point to the metal center. In order to determine which of these effects were in play, a homogeneous analog of the surface species was synthesized by reacting the aldehyde functionalized cobalt salen catalyst with n-propylamine (Figure 4.12). This catalyst also showed minimal reactivity in the HKR of epichlorohydrin, achieving less than 5% conversion of the starting epoxide and no enhancement in the enantiomeric excess. It is hypothesized that the imine nitrogen of the linker is close enough to the metal center that it is able to block the coordination of the epoxide.

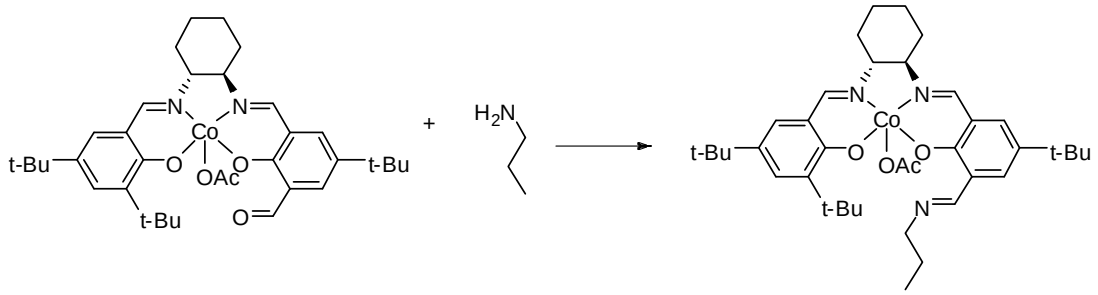

Figure 4.12. Reaction of the aldehyde functionalized salen with n-propylamine to form a homogeneous catalyst with a similar metal environment as the immobilized catalyst.

Therefore, this data indicates that contrary to published reports, grafting of the cobalt salen catalyst via a Schiff base reaction with an aldehyde in this position and an amine does not yield an active catalyst for the HKR of epichlorohydrin.[11] It may be that some other moiety generated during the step-wise grafting approach exists on the surface that promotes the reaction. This may also provide insight into why this grafting approach failed to produce very active or selective catalysts in other reactions reported in the literature.[9,10,12]

4.3.2. Chloromethyl functionalized salen ligand (2)

Since the aldehyde functionalized salen ligand was found to be unsuitable in terms of activity and selectivity, a second amine-reactive salen ligand was investigated. Reports in the literature indicated that a chloromethyl functionality on the 5 position of one of the salen phenyl rings was capable of reacting with aminosilica materials under relatively mild reaction conditions.[13-15,25] However, in most of these cases, the synthesis procedure leads to multiple types of sites on the aminosilica surfaces (Figure 4.13).[13,14,25] This again makes accurate assignment of catalytic activity difficult, as demonstrated in section 4.3.1. To minimize the multiple surface moieties, a synthesis was developed to generate the pre-assembled chloromethyl salen catalyst via a method similar to the one reported by Kureshy and co-workers.[15]

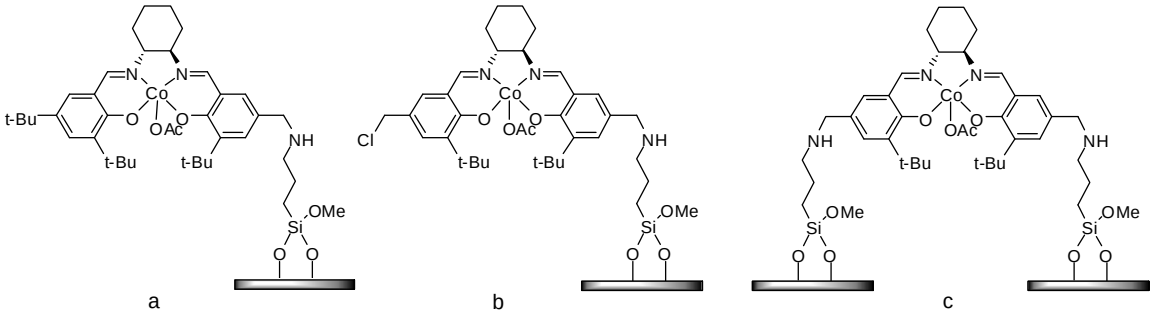

Figure 4.13. Possible products of literature methods for grafting salen catalysts using a chloromethyl/amine reaction, where (a) is the desired functionality and (b) and (c) are undesired side products.

Although this previous report indicated a yield of ~80% for the chloromethyl functionalized unsymmetrical salen ligand, these results were not able to be reproduced in this work. When the reported synthesis procedure was attempted, more than 50% of the crude product was found to be un-reacted starting materials. Since this approach was not successful, the synthesis of compound **2** was attempted using the same protocol as used for the aldehyde functionalized salen (Figure 4.7). During the synthesis of the ligand, a mixture of un-reacted aldehydes as well as both symmetrical salen ligands was generated (Figure 4.14). Many attempts were made to improve the synthesis method as well as the purification procedures. If the chloromethyl aldehyde was added first to the protected cyclohexane diamine, a reaction between the chloromethyl group and the cyclohexane diamine was observed. When a smaller equivalent of the chloromethyl aldehyde was added to the mono-functionalized cyclohexane diamine, the product was not able to be purified sufficiently. To improve the purification procedure, different silica gels were tried including standard silica gel, premium silica gel, and Florisil. Also, if the columns were pre-treated with methanol to remove water, some of the chloromethyl

groups were exchanged to hydroxymethyl groups. Despite great effort, the desired compound was never obtained in greater than 10% yield. For this reason, this grafting method was ultimately abandoned.

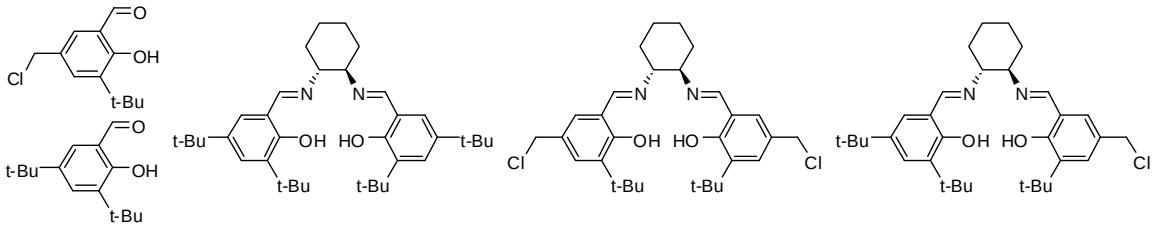

Figure 4.14. Mixture of compounds obtained using synthesis from Figure 4.7 to produce the chloromethyl functionalized salen.

However, in order to provide a rough test of the utility of the spaced aminosilicas, the statistical mixture method reported by Baleizao and co-workers was used to functionalize aminosilica materials with the salen ligand (Figure 4.15).[13] The mixture of salen ligands was metalated with cobalt for use in the hydrolytic kinetic resolution (HKR) of epichlorohydrin and then immobilized. All three aminosilica materials were functionalized: the trityl de-protected aminosilica, the benzyl de-protected aminosilica, and the traditionally grafted aminosilica.

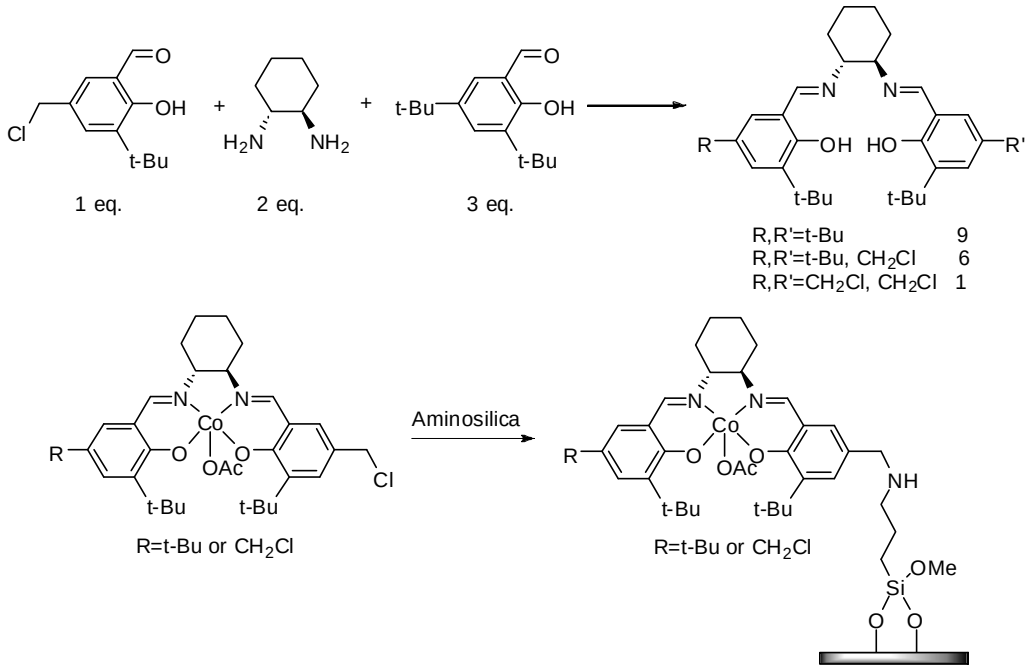

Figure 4.15. Statistical mixture method for immobilizing a chloromethyl functionalized salen catalyst onto an aminosilica.

When used in the HKR reaction, the materials were not exceptionally active catalysts. However, differences between the aminosilica scaffolds were observed (Figure 4.16). The catalyst which was grafted onto the trityl de-protected aminosilica (most opportunity for isolation) exhibited the least reactivity in the HKR reaction. Again, due to the bi-metallic nature of the reaction pathway, this result indicates that the catalytic sites are likely too far apart for two sites to be able to efficiently come together to complete the reaction. The benzyl de-protected aminosilica showed slightly more activity than the trityl de-protected material, which can be explained by the fact that, while isolated, the amine sites are still closer together than on the trityl de-protected aminosilica. Finally, the traditionally grafted aminosilica material exhibited the highest reactivity for the HKR of

epichlorohydrin. As this scaffold allows the most opportunity for the grafting of salen catalytic sites in close proximity, this result is in line with the initial hypothesis.

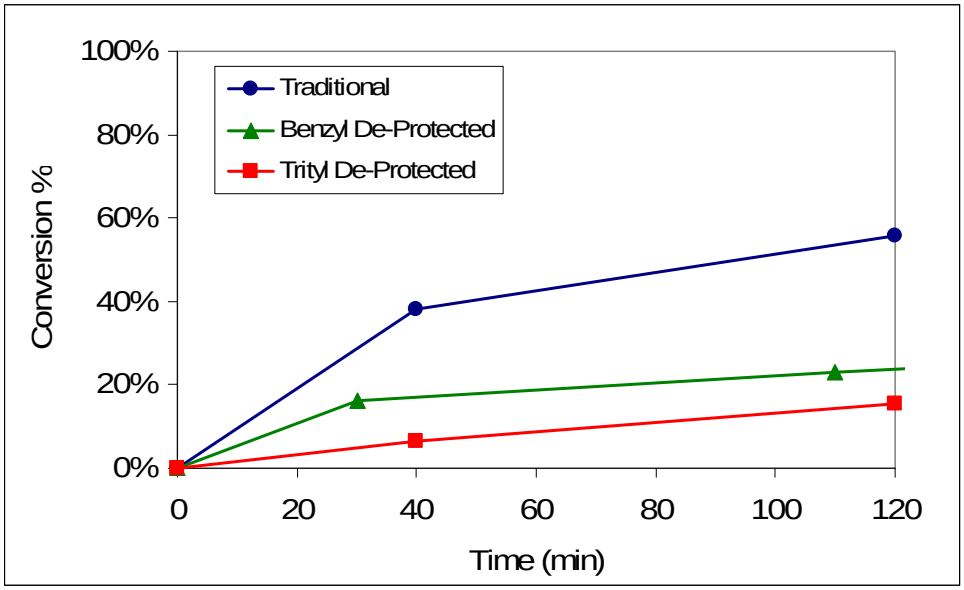

Figure 4.16. Conversion of R-epichlorohydrin (0.5 mol% catalyst) using a cobalt(III) salen catalyst grafted onto three aminosilica scaffolds.

Although these results show that the starting scaffolds onto which the catalyst is grafted can influence activity, the inability to thoroughly characterize the surface species on these materials rendered this method undesirable. The statistical nature of the synthesis procedure coupled with the difficulty in purifying the desired species in sufficient yield for study led to the exploration of a third technique for grafting the salen catalyst onto aminosilica surfaces. However, valuable information was obtained which showed that these materials could be included in an immobilized catalyst's design criteria if a suitable analog could be synthesized.

4.3.3. Carboxylic acid functionalized salen ligand (3)

In a last effort to synthesize a well-defined salen catalyst on an aminosilica surface, a method reported in the literature utilizing a carboxylic acid functionalized salen ligand was explored.[26] While reaction results were reported, no characterization of the immobilized catalyst was provided. Therefore, the isolation of products at individual steps was attempted in this work so as to be able to more thoroughly characterize the immobilized catalyst. Two paths were explored, with the first being the synthesis of the salen catalyst with an unprotected carboxylic acid functionality (Figure 4.7) and the second being the synthesis of the salen catalyst using a self-protecting method (Figure 4.8).[32]

In the first case, the carboxylic acid functionalized aldehyde was reacted in the same manner as the aldehyde and chloromethyl functionalized aldehydes used for compounds **1** and **2**. The crude product mixture was purified by column chromatography, and the resulting fractions showed a mixture of the desired product, symmetrical di-*tert*-butyl substituted salen, and un-reacted starting aldehydes. The least impure fraction of the target compound still contained 30% un-reacted starting materials. Additional attempts were made to purify the product with column chromatography, but the pure product was not isolated in >10% yield.

The second synthesis that was attempted was a self-protecting method whereby the carboxylic acid functionalized aldehyde was reacted with cyclohexane diamine to generate a zwitterionic product.[32] The reaction was attempted multiple times, but in each case, the zwitterionic solid product never precipitated from the methanol solution. The solution phase was analyzed by ^{1}H NMR, and the result showed that some Schiff base

formation had occurred. Considering that the product might simply be soluble in methanol, the methanol was removed, and a portion of the residue was re-dissolved in methylene chloride and another portion in ether in attempts to precipitate the desired product. These solvents did cause the precipitation of some solid material, but it was not at all pure. Attempts to further purify the product were unsuccessful. In the original report of this procedure, the carbonyl carbon of the acid functionality was directly off the phenyl ring (a benzoic acid), whereas in this work, there is a methylene group between the phenyl ring and the carboxylic acid functionality (a phenyl acetic acid). It is hypothesized that the change in chemical environment due to the extra methylene group may prevent the efficient formation of the desired zwitterion.

Since compound **3** was not able to be synthesized in a pure form, this method of grafting to aminosilicas was not pursued further.

4.4. Conclusions

The results presented in this chapter highlight efforts toward the synthesis of well-defined salen catalysts immobilized onto aminosilica materials. While the three methods that were attempted did not achieve the complete goal of a defined, active, and selective immobilized catalyst, the results that were obtained did reveal a number of important findings. First, although reported to be a successful catalyst, the aldehyde functionalized cobalt salen catalyst was shown to be inactive toward the HKR reaction once reacted with an amine group either on a surface or in solution. This may explain why other literature reports where this grafting method was utilized for other catalysts/reactions did not produce highly active catalysts. The second important result revealed that even with a multi-sited immobilized catalyst, a trend was seen in reactivity based on the aminosilica

scaffold that was used. This lends credence to the original hypothesis that the differently spaced aminosilicas could be included in the design parameters when immobilizing a catalyst with a known mechanism, or they could be used to help establish a previously unknown reaction mechanism. Lastly, some synthetic challenges were highlighted to provide guidance for future work in this area.

4.5. REFERENCES

[1] Kramer, J., Garcia, A. R., Driessen, W. L., and Reedijk, J., *Chem. Commun.* (2001) 2420.

[2] Walcarius, A., Etienne, M., and Bessiere, J., *Chem. Mater.* 14 (2002) 2757.

[3] Hicks, J. C., Drese, J. H., Fauth, D. J., Gray, M. L., Qi, G., and Jones, C. W., *J. Am. Chem. Soc.* 130 (2008) 2902.

[4] Yoo, S., Lunn, J. D., Gonzalez, S., Ristich, J. A., Simanek, E. E., and Shantz, D. F., *Chem. Mater.* 18 (2006) 2935.

[5] Wight, A. P., and Davis, M. E., *Chem. Rev.* 102 (2002) 3589.

[6] McKittrick, M. W., and Jones, C. W., *Chem. Mater.* 15 (2003) 1132.

[7] McKittrick, M. W., and Jones, C. W., *J. Am. Chem. Soc.* 126 (2004) 3052.

[8] Yu, K., McKittrick, M. W., and Jones, C. W., *Organometallics* 23 (2004) 4089.

[9] Kim, G.-J., and Shin, J.-H., *Catal. Lett.* 63 (1999) 205.

[10] Kim, G.-J., and Shin, J.-H., *Tetrahedron Lett.* 40 (1999) 6827.

[11] Kim, G.-J., and Park, D.-W., *Catal. Today* 63 (2000) 537.

[12] Alvaro, M., Baleizao, C., Carbonell, E., Ghoul, M. E., Garcia, H., and Gigante, B., *Tetrahedron* 61 (2005) 12131.

[13] Baleizao, C., Gigante, B., Sabater, M. J., Garcia, H., and Corma, A., *Appl. Catal. A* 228 (2002) 279.

[14] Alvaro, M., Baleizao, C., Das, D., Carbonell, E., and Garcia, H., *J. Catal.* 228 (2004) 254.

[15] Kureshy, R. I., Ahmad, I., Khan, N.-u. H., Abdi, S. H. R., Pathak, K., and Jasra, R. V., *J. Catal.* 238 (2006) 134.

[16] Burkett, S. L., Sims, S. D., and Mann, S., *Chem. Commun.* (1996) 1367.

[17] Beck, J. S., Vartuli, J. C., Roth, W. J., Leonowicz, M. E., Kresge, C. T., Schmitt, K. D., Chu, C. T.-W., Olson, D. H., Sheppard, E. W., McCullen, S. B., Higgins, J. B., and Schlenker, J. L., *J. Am. Chem. Soc.* 114 (1992) 10834.

[18] Hicks, J. C., and Jones, C. W., *Langmuir* 22 (2006) 2676.

[19] Hicks, J. C., Dabestani, R., Buchanan III, A. C., and Jones, C. W., *Chem. Mater.* 18 (2006) 5022.

[20] Baleizao, C., and Garcia, H., *Chem. Rev.* 106 (2006) 3987.

[21] Doyle, A. G., and Jacobsen, E. N., *Angew. Chem. Int. Ed.* 46 (2007) 3701.

[22] Zhang, W., Loebach, J. L., Wilson, S. R., and Jacobsen, E. N., *J. Am. Chem. Soc.* 112 (1990) 2801.

[23] Nielsen, L. P. C., Stevenson, C. P., Blackmond, D. G., and Jacobsen, E. N., *J. Am. Chem. Soc.* 126 (2004) 1360.

[24] Mazet, C., and Jacobsen, E. N., *Angew. Chem. Int. Ed.* 47 (2008) 1762.

[25] Lou, L.-L., Yu, K., Ding, F., Peng, X., Dong, M., Zhang, C., and Liu, S., *J. Catal.* 249 (2007) 102.

[26] Hajji, C., Roller, S., Beigi, M., Liese, A., and Haag, R., *Adv. Synth. Catal.* 348 (2006) 1760.

[27] Zhao, D., Huo, Q., Feng, J., Chmelka, B. F., and Stucky, G. D., *J. Am. Chem. Soc.* 120 (1998) 6024.

[28] Pangborn, A. B., Giardello, M. A., Grubbs, R. H., Rosen, R. K., and Timmers, F. J., *Organometallics* 15 (1996) 1518.

[29] Campbell, E. J., and Nguyen, S. T., *Tetrahedron Lett.* 42 (2001) 1221.

[30] Holbach, M., Zheng, X., Burd, C., Jones, C. W., and Weck, M., *J. Org. Chem.* 71 (2006) 2903.

[31] Canali, L., Cowan, E., Deleuze, H., Gibson, C. L., and Sherrington, D. C., *J. Chem. Soc., Perkin Trans. I* (2000) 2055.

[32] Jeon, Y.-M., Heo, J., and Mirkin, C. A., *Tetrahedron Lett.* 48 (2007) 2591.

[33] McKittrick, M. W., and Jones, C. W., *Chem. Mater.* 17 (2005) 4758.

[34] Hicks, J. C., Dabestani, R., Buchanan III, A. C., and Jones, C. W., *Inorg. Chim. Acta* (2008) in press.

CHAPTER 5

SUMMARY, CONCLUSIONS, AND FUTURE WORK

5.1. Summary

The main goals of this dissertation were: 1) to synthesize, characterize, and evaluate the reactivity of immobilized catalysts for different applications so that new catalysts would be made available, and 2) to compare the different catalyst systems to gain insight on how immobilization parameters effect catalytic activity. To this end, immobilized catalysts were developed and tested for application in the formation of cyclic carbonates from epoxides and carbon dioxide, the oxidative kinetic resolution of α-hydroxy esters, and the exploitation of aminosilica scaffolds with varied degrees of grafting site isolation.

In the first application, a new immobilized Lewis base catalyst was developed on SBA-15 mesoporous silica for the reaction of propylene oxide with carbon dioxide.[1] The homogeneous base selected for immobilization was 4-(dimethylamino)pyridine (DMAP) due to its high activity in this reaction as well as its use in many other organic transformations. While previously reported to function only as a co-catalyst, the results presented in this work show that the base gives yields of 80-85% with no additional catalyst present. The reaction, which was conducted at 120 °C and 17.2 bar CO_2 pressure, was tested with homogeneous DMAP, the new silica supported DMAP, and a commercially available poly(styrene) supported DMAP. All three catalysts performed similarly in the first runs. However, the recycle performance of the silica supported catalyst, while not as high as the initial run, was superior to that of the polymer supported catalyst. This could potentially be attributed to degradation of the polymer catalyst

caused by the elevated reaction temperature and pressure. This work served to clarify the importance of the Lewis base in this reaction as well as to provide a comparison of support materials for high temperature/pressure reactions.

The second application for which new immobilized catalysts were developed is the oxidative kinetic resolution of α-hydroxy esters. Since enantiomerically pure α-hydroxy esters are used in pharmaceutical and fine chemical production, enantioselective reactions are attractive because they facilitate the separation of enantiomers. The homogeneous catalyst selected for immobilization in this case was a tridentate Schiff base vanadium catalyst derived from salicylaldehyde and S-*tert*-leucinol.[2] One silica supported and two polymer supported catalysts were created. The polymer supported catalysts were synthesized via the polymerization of a styryl functionalized catalyst monomer alone (homopolymer) or with styrene (copolymer). Other parameters that were studied for this reaction system included the method of polymer metalation (*in situ* or prior to reaction) and the reaction solvent. All three immobilized catalysts were active for the resolution reaction, although the polymer catalysts outperformed the silica supported catalyst, with the copolymer being the most active catalyst. Acetone was found to be the optimal reaction solvent for all of the catalysts studied, and the most effective metalation protocol was found to depend on the polymer catalyst used.

The final area which was studied was the utilization of support scaffold materials with varied degrees of grafting site isolation to create spaced salen catalysts anchored to silica surfaces. Previous researchers in our group had developed protocols for the syntheses of amine functionalized mesoporous silicas with increasing degrees of amine group isolation on the surface.[3,4] The homogeneous catalyst selected for immobilization

on these materials was the salen catalyst due to its activity for many types of reactions.[5,6] It was also selected because salen catalysts are known to function in a bimetallic manner in some reactions (catalytic cycle involves two active sites)[7] and in a monometallic manner in other reactions (catalytic cycle involves one active site).[8] It was surmised that the same salen catalyst grafted on different amine scaffolds would exhibit differences in activity depending on the reaction mechanism that was occurring, with greater spacing favoring monometallic reactions and less spacing favoring bimetallic reactions. A number of difficulties in the syntheses of amine reactive salen catalyst analogs were discussed, most of which related to the development of analogs that could be thoroughly characterized prior to grafting. One such analog was shown to be completely ineffective when the pure compound was used, contrary to reports that indicated its activity when grafted onto silica in a step-wise manner. However, tests were conducted with other spaced salen materials that did show decreasing activity with increasing catalyst isolation in the hydrolytic kinetic resolution of epichlorohydrin, a bimetallic reaction.

5.2. Conclusions

While a concrete algorithm for designing new immobilized catalysts does not yet exist, there are a number of design parameters which can be ascertained from a review of the results found in this work. One factor that complicates this analysis in the reported literature is the considerable variation in the degree of characterization of immobilized catalysts. Particularly if the immobilization procedure involves multiple surface reactions, it can be extremely difficult to properly assign catalytic behavior. This is because most readily available characterization techniques for solid materials do not have the resolution to detect or quantify small amounts of impurities which can alter the

catalytic properties of the material. Therefore, in this work, every attempt was made to synthesize the supported catalysts in such a way as to minimize the number of surface reactions and to produce well-defined materials.

There are three general components to immobilized catalysts that are made from the grafting of catalyst analogs onto support structures or from the incorporation of catalyst analogs into the support structure.[9] These are the support, the linker, and the catalyst analog. When selecting a support, the most important considerations are the reaction temperature and pressure. In general, polymer supports are very attractive for mild reaction conditions. Their properties can be tuned for a specific application more easily than silica materials.[10] For instance, altering the catalyst loading and the degree of isolation between two sites can be accomplished simply by changing the monomer ratios in a copolymer. Also, the polymer backbone can be altered to adjust the catalyst's solubility in the reaction solvent. If a totally heterogeneous process is desired, the polymer can be made insoluble. If higher reaction rates are desired, the polymer backbone can be selected so that it will be dissolved during the reaction but easily precipitated after the reaction. However, polymer catalysts are more susceptible to degradation under high temperatures and pressures than inorganic materials. Even a very active polymer catalyst would fail to be an "ideal" immobilized catalyst if degradation during the initial reaction rendered it unable to be recycled. For these conditions, silica materials are more appropriate supports.[11,12] Mesoporous silicas have very high thermal stabilities, high surface areas, and are easy to functionalize. Although there is less opportunity to tune the support structure itself, the surface can be tailored to a specific application through processes which can adjust the isolation of grafting sites.

The linker, or group which connects the catalyst analog to the support structure, is the next important consideration when designing a new immobilized catalyst. With both polymer and silica supports, the linker is typically the component which most affects the mobility of the catalytic sites. A rigid linker that minimizes interactions between two catalytic sites would be appropriate for monometallic reactions as it should increase accessibility to the active site and minimize site deactivation by other active sites. A long, flexible linker would be appropriate when two catalytic sites must interact during the course of the reaction. The exact linker length that is optimal may be different for each catalyst/reaction combination, though.[9,13] Here, two options exist to address this problem. The first option is to test similarly flexible linkers of different lengths until the optimized distance is found. This can be very synthetically taxing. The second option is to combine modeling of the reaction transition state with modeling of the linker length to hone in on an ideal length. This method is rarely reported, but it is anticipated to become increasingly important as this field continues to mature.

The last consideration in designing supported catalysts is the structure of the catalyst analog itself. This area is likely to be the last for which true, *a priori* criteria can be developed. Even the design of new homogeneous catalysts often requires trial and error when determining the most active ligand structures.[14] However, it can be said that ensuring that the point of attachment is far away from the active site is desirable because it decreases the opportunity for the linker to coordinate with or otherwise block access to the active site. So, while general guidelines can be offered for the design of immobilized catalysts, more detailed criteria must continue to be determined from on-going research in this area.

5.3. Recommendations for Future Work

5.3.1. Aluminum salen catalyzed formation of cyclic carbonates

In chapter 2, it was demonstrated that a Lewis base alone could catalyze the reaction of propylene oxide with carbon dioxide in moderate yields (~80%). However, the yield can be increased to almost quantitative values with the use of metal catalysts. Specifically, metal salen catalysts have been shown to give excellent yields and high selectivity toward the desired cyclic carbonate.[15-21] Nonetheless, most of these systems still require elevated carbon dioxide pressures and the use co-catalysts to be effective. The following paragraphs outline research opportunities to address these issues using supported catalysts.

5.3.1.1. Macrocyclic oligomeric aluminum salen catalysts

A recent publication by Melendez and coworkers reported the use of an aluminum salen catalyst for the reaction of epoxides with carbon dioxide at room temperature and atmospheric carbon dioxide pressure.[22] In this report, the authors claim based on mass spectroscopy results that the added aluminum salen (with an ethoxide counterion) forms a dimeric species in solution (Figure 5.1). They hypothesize that the formation of the dimer is the cause of its catalytic efficiency.

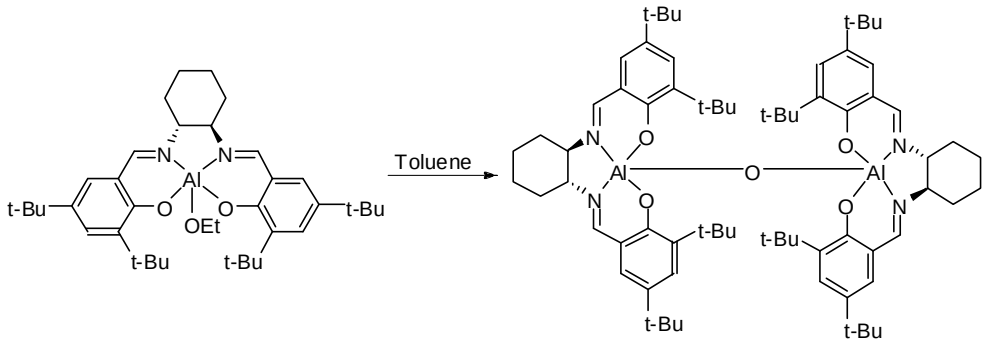

Figure 5.1. Proposed dimer formation from an aluminum salen catalyst with an ethoxide counterion.

If the catalysis is truly enhanced by the aluminum salen existing in dimeric versus monomeric form, it would be of interest to investigate other aluminum salen catalysts where multiple active sites are forced to be in close proximity to one another. Previous research in our group has led to the discovery of cyclic, oligomeric, cobalt salen catalysts which are highly effective for the hydrolytic kinetic resolution of epoxides.[23] These oligomeric ligands are excellent candidates for use in a more detailed study of the aluminum salen catalyzed cyclic carbonate reaction.

A preliminary investigation was conducted using two macrocyclic oligomeric catalysts (Figure 5.2). For the conversion of styrene oxide using the small molecule aluminum salen catalyst (Figure 5.1) and tetrabutylammonium bromide as a co-catalyst, Melendez reported an epoxide conversion of 62% in 3 h. With oligomeric catalysts **a** and **b** (Figure 5.2), styrene oxide conversions of 42% and 13% respectively were observed after 3 h under the same reaction conditions. While these initial results show the reported catalyst to be more active, it must be noted that the oligomeric catalysts were prepared with chloride counter-ions. When the reported aluminum salen catalyst (Figure 5.1) was

synthesized with a chloride counter-ion and re-tested, no reaction occurred, indicating the oligomeric catalysts outperformed their homogeneous counterpart.

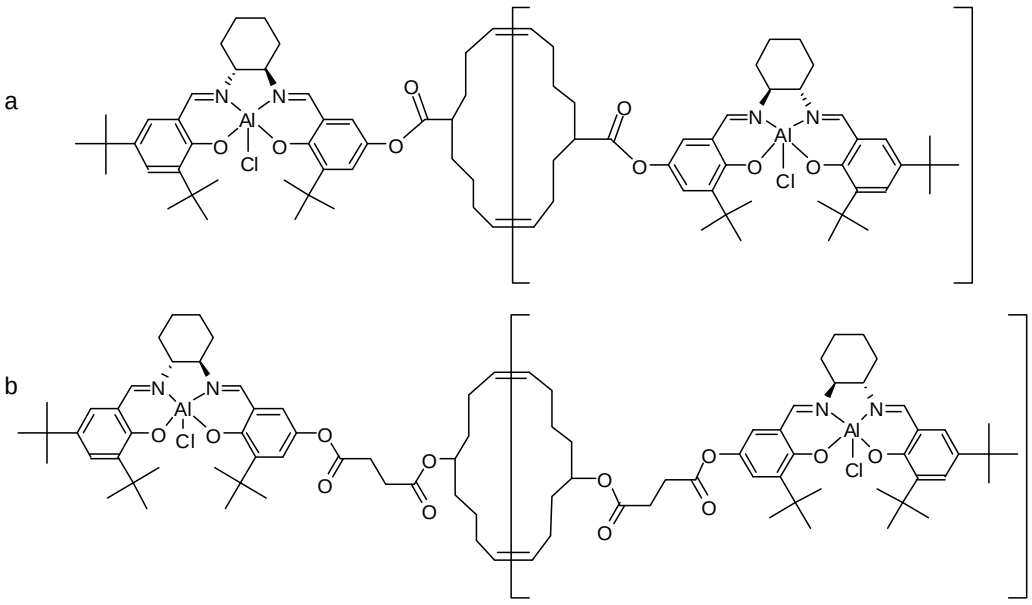

Figure 5.2. Oligomeric aluminum salen catalysts used for cyclic carbonate synthesis.

Based on these findings, it is hypothesized that replacement of the chloride counter-ions on the oligomeric catalysts will increase their activities, quite possibly beyond that of the reported catalyst. Also, the activity might further be increased with the addition of a co-solvent such as methylene chloride. In the preliminary studies, the oligomeric catalysts were only partially soluble in the starting epoxide, potentially limiting their efficiency. Since the reaction is effective with a wide range of epoxides and occurs at ambient temperature and pressure, the optimized catalysts would be broadly applicable and attractive.

5.3.1.2. Catalyst/co-catalyst copolymers

As stated, Lewis basic co-catalysts are almost always required to achieve quantitative yields of cyclic carbonates even with the use of metal salen catalysts.[15,16,24,25] There are many reports of immobilized metal salen catalysts for this reaction, although the co-catalyst is still typically dissolved in the liquid phase.[24-26] It would be desirable for a heterogeneous system to have both the catalyst and co-catalyst immobilized, particularly if both species were present on the same support.

To this end, a copolymer system of an aluminum salen catalyst and a 4-(dimethylamino)pyridine (DMAP) analog could potentially promote the formation of cyclic carbonates at atmospheric pressure with very high activity, selectivity, and catalyst recoverability (Figure 5.3). Early research in our group on polymer supported salen catalysts focused on the direct polymerization of a styryl functionalized salen monomer either alone or with styrene.[27] Later studies investigated more flexible monomers by introducing ethylene glycol spacer units in the linker (Figure 5.4).[13] Both of these monomer structures are suitable for copolymerization with a co-catalyst, and comparison of the resulting polymers could lead to the determination of an optimal structure. Metals other than aluminum, such as cobalt and chromium, could also be used in the salen ligand, as these previously have been reported to produce active cyclic carbonate catalysts. However, carbon dioxide pressures above atmospheric would likely be required to obtain sufficient carbonate yields.

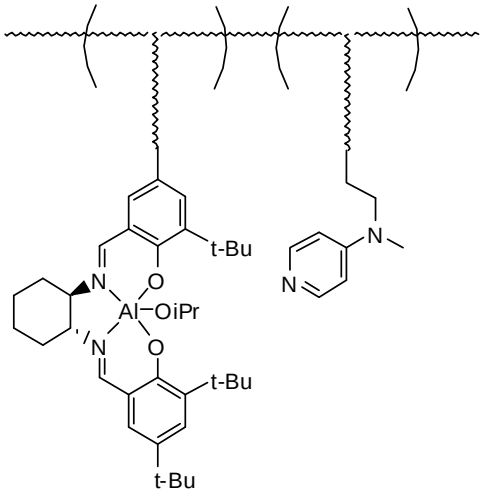

Figure 5.3. Conceptual schematic of a catalyst/co-catalyst copolymer for cyclic carbonate synthesis.

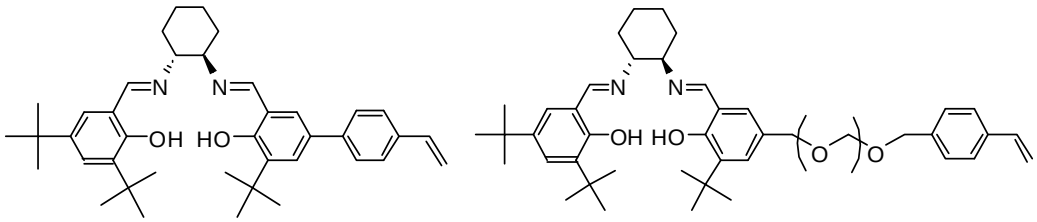

Figure 5.4. Polymerizable salen monomers.

A 4-(dimethylamino)pyridine (DMAP) analog functionalized with a styryl group could provide the necessary Lewis base functionality in the copolymer. In order to increase the ability of the base and salen to interact, the DMAP analog could be synthesized with a propyl spacer as the linker. This could be accomplished through the deprotonation of 4-(methylamino)pyridine (MAP) followed by its reaction with 4-(3-

chloropropyl)styrene (Figure 5.5). MAP is commercially available, and 4-(3-chloropropyl)styrene can be prepared in two steps following literature procedures.[28]

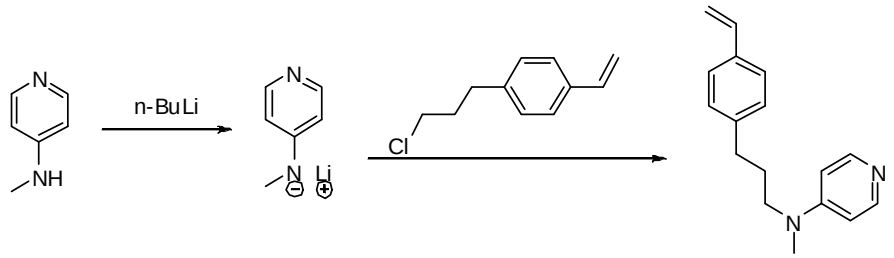

Figure 5.5. Proposed synthesis of flexible, styryl functionalized DMAP analog.

5.3.2. Tridentate Schiff base vanadium catalysts

5.3.2.1. Optimization of vanadium copolymer catalyst

In Chapter 3 of this dissertation, polymeric, tridentate vanadium Schiff base catalysts were developed for the oxidative kinetic resolution of secondary alcohols. Two polymers were tested, with the first being a homopolymer of the monomer functionalized catalyst, and the second being a copolymer of the same monomer and styrene (Figure 5.6). The reactivity results showed that the copolymer (2:5 catalyst:styrene ratio) was a more active catalyst than the homopolymer. However, the ratio of catalyst monomer to styrene was not varied. One possibility for the improvement of the polymer catalyst is to synthesize copolymers with incrementally increasing styrene ratios to determine if there exists an optimal copolymer ratio for maximum catalytic activity.

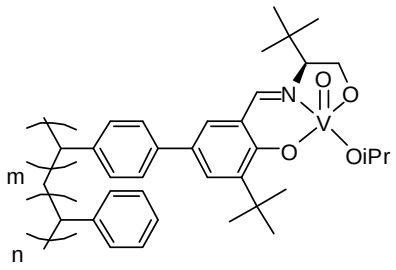

Figure 5.6. Vanadium polymer catalyst for oxidative kinetic resolution. Homopolymer: m=0; copolymer: m=0, n varied.

Another possibility for improvement of the polymer catalysts is to use a different linker between the Schiff base ligand and styryl functionalities on the catalyst monomer to potentially improve solubility. Currently, the metalated polymers are insoluble in common organic solvents, including those in which the catalytic reactions take place. A salicylaldehyde derivative with an ethylene glycol functionality has been reported which could be used in the polymer and copolymer syntheses to alter the solubilities (Figure 5.7).

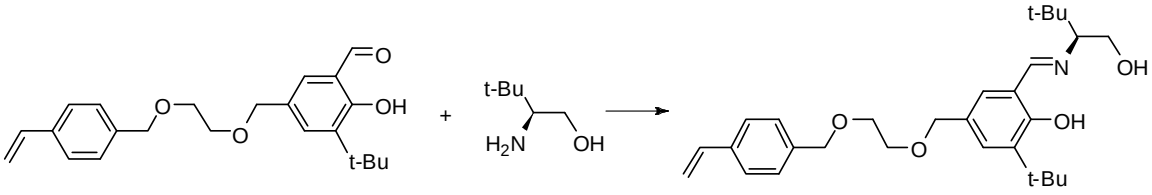

Figure 5.7. Styryl functionalized monomer with ethylene glycol linker.

5.3.2.2. Other asymmetric reactions utilizing tridentate Schiff base vanadium catalysts

There are other asymmetric reactions of interest which use similar catalysts to the vanadium Schiff base catalyst used in this work. Two specific examples are the oxidative kinetic resolution of α-hydroxy amides and the oxidative kinetic resolution of α-hydroxy phosphonates, which are both reported to occur with high yields and enantiomeric excesses (Figure 5.8).[29,30] These reactions use tridentate Schiff base catalysts derived from *tert*-leucine instead of *tert*-leucinol. The polymer and silica supported catalysts described in Chapter 3 could be easily synthesized with this functionality similarly to reported procedures.[29]

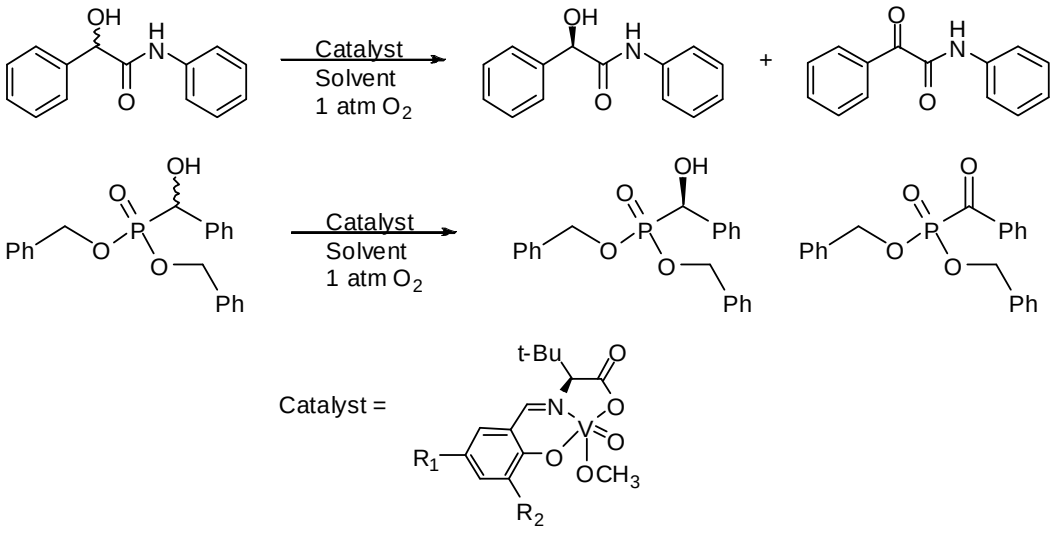

Figure 5.8. Asymmetric reactions utilizing a tridentate Schiff base vanadium catalyst.

Since the leucine derived catalyst (Figure 5.8) is also active for the oxidative kinetic resolution of α-hydroxy esters, a study of the polymer and silica immobilized

catalysts for these three reactions would provide a basis set for comparison of immobilization effects across multiple support structures and reactions. Also, there is one known report of a similar catalyst grafted onto a poly(styrene) bead.[31] This catalyst could be prepared and tested as well and would provide an additional comparison of a grafted polymer catalyst versus a polymerized catalyst monomer.

5.3.3. Salen catalysts grafted on aminosilicas

Although the synthesis attempts outlined in Chapter 4 of this dissertation were not successful for immobilizing well-defined salen catalysts onto aminosilicas, the preliminary reaction results showed that the spaced amine scaffolds could be used to alter the grafted catalyst's activity. This is still a very desirable quality, particularly when attempting to exploit a known catalytic mechanism or determine a new catalytic mechanism.

There are two paths toward the development of salen catalysts on aminosilicas that are promising. The first is an improved synthesis for the carboxylic acid functionalized salen ligand. As postulated, the use of a phenyl acetic acid functionalized aldehyde instead of a benzoic acid functionalized aldehyde may likely have interfered with the formation of the zwitterion, as all of the previously reported zwitterions did not have the methylene spacer (Figure 5.9).[32]

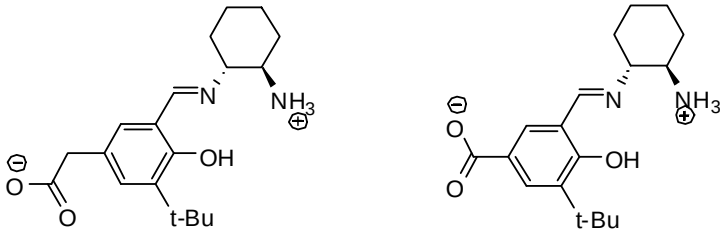

Phenylacetic acid functionalized Benzoic acid functionalized

Figure 5.9. Carboxylic acid functionalized half-salen ligands.

Therefore, repeating the salen synthesis with 3-*tert*-butyl-5-formyl-4-hydroxybenzoic acid might generate pure product yields in line with the reported compounds (75% - 99%). In this case, the benzoic acid functionalized salen could be coupled to the aminosilica surface using a N,N'-diisopropylcarbodiimide (DIC) coupling (Figure 5.10). N,N'-dicyclohexylcarbodiimide (DCC) is a more common activating agent for carboxylic acids than DIC, but the DCC urea by-product is insoluble in most organic solvents, making it difficult to remove from the silica surface. However, the DIC urea by-product is soluble in organic solvents, making the removal of this by-product from the silica surface much easier.

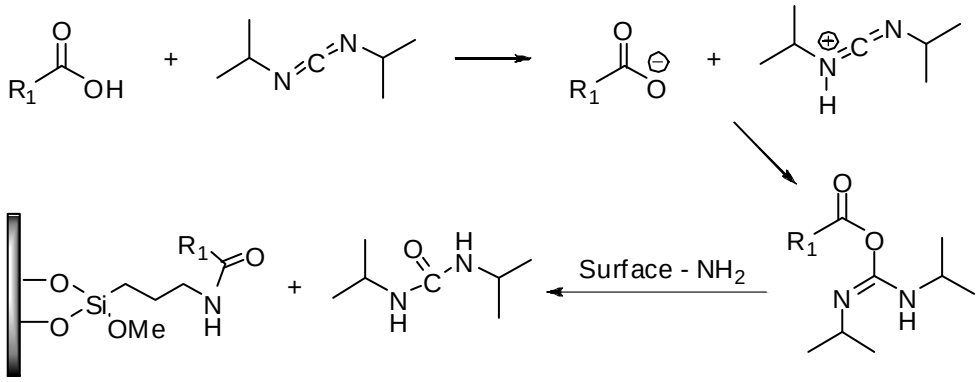

Figure 5.10. DIC coupling of a carboxylic acid to aminosilica.

The second promising path toward the synthesis of salen catalysts on aminosilicas is significantly more synthetically challenging. A pyrrolidine–based salen catalyst grafted to an amine functionalized resin has been previously reported (Figure 5.11).[33] Following a similar procedure, it is expected that the same ligand could be grafted to aminosilicas. The starting pyrrolidine dimesylate is first synthesized in three steps from L-tartaric acid.[34] Then, through a series of transformations, the diamine functionalized pyrrolidine is obtained and subsequently reacted with 3,5-di-*tert*-butyl-2-hydroxybenzaldehyde to form the salen ligand.[35,36] The pyrrolidine salen is then reacted with glutaric anhydride to add a carboxylic acid functionality to the ligand. Finally, this compound could then be anchored to the aminosilica using a DIC coupling.[33] Obtaining the product in sufficient yield for study, however, could be difficult.

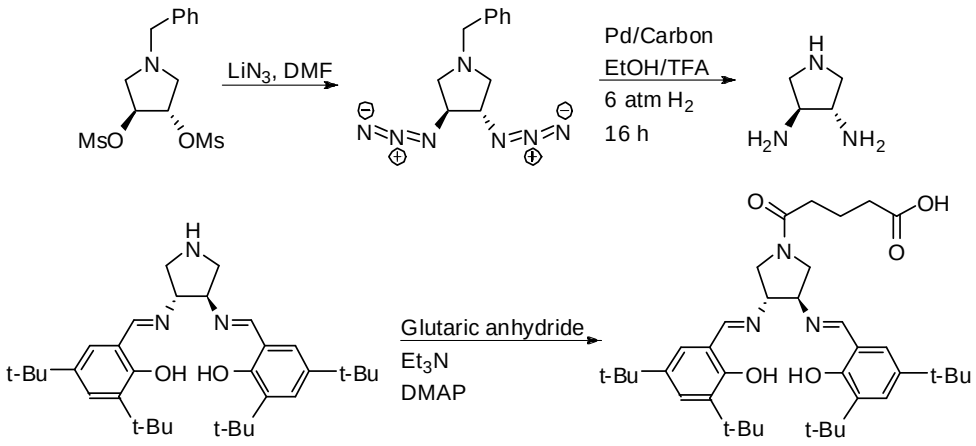

Figure 5.11. Synthesis of pyrrolidine salen for aminosilica grafting.

One particular application where "spaced" salen catalysts could provide useful information is the aluminum salen catalyzed reaction of epoxides with carbon dioxide. There is a great deal of disagreement in the existing literature concerning the mechanism of this reaction (see Appendix A). While it is generally accepted that the metal salen coordinates with the epoxide to activate it for ring-opening, it is unclear whether a second metal salen is required to activate the carbon dioxide before its attachment to the ring-opened epoxide. Data from the use of spaced, aminosilica supported salen catalysts in conjunction with data from the oligomeric catalysts discussed in section 5.3.1.1 could provide valuable insight to establish the true reaction mechanism, which could allow for the design of even more active catalysts.

Another application where "spaced" salen catalysts could be used is the ring-opening polymerization of lactide. Aluminum salen catalysts are known to promote this reaction through a coordination insertion mechanism, meaning that access to the aluminum center is critical for successful polymerization (Figure 5.12).[37-39] Since there is a tradeoff between catalyst isolation and catalyst loading on the spaced aminosilica

surfaces, these materials could be used to determine an optimal balance between surface loading and active site accessibility for lactide polymerizations with silica immobilized catalysts.

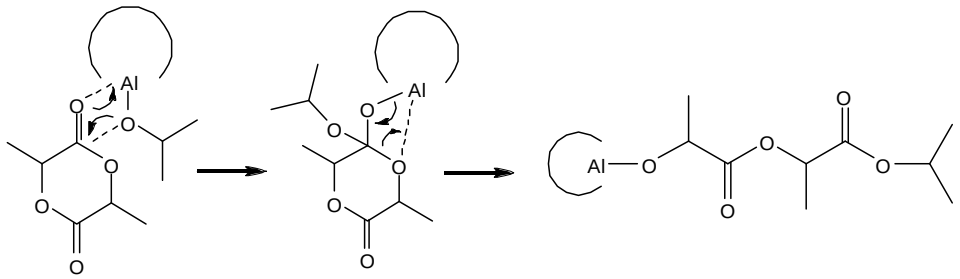

Figure 5.12. Mechanism of the polymerization of lactide with an aluminum salen catalyst.

Overall, the development of immobilized catalysts has been significantly advanced by the research efforts of the past few decades. For some reactions, thorough examinations of many immobilized catalysts have brought to light design parameters which can be used to create highly active and selective “next generation” catalysts. For other reactions, much of the design of new catalysts is still left to some degree of trial and error. This dissertation has contributed to the study of new immobilized catalysts and offered perspectives on future opportunities for catalyst optimization and for the establishment of new design criteria. As the need for effective and recoverable catalysts only grows, it is anticipated that catalyst immobilization will be a continued topic of research for many years.

5.4. REFERENCES

[1] Shiels, R. A., and Jones, C. W., *J. Mol. Catal. A: Chem.* 261 (2007) 160.

[2] Radosevich, A. T., Musich, C., and Toste, F. D., *J. Am. Chem. Soc.* 127 (2005) 1090.

[3] McKittrick, M. W., and Jones, C. W., *Chem. Mater.* 15 (2003) 1132.

[4] Hicks, J. C., Dabestani, R., Buchanan III, A. C., and Jones, C. W., *Chem. Mater.* 18 (2006) 5022.

[5] Canali, L., and Sherrington, D. C., *Chem. Soc. Rev.* 28 (1999) 85.

[6] Baleizao, C., and Garcia, H., *Chem. Rev.* 106 (2006) 3987.

[7] Nielsen, L. P. C., Stevenson, C. P., Blackmond, D. G., and Jacobsen, E. N., *J. Am. Chem. Soc.* 126 (2004) 1360.

[8] Doyle, A. G., and Jacobsen, E. N., *Angew. Chem. Int. Ed.* 46 (2007) 3701.

[9] Corma, A., *Catal. Rev.* 46 (2004) 369.

[10] Mastrorilli, P., and Nobile, C. F., *Coord. Chem. Rev.* 248 (2004) 377.

[11] Thomas, J. M., and Raja, R., *J. Organomet. Chem.* 689 (2004) 4110.

[12] De Vos, D. E., Dams, M., Sels, B. F., and Jacobs, P. A., *Chem. Rev.* 102 (2002) 3615.

[13] Zheng, X., Jones, C. W., and Weck, M., *Adv. Synth. Catal.* 350 (2008) 255.

[14] Blaser, H.-U., Indolese, A., Naud, F., Nettekoven, U., and Schnyder, A., *Adv. Synth. Catal.* 346 (2004) 1583.

[15] Paddock, R., and Nguyen, S.-B. T., *J. Am. Chem. Soc.* 123 (2001) 11498.

[16] Paddock, R., and Nguyen, S.-B. T., *Chem. Commun.* (2004) 1622.

[17] Jing, H., Edulji, S. K., Gibbs, J. M., Stern, C. L., Zhou, H., and Nguyen, S.-B. T., *Inorg. Chem.* 43 (2004) 4315.

[18] Shen, Y.-M., Duan, W.-L., and Shi, M., *J. Org. Chem.* 68 (2003) 1559.

[19] Darensbourg, D. J., Fang, C. C., and Rogers, J. L., *Organometallics* 23 (2004) 924.

[20] Darensbourg, D., and Holtcamp, M. W., *Coord. Chem. Rev.* 153 (1996) 155.

[21] Lu, X.-B., Zhang, Y.-J., Jin, K., Luo, L.-M., and Wang, H., *J. Catal.* 227 (2004) 537.

[22] Melendez, J., North, M., and Pasquale, R., *Eur. J. Inorg. Chem.* (2007) 3323.

[23] Zheng, X., Jones, C. W., and Weck, M., *J. Am. Chem. Soc.* 129 (2007) 1105.

[24] Alvaro, M., Baleizao, C., Carbonell, E., Ghoul, M. E., Garcia, H., and Gigante, B., *Tetrahedron* 61 (2005) 12131.

[25] Alvaro, M., Baleizao, C., Das, D., Carbonell, E., and Garcia, H., *J. Catal.* 228 (2004) 254.

[26] Song, C. E., and Lee, S.-G., *Chem. Rev.* 102 (2002) 3495.

[27] Zheng, X., Jones, C. W., and Weck, M., *Chem. Eur. J.* 12 (2006) 576.

[28] Montheard, J. P., Boinon, B., and Benayad, B., *J. Polym. Sci. Part A* 27 (1989) 2539.

[29] Weng, S.-S., Shen, M.-W., Kao, J.-Q., Munot, Y. S., and Chen, C.-T., *PNAS* 103 (2006) 3522.

[30] Pawar, V. D., Bettigeri, S., Weng, S.-S., Kao, J.-Q., and Chen, C.-T., *J. Am. Chem. Soc.* 128 (2006) 6308.

[31] Maurya, M. R., Sikarwar, S., and Kumar, M., *Catal. Commun.* 8 (2007) 2017.

[32] Jeon, Y.-M., Heo, J., and Mirkin, C. A., *Tetrahedron Lett.* 48 (2007) 2591.

[33] Song, C. E., Roh, E. J., Yu, B. M., Chi, D. Y., Kim, S. C., and Lee, K.-J., *Chem. Commun.* (2000) 615.

[34] Nagel, U., *Angew. Chem. Int. Ed.* 23 (1984) 435.

[35] Reddy, D. R., and Thornton, E. R., *J. Chem. Soc., Chem. Commun.* (1992) 172.

[36] Konsler, R. G., Karl, J., and Jacobsen, E. N., *J. Am. Chem. Soc.* 120 (1998) 10780.

[37] Nomura, N., Ishii, R., Yamamoto, Y., and Kondo, T., *Chem. Eur. J.* 13 (2007) 4433.

[38] Yang, J., Yu, Y., Li, Q., Li, Y., and Cao, A., *J. Polym. Sci. Part A* 43 373.

[39] Dechy-Cabaret, O., Martin-Vaca, B., and Bourissou, D., *Chem. Rev.* 104 (2004) 6147.

APPENDIX A

COUPLING OF CARBON DIOXIDE WITH EPOXIDES USING SALEN CATALYSTS - MECHANISTIC CONSIDERATIONS

Salen catalysts are very active and selective catalysts for the formation of cyclic carbonates from carbon dioxide and epoxides. There are reports in the literature of salen or salen-like complexes of aluminum, cobalt, chromium, manganese, tin, zinc, ruthenium and copper which are used to synthesize cyclic carbonates with varying degrees of activity. These catalysts are typically used in conjunction with a nucleophilic co-catalyst such as a Lewis base or a quaternary ammonium salt, and in most if not all cases, control experiments with no co-catalyst generate greatly reduced or completely suppressed yields. These reports are summarized in Table A.1.

One aspect of this reaction about which literature reports are very inconsistent is the reaction mechanism. While it is generally accepted that the metal salen catalyst activates the epoxide, the role of the co-catalyst differs significantly among proposed mechanisms. The purpose of this appendix is to present a critical analysis of the most often cited proposed mechanisms. In addition, evidence from reported mechanisms for other catalytic systems for this reaction will be included where informative. Discussion of the mechanism for the copolymerization of epoxides and carbon dioxide with salen catalysts has been omitted. This mechanism is far more well-established, and a thorough explanation of it can be found in existing reviews on this topic.[1-3]

Table A.1. Salen or salen-like catalyst systems for cyclic carbonate production.

Metal	Co-catalyst	Homogeneous Systems	Heterogeneous Systems
Al	Lewis base	[4,5]	[6]
Al	Quaternary ammonium salts or other nucleophiles	[4,5,7-10]	
Co	Lewis base	[4,5,11-14]	
Co	Quaternary ammonium salts or other nucleophiles	[4,5,15-18]*	[18,19]
Cr	Lewis base	[4,5,20,21]	[22]
Cr	Quaternary ammonium salts or other nucleophiles	[4,5]	
Mn, Cu, Sn, Zn	Lewis base	[14,23-25]*	[25]*
Ru	Quaternary ammonium salts	[26]	

* These reactions were conducted without co-catalyst addition.

Proposed Mechanism 1

The first reaction mechanism that is commonly proposed involves activation of the epoxide by the metal salen catalyst followed by attack of the nucleophilic co-catalyst to ring-open the epoxide at the least hindered carbon (Figure A.1).[4,8,11,14,16,20,24,26] After this occurs, the ring-opened epoxide attacks the un-activated carbon dioxide. Finally, the molecule cyclizes to give the carbonate product, and the catalytic cycle repeats.

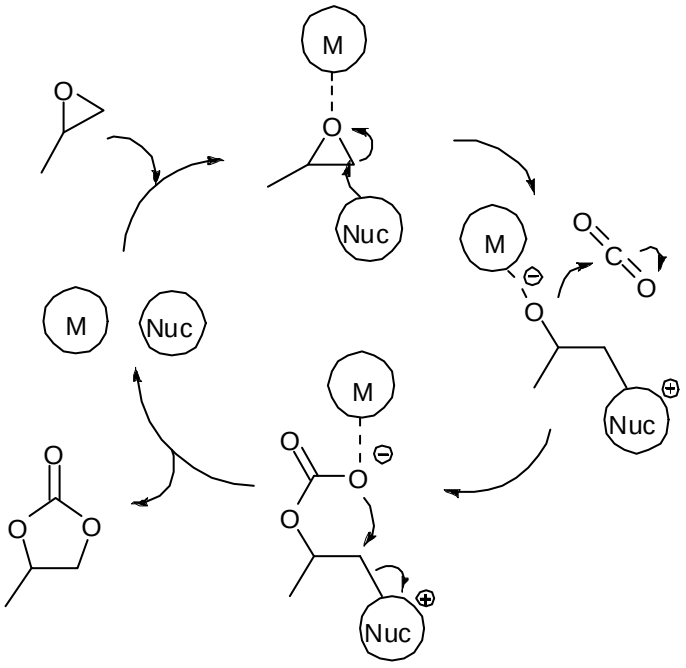

Figure A.1. Proposed cyclic carbonate mechanism 1.

The main evidence offered for this mechanism comes from labeling studies.[8,14] In these studies, *trans*-deuterio epoxide was synthesized and used in the carbonate reaction to test between two possible reaction paths (Figure A.2). Path A occurs by mechanism 1 (Figure A.1), whereas path B occurs by activation of carbon dioxide by the nucleophile and its subsequent attack on the salen activated epoxide. The compound then cyclizes and gives the product with an inversion of configuration. Since the inversion product from path B was not observed, it was proposed that path A was the proper mechanism. The same labeling study has also been conducted with phenol or the metal free ligand in place of the metal salen with the same results.[27,28] While these results suggest that the added co-catalyst does not coordinate with the carbon dioxide, they do not rule out the possibility

that the co-catalyst may coordinate with the salen catalyst, or that the salen catalyst may activate the carbon dioxide.

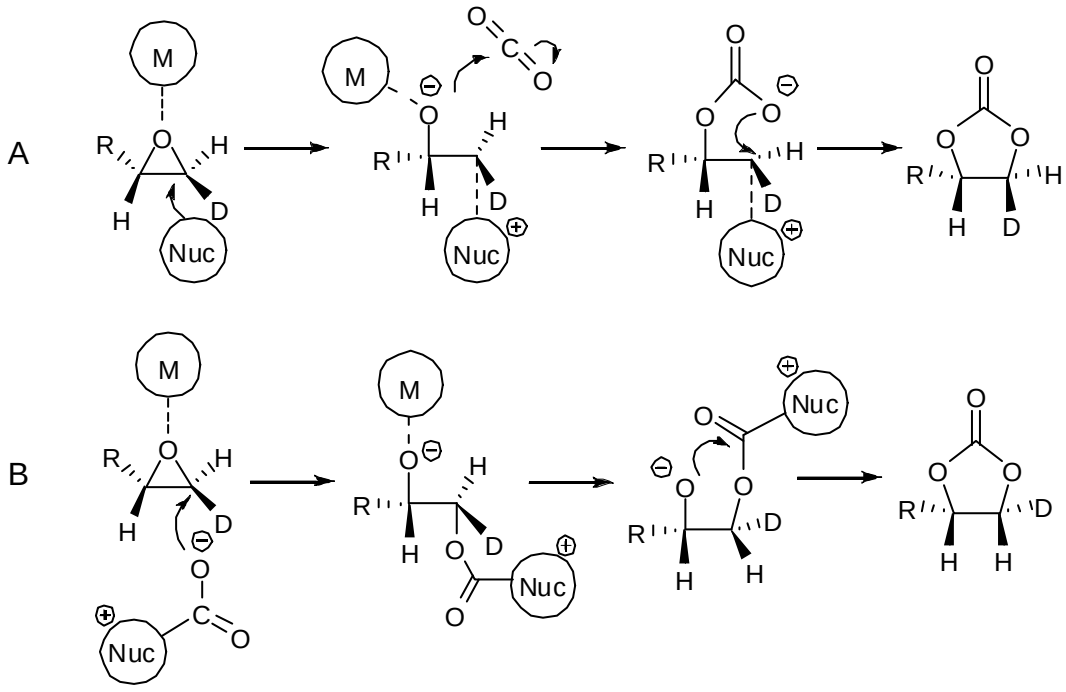

Figure A.2. Labeling studies. Path A – retention of configuration; Path B – inversion of configuration.

Proposed Mechanism 2

The second proposed mechanism cited in the literature involves coordination of both a Lewis base and the epoxide with the salen catalyst (Figure A.3).[12,13] Here, the base serves dual roles of ring-opening the epoxide and coordinating with the metal salen to facilitate the carbon dioxide insertion. This is given as the reason why two equivalents of base are found to be optimal. It is also rationalized that the reason further increases in

base concentration slow the reaction is because of competitive binding between the base and the epoxide with the metal salen. The activation of carbon dioxide is not included in this mechanism, although a deactivation pathway is hypothesized in which a large fraction of base coordinates with carbon dioxide at high pressures which prevents the coordination of the base with the metal salen.

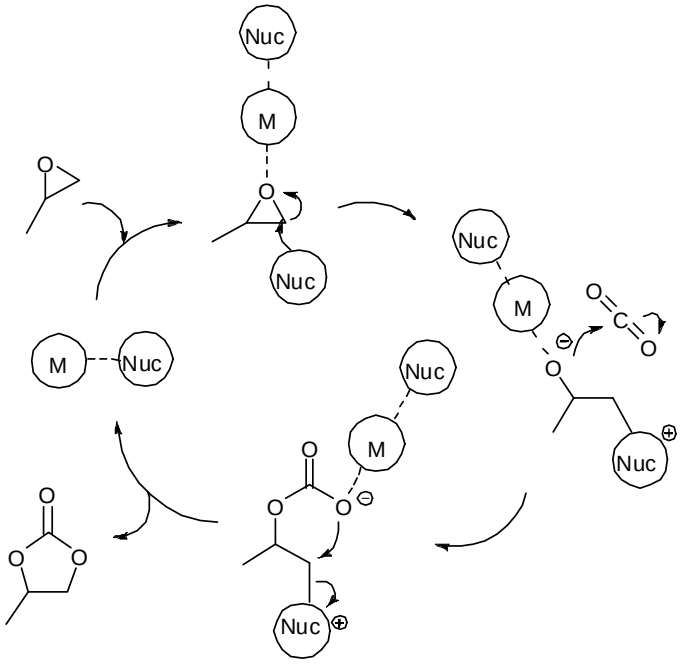

Figure A.3. Proposed cyclic carbonate mechanism 2.

One study has suggested that the Lewis base coordination with the metal salen proposed above is not a requirement in the catalytic cycle.[6] In this work, both the salen catalyst and the base were supported on different solid materials. It was surmised that if the direct interaction between the metal salen and the base was a requirement of the

catalytic cycle, the yield of cyclic carbonate should be dramatically reduced due to the presence of two solid phases. However, the activity was only partially suppressed, indicating that this interaction may not be critical. This evidence could also be used in support of proposed mechanism 1.

Proposed Mechanism 3

The third mechanism reported in the literature suggests a similar coordination between the nucleophile and the metal salen as in proposed mechanism 2, but in this case, this complex serves to activate the carbon dioxide (Figure A.4).[21,23] The epoxide is activated by a salen catalyst not coordinated with the nucleophile. Here, the activated carbon dioxide ring-opens the epoxide and subsequently adds to it. The molecule then cyclizes and forms the carbonate. This proposed mechanism appears to be in direct opposition to the labeling studies presented for proposed mechanism 1 (Figure A.2). Also, there does not seem to be reason given as to why the nucleophile would not also coordinate with the salen which activates the epoxide. However, FT-IR, UV-vis, and EPR spectroscopic results do indicate the presence of carbon dioxide bound to the salen and nucleophile, indicating this pathway may be plausible.[23]

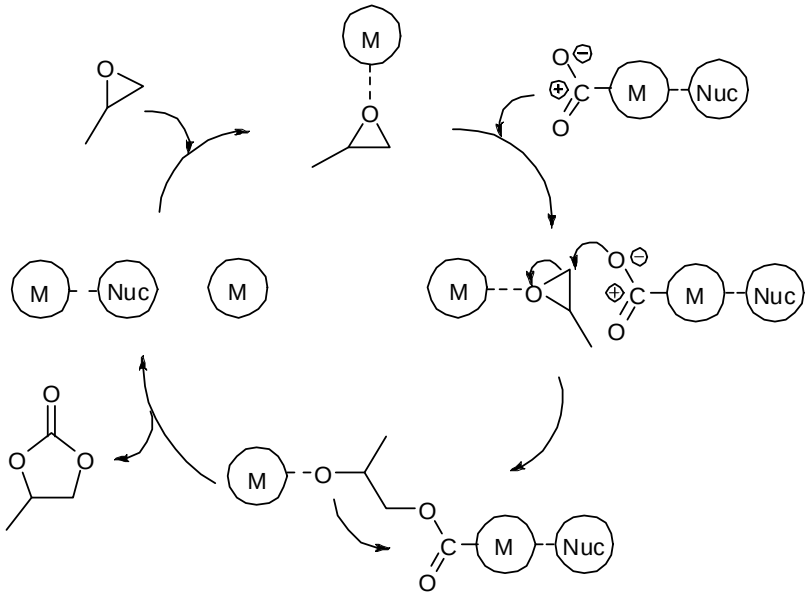

Figure A.4. Proposed cyclic carbonate mechanism 3.

Proposed Mechanism 4

The last reported mechanism which will be covered involves the use of an aluminum salen catalyst that is proposed to exist in dimeric form (Figure A.5).[7] The mechanism is based on reactivity results which show that this catalyst is able to produce cyclic carbonates at much milder reaction conditions than other catalysts (25 °C, 1 atm carbon dioxide).

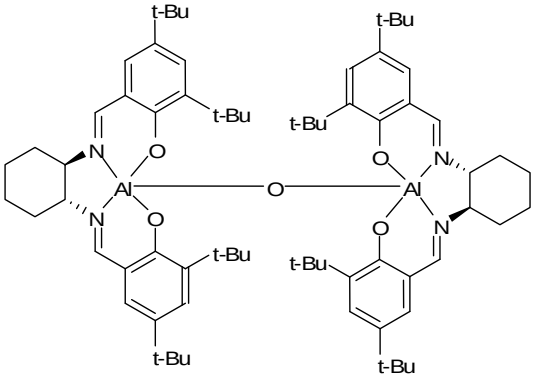

Figure A.5. Dimeric aluminum salen.

In this mechanism, one aluminum center binds the epoxide, which is subsequently ring-opened by a quaternary ammonium salt (Figure A.6). Then, the second aluminum center on the dimer binds and activates carbon dioxide. Intramolecular transfer of the alkoxide and cyclization of the carbonate complete the catalytic cycle. The suggested mode of CO_2 binding on the second aluminum center is supported by previously reported theoretical and spectroscopic results.[29,30] When the reaction was conducted without the ammonium salt, no carbonate was produced, indicating the activated carbon dioxide does not directly attack the epoxide ring. While a dual sited salen catalyst may not be required for cyclic carbonate production, it does appear to enhance the activity of the catalyst.

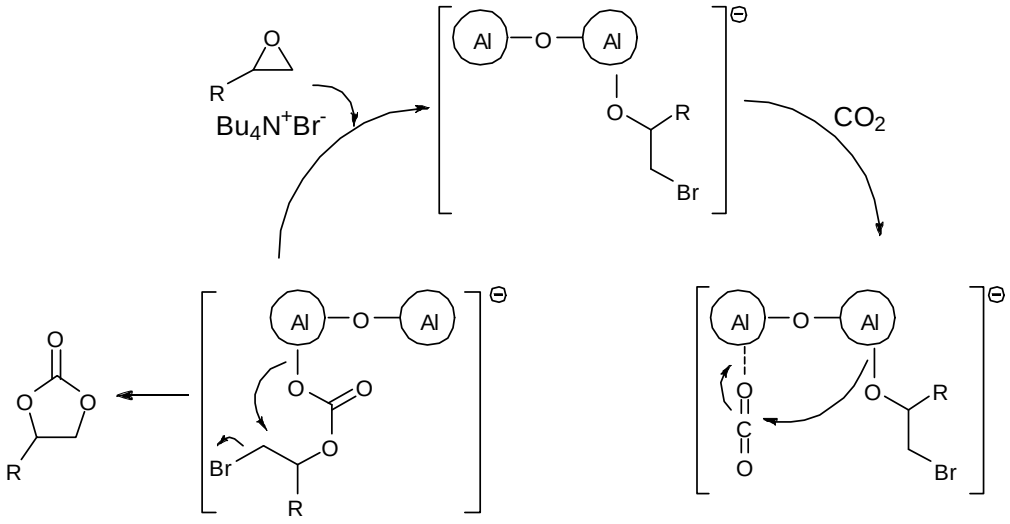

Figure A.6. Proposed cyclic carbonate mechanism 4.

The four mechanisms outlined here are the most commonly proposed, although other reaction mechanisms have been reported.[4,5,10,15] As suggested by Lu, it appears that multiple reaction pathways can occur simultaneously, with one or more predominating under a given set of reaction conditions.[31] However, close examination of these possible mechanisms could still prove useful in designing catalytic systems that take advantage of the most active and efficient pathways.

REFERENCES

[1] Darensbourg, D. J., *Chem. Rev.* 107 (2007) 2388.

[2] Coates, G. W., and Moore, D. R., *Angew. Chem. Int. Ed.* 43 (2004) 6618.

[3] Darensbourg, D. J., Mackiewicz, R. M., Phelps, A. L., and Billodeaux, D. R., *Acc. Chem. Res.* 37 (2004) 836.

[4] Berkessel, A., and Brandenburg, M., *Org. Lett.* 8 (2006) 4401.

[5] Lu, X.-B., Feng, X.-J., and He, R., *Appl. Catal. A* 234 (2002) 25.

[6] Alvaro, M., Baleizao, C., Carbonell, E., Ghoul, M. E., Garcia, H., and Gigante, B., *Tetrahedron* 61 (2005) 12131.

[7] Melendez, J., North, M., and Pasquale, R., *Eur. J. Inorg. Chem.* (2007) 3323.

[8] Lu, X.-B., Zhang, Y.-J., Jin, K., Luo, L.-M., and Wang, H., *J. Catal.* 227 (2004) 537.

[9] Lu, X.-B., Zhang, Y.-J., Liang, B., Li, X., and Wang, H., *J. Mol. Catal. A: Chem.* 210 (2004) 31.

[10] Lu, X.-B., He, R., and Bai, C.-X., *J. Mol. Catal. A: Chem.* 186 (2002) 1.

[11] Tanaka, H., Kitaichi, Y., Sato, M., Ikeno, T., and Yamada, T., *Chem. Lett.* 33 (2004) 676.

[12] Paddock, R. L., Hiyama, Y., McKay, J. M., and Nguyen, S.-B. T., *Tetrahedron Lett.* 45 (2004) 2023.

[13] Paddock, R., and Nguyen, S.-B. T., *Chem. Commun.* (2004) 1622.

[14] Shen, Y.-M., Duan, W.-L., and Shi, M., *J. Org. Chem.* 68 (2003) 1559.

[15] Chen, S.-W., Kawthekar, R. B., and Kim, G.-J., *Tetrahedron Lett.* 48 (2007) 297.

[16] Chang, T., Jing, H., Jin, L., and Qiu, W., *J. Mol. Catal. A: Chem.* 264 (2007) 241.

[17] Lu, X.-B., Liang, B., Zhang, Y.-J., Tian, Y.-Z., Wang, Y.-M., Bai, C.-X., Wang, H., and Zhang, R., *J. Am. Chem. Soc.* 126 (2004) 3732.

[18] Ramin, M., Jutz, F., Grunwaldt, J.-D., and Baiker, A., *J. Mol. Catal. A: Chem.* 242 (2005) 32.

[19] Lu, X.-B., Xiu, J.-H., He, R., Jin, K., Luo, L.-M., and Feng, X.-J., *Appl. Catal. A* 275 (2004) 73.

[20] Darensbourg, D. J., Fang, C. C., and Rogers, J. L., *Organometallics* 23 (2004) 924.

[21] Paddock, R., and Nguyen, S.-B. T., *J. Am. Chem. Soc.* 123 (2001) 11498.

[22] Alvaro, M., Baleizao, C., Das, D., Carbonell, E., and Garcia, H., *J. Catal.* 228 (2004) 254.

[23] Srivastava, R., Bennur, T. H., and Srinivas, D., *J. Mol. Catal. A: Chem.* 226 (2005) 199.

[24] Jing, H., Edulji, S. K., Gibbs, J. M., Stern, C. L., Zhou, H., and Nguyen, S.-B. T., *Inorg. Chem.* 43 (2004) 4315.

[25] Jutz, F., Grunwaldt, J.-D., and Baiker, A., *J. Mol. Catal. A: Chem.* 279 (2008) 94.

[26] Jing, H., Chang, T., Jin, L., Wu, M., and Qiu, W., *Catal. Commun.* 8 (2007) 1630.

[27] Shen, Y.-M., Duan, W.-L., and Shi, M., *Eur. J. Org. Chem.* (2004) 3080.

[28] Shen, Y.-M., Duan, W.-L., and Shi, M., *Adv. Synth. Catal.* 345 (2003) 337.

[29] Panek, J., and Latajka, Z., *J. Phys. Chem. A* 103 (1999) 6845.

[30] Walters, R. S., Brinkmann, N. R., Schaefer, H. F., and Duncan, M. A., *J. Phys. Chem. A* 107 (2003) 7396.

[31] Lu, X.-B., Wang, H., and He, R., *J. Mol. Catal. A: Chem.* 186 (2002) 33.

VITA

Rebecca A. Shiels (Hicks)

Rebecca was born in Atlanta, GA to Charles and Mary Shiels (and siblings Brian, Suzanne, and Renee). She attended public schools in Gwinnett County, GA and graduated from Norcross High School in 1995. She went on to receive a B.E. in Chemical Engineering (summa cum laude) with minors in mathematics and piano performance from Vanderbilt University (1999). After graduation, she worked as an engineer for Merck & Co., Inc. in Albany, GA in their Technical Operations group and later for Lucent Technologies/OFS in Norcross, GA in their Modified Chemical Vapor Deposition group.

In 2003, Rebecca entered graduate school at Georgia Tech to pursue a Ph.D. in Chemical Engineering under the direction of Prof. Chris Jones. In January 2008, she was married to Dr. Jason C. Hicks, a fellow graduate of the Jones group. After completing her degree, Rebecca will work for Chevron Energy Technology Corporation in their Process Technology Division.